International Atomic Energy Agency

INDC(NDS)-263
Distr.: G+Sp

INDC INTERNATIONAL NUCLEAR DATA COMMITTEE

ACTIVATION CROSS SECTIONS FOR THE GENERATION OF LONG-LIVED RADIONUCLIDES OF IMPORTANCE IN FUSION REACTOR TECHNOLOGY

Texts of Papers Presented at the
First Meeting of a Co-ordinated Research Programme
organized by the IAEA and held in Vienna, 11-12 November 1991

Compiled by
Wang DaHai
IAEA Nuclear Data Section

July 1992

IAEA NUCLEAR DATA SECTION, WAGRAMERSTRASSE 5, A-1400 VIENNA

INDC(NDS)-263
Distr.: G+Sp

ACTIVATION CROSS SECTIONS FOR THE GENERATION OF LONG-LIVED RADIONUCLIDES OF IMPORTANCE IN FUSION REACTOR TECHNOLOGY

Texts of Papers Presented at the
First Meeting of a Co-ordinated Research Programme
organized by the IAEA and held in Vienna, 11-12 November 1991

Compiled by
Wang DaHai
IAEA Nuclear Data Section

July 1992

Reproduced by the IAEA in Austria
July 1992

92-02668

Foreword

Following the recommendations of the International Nuclear Data Committee (INDC), the IAEA Nuclear Data Section has established a Co-ordinated Research Programme (CRP) on activation cross sections for the generation of long-lived radionuclides of importance in concentrating on the cross sections for the reactions suggested by the 16th INDC meeting.

The first Research Coordination Meeting of the CRP was held at the IAEA Headquarters, Vienna, Austria, from 11 to 12 November 1992. The main objectives of the meeting were to review the results under the CRP and the status of long-lived activation cross section data and to fix the future working programme for the CRP.

The proceedings contain the progress reports of the CRP and the contributed papers presented at the meeting as well as the summary of the conclusions and recommendations of the meeting.

The Scientific Secretary of the meeting wishes to express his appreciation to Dr. E.T. Cheng and Prof. Dr. H. Vonach for acting as Chairmen and preparing the summary of the conclusions and recommendations of the meeting.

Contents

Conclusions and Recommendations

(1) Status of Cross-Sections measured under the CRP

The status of the neutron cross section measurements performed under the CRP is summarized in Tables 1-4. Tables 1 and 2 give the results for threshold reaction measurements around and below 14 MeV respectively, Table 3 summarizes the status for the neutron capture reactions included in the CRP, and Table 4 lists the half-lives of the relevant radioisotopes.

The tables show that considerable progress has been achieved since the already quite favourable situation at the Consultants Meeting on Activation Cross Sections for the Generation of Long-lived Radionuclides at Argonne National Laboratory in September 1989.

In detail the present situation was judged to be as follows:

a) For the reactions $^{94}Mo(n,p)^{94}Nb$, $^{109}Ag(n,2n)^{108m}Ag$, $^{179}Hf(n,2n)^{178m2}Hf$, $^{151}Eu(n,2n)^{150m}Eu$, $^{153}Eu(n,2n)^{152g}Eu$ and $^{159}Tb(n,2n)^{158g}Tb$ a sufficient number of reliable measurements has been performed around 14 MeV and no more experimental work is needed at that energy.

b) For the reaction $^{187}Re(n,2n)^{186m2}Re$ only one measurement has been performed and there are also considerable discrepancies in the measurements of the cross-sections for $^{187}Re(n,2n)^{186g+m1}Re$. Thus a new measurement of both cross-sections was felt desirable.

c) Concerning the reaction $^{182}W(n,n'\alpha)^{178m2}Hf$ two mutually consistent results are available, a third one is expected to be supplied by Patrick/Harwell in the near future. If this confirms the other measurements, no additional measurements will be needed.

d) $^{158}Dy(n,p)^{158g}Tb$. The majority of the participants felt that the existing estimates of this cross-section from systematics should be confirmed by at least one measurement. There was general agreement, however, that a successful measurement can only be performed if isotopically enriched

Table 1

14 MeV Cross-Sections (mb)

	$^{63}Cn(n,p)^{63}Ni$	$^{94}Mo(n,p)^{94}Mo$	$^{109}Ag(n,2n)^{108m*}Ag$	$^{151}Eu(n,2n)^{150m}Eu$	$^{153}Eu(n,2n)^{152m}Eu$	$^{159}Tb(n,2n)^{159}Tb$
IRK-89 Eval.			665 ± 73	1325 ± 94	1442 ± 60	1930 ± 49
Debrecen			865 ± 66			
JAERI/ANL			734 ± 30	1282 ± 75		2110 ± 168
"			628 ± 46	1162 ± 66	(1970 ± 95)	2050 ± 10
Beijing			727 ± 23	1219 ± 28	1544 ± 42	1968 ± 56
JAERI		50 ± 18	698 ± 35	1220 ± 58	1506 ± 78	
St. Petersburg			685 ± 122	1090 ± 84	~1580 ± 110	
ANL (Greenwood)	54 ± 4	50.1 ± 5.3				
Jülich	~ 120 (new measurem. in progress)					
Lanzhon Univ.			746 ± 30			

Table 1 (continued)

	$^{179}Hf(n,2n)^{178m2}Hf$	$^{182}W(n,n'alpha)^{178m2}Hf$	$^{158}Dy(n,p)^{158}Tb$	$^{193}Ir(n,2n))^{192m2}Tb$	$^{187}Re(n,2n)^{186m}Re$
IRK-89 Eval.			< 100	184 ± 44	592 ± 122
Debrecen					
JAERI/ANL	6.3 ± 5				
JAERI	6.3 ± .6	.014 ± .008	100 ± 80		135 ± 65
Beijing	7.7 ± .6				340 ± 192
St. Petersburg		< .040			
ANL /Greenwood					
Jülich					
Lanzhon Univ.	6.04 ± 32				
Harwell/Patrick	5.9 ± .6	?			

* all cross-section reported to the CRP were renormalized to the new half-life of 418 years for ^{108m}Ag

Table 2

Cross Sections below 14 MeV

$^{63}Cu(n,p)^{63}Ni$	Jülich/Debrecen Measurements in progress
$^{94}Mo(n,p)^{94}Nb$	
$^{109}Ag(n,2n)^{108m}Ag$	40.8 mb ± 8.5 % at 10.3 MeV ANL/LANL
$^{151}Eu(n,2n)^{150m}Eu$	198 ± 16 mb at 10.3 MeV ANL/LANL; 9.7 - 10.7 MeV Jülich/Debrecen
$^{153}Eu(n,2n)^{152g}Eu$	
$^{159}Tb(n,2n)^{158}Tb$	536 ± 53 mb at 10.3 MeV ANL/LANL; 8.6 - 10.7 MeV Jülich/Debrecen
$^{179}Hf(n,2n)^{178m2}Hf$	
$^{182}W(n,n'\alpha)^{178m2}Hf$	
$^{158}Dy(n,p)^{158}Tb$	
$^{193}Ir(n,2n)^{192m2}Ir$	
$^{187}Re(n,2n)^{186m}Re$	

Table 3

(n,γ) Reactions

$^{98}Mo(n,\gamma)^{99}Mo \rightarrow {}^{99}Tc$

E_n = 29 - 1100 KeV	Chengdu	) reasonable agreement
E_n = 700 - 2000 KeV	St. Petersburg	) in overlapping region

$^{165}Ho(n,\gamma)^{166m}Ho$ 2.92 ± 0.6 mb at E_n = 674 KeV
in conjunction with $\sigma(n,\gamma)$ (E_n) gives isomer cross-section (E_n)

$^{191}Ir(n,\gamma)^{192m2}Ir$ no work done

Table 4

Half-life of some Radioisotopes

Radio-isotope		$T_{1/2}$ from: ENSDF (1989 Version)	(uncertainty) (Y)	$T_{1/2}$ from: "Table of Radioactive Isotopes" (1986) (E. Browne, R.B. Firestone and V.S. Shirley)
14C		5730 Y	40	5730 ± 40 Y
26AL		7.2E+5 Y	3	$7.2_3 \times 10^5$Y = (7.2 ± 0.3)x10^5 Y
36CL		3.01E5 Y	2	$3.01_2 \times 10^5$Y = (3.01 ± 0.02)x10^5 Y
39AR		269 Y	3	269_3 Y = (269 ± 3) Y
59NI		7.5E+4 Y	13	$7.5_{13} \times 10^4$Y = (7.5 ± 1.3)x10^4 Y
60FE		1.5E+6 Y	3	~ 1 x 10^5Y
63NI		100.1 Y	20	100.1_{20} Y = (100.1 ± 2.0) Y
92NB		3.5E+7 Y	3	$3.6_3 \times 0^7$Y = (3.6 ± 0.3)10^7 Y
94NB		2.03E+4 Y	16	$2.03_{16} \times 10^4$ Y = (2.03 ± 0.16)10^4 Y
99TC		2.111E+5 Y	12	$2.13_5 \times 10^5$ Y = (2.13 ± 0.05)10^5 Y
108AG		418 Y	12	
150EU		35.8 Y	10	35.8_{10} Y = (35.8 ± 1.0) Y
152EU		13.542 Y	10	13.33_4 Y = (13.33 ± 0.04) Y
158TB	*	180 Y	11	150_{30} Y = (150 ± 30) Y
166HO		1.20E3 Y	18	1200_{180} Y = (1200 ± 180) Y
178HF		31 Y	1	31_1 Y = (31 ± 1) Y
186RE		2.0E+5 Y	5	2 x 10^5 Y
192IR		241 Y	9	241_9 Y = (241 ± 9) Y
208BI		3.68E+5 Y	4	$3.68_4 \times 10^5$ Y = (3.68 ± 0.04)x10^5 Y
210BI		3.0E+6 Y	1	$3.00_{20} \times 10^6$ Y = (3.00 ± 0.20)10^6 Y

* See Nuclear Data Sheets 1989. Experimental data were obtained in 1984.

^{158}Dy (natural concentration .1%) can be made available (~ 100 mg).

e) The experimental situation for the reactions $^{98}Mo(n,\gamma)^{99}Mo$ and $^{165}Ho(n,\gamma)^{166m}Ho$ was considered to be satisfactory, however, for $^{165}Ho(n,\gamma)^{166m}Ho$ measurements at some more energies are still needed.

f) The reaction $^{191}Ir(n,\gamma)^{192m2}Ir$ is still an open question as the measurement of the activation resonance integral at Chalk River proposed at the Argonne CM has not been possible and no volunteer for a study of this reaction could be found.

g) For the $^{63}Cu(n,p)^{63}Ni$ reaction, the new result of Greenwood at 14 MeV (table 1) strongly differs from the Jülich value measured some time ago. Further discussion of this problem will have to wait for the result of the ongoing new measurement at Jülich. As this reaction has a rather low threshold (~ 2 MeV) it was felt that measurements for a number of energies below 14 MeV are needed if the activation in moderated fusion neutron energy spectra is to be calculated reliably. New measurements are in progress in collaboration between Jülich and Debrecen. Copper samples have been irradiated in Debrecen at different neutron energies between 6 and 12 MeV and at 14.5 MeV. After the radiochemical separation of ^{63}Ni isotope in Jülich the activities will be measured in Jülich and Debrecen.

(2) Cross-Section Calculations

a) Calculations of the excitation functions for the reactions $^{63}Cu(n,p)^{63}Ni$, $^{94}Mo(n,p)^{94}Nb$, $^{109}Ag(n,2n)^{108m}Ag$ and $^{159}Tb(n,2n)^{158}Tb$ have been transmitted to Prof. Vonach by Prof. Yamamuro. These results are in very good agreement with the CRP measurements at 14 MeV.

b) Calculations of excitation functions for almost all CRP reactions have been performed by the Obninsk group, also in good agreement with the experimental 14 MeV cross-sections for most reactions.

c) There was agreement that in case of total (n,2n) cros-sections the calculated excitation functions normalized to the experimental 14 MeV values will probably fulfill the data needs. For low threshold reactions like $^{63}Cu(n,p)^{63}Ni$, however, it was not felt safe to rely on theory only for energies below 14 MeV especially in the threshold region.

d) There are deficiencies in calculation of formation cross-sections of isomeric states. In calculations of absolute cross-sections or formation of high-spin isomers (e.g. $^{178m2}Hf$) the uncertainty is still of the order of a factor of two.

(e) There are very strong deficiencies in calculation of cross-sections of reactions involving emission of complex particles like ^{3}H, ^{3}He etc.

(3) Decay Data.

It was decided to use the half-lives published in the Nuclear Data Sheets (or contained in the ENSDF-file) for the long-lived radionuclides considered under the CRP with the exception of ^{108m}Ag. For this nuclide (see table 1) the new half-life of 418 ± 12 years measured at the PTB/Braunschweig and presented at the 1991 Jülich Conference is recommended.

It is further stressed that uncertainties in half-lives and branching ratios are still among the largest sources of uncertainty for some cross-sections included in the CRP.

(4) Plan for future work

In order to solve the relatively few still open problems, the following working plan was adopted by the participants:

a) IRK Vienna will perform an evaluation of the 14 MeV cross-sections for those reactions where the present data base appears to be satisfactory, that is for $^{94}Mo(n,p)^{94}Nb$, $^{109}Ag(n,2n)^{108m}Ag$, $^{151}Eu(n,2n)^{150m}Eu$, $^{153}Eu(n,2n)^{152m}Eu$, $^{159}Tb(n,2n)^{158}Tb$ and $^{179}Hf(n,2n)^{178m2}Hf$.

b) IAE Beijing will measure the activation cross-sections for the reactions $^{108}Cd(n,p)^{108m}Ag$ and $^{187}Re(n,2n)^{186m}Re$ at 14 MeV and $^{151}Eu(n,\gamma)^{152}Eu$ and $^{153}Eu(n,\gamma)^{154}Eu$ at 60 keV - 1.2 MeV. IEP Debrecen will measure the $^{108}Cd(n,p)^{108m}Ag$ reaction around 14 MeV and in a few points between 6 and 12 MeV.

c) KFA Jülich in collaboration with Debrecen will continue will continue the measurement and analysis of irradiated Cu samples for $^{63}Cu(n,p)^{63}Ni$ cross-sections at 14 MeV and a few lower energies. Debrecen will collaborate with KFA Jülich to measure the cross sections for $^{151}Eu(n,2n)^{150m}Eu$ and $^{159}Tb(n,2n)^{158}Tb$ at 8.6 - 10.7 MeV.

d) KRI St. Petersburg will measure the $^{182}W(n,n'\alpha)^{178m2}Hf$ and $^{158}Dy(n,p)^{158g}Tb$ cross-sections at 14 MeV if enriched isotope samples can be made available.

e) E. Cheng will investigate the problem of availability and cost of enriched ^{158}Dy and ^{182}W and transmit the information to the NDS.

f) ANL will check the energy scale for the incident neutrons for the Los Alamos irradiations (~ 10 MeV measurements) and compare the results for the $^{151}Eu(n,2n)^{150m}Eu$ and $^{159}Tb(n,2n)^{158}Tb$ reactions with the Jülich/Debrecen results to see if any adjustments are necessary. It will also compare the experimental cross-sections for the $^{9}Be(d,n)$ spectrum with calculations based on the calculated excitation functions reported by the CRP (see section 2) and investigate the differences from the separate JAERI and ANL cross-section determinations from the 14.7 MeV sample irradiations.

g) ENEA Bologna will calculate the cross-sections for the $^{109}Ag(n,2n)^{108m}Ag$, $^{63}Cu(n,p)^{63}Ni$, $^{158}Dy(n,p)^{158g}Tb$ and $^{62}Ni(n,\gamma)^{63}Ni$ reactions.

h) Chadwick/LANL will continue theoretical calculations for long-lived isomers studying particularly charged particle emission processes and investigate theoretical estimates for the transmutation of long-lived isomers and cooperate with D.L. Smith on the interpretation of the $^{9}Be(d,n)$ results.

i) JAERI will do some new measurements of activation cross-sections using isotopically enriched targets of ^{94}Mo, ^{95}Mo and ^{179}Hf.

j) The Obninsk group will calculate the transmutation cross sections for the long-lived radionuclides ^{26}Al, ^{94}Nb, ^{108m}Ag, ^{158}Tb, ^{166m}Ho, ^{178m}Hf, ^{186m}Re and ^{192m}Ir, analyze the isomer ratios for different reactions leading to the same isomer state and the energy dependence of the high-spin isomer ratio in the $^{179}Hf(n,2n)$ reaction, and construct more accurate systematics of isomer ratios for the threshold reactions.

(5) Data compilation in EXFOR

All groups are urged to send their experimental, evaluated, and calculated data to the respective nuclear data center for compilation in EXFOR (for more detail, see the appendix) and copy to NDS.

(6) Date and place of next meeting

It was proposed that the next CRP meeting will be held either in conjunction with the first CRP meeting on (n,α) cross-sections or in conjunction with the next fusion nuclear data review to be held at San Diege, USA, in spring 1993.

Activation cross section measurement and evaluation for the $^{23}Na(n,2n)^{22}Na$ reaction

Lu Hanlin, Zhao Wenrong and Yu Weixiang

(China Institute of Atomic Energy, P.O.Box 275, Beijing 102413)

Abstract: A large serious discrepancy exists in the published literatures and in the two recent evaluations for the cross sections of $^{23}Na(n,2n)^{22}Na$ reaction. New experimental measurements have been performed in neutron energy range of 13–18 MeV by activation method for $^{23}Na(n,2n)^{22}Na$ reaction. Based on the new measurements and the trend of excitation function, the recommended data are given.

Key words: Activation cross section, $^{23}Na(n,2n)^{22}Na$.

The excitation function of cross sections for $^{23}Na(n,2n)^{22}Na$ reaction is very important for safety and cnviromental assessments of fast breeder reactors in accidental hazard potential, decay heat and shut down doserate[1]. The published literatures[2–13] show a large discrepancy in existing measurement data and between two most famous evaluations for ENDF / B–V[14] and the International Reactor Dosimetry File[15] of the IAEA. In order to distinguish the published data, a new measurement was carried out by activation method in the neutron energy range from 13 to 18 MeV for $^{23}Na(n,2n)^{22}Na$ reaction.

The $T(d,n)^4He$ reaction was used for neutron production at the Van–de–Graaff accelerator and Cockcroft–Walton accelerator of CIAE. The NaF powder was pressed tablets with 20 mm in diameter and 2.5 mm in thickness used as samples and they were sandwiched between two Nb foils with 0.03 mm in thickness and the same diameter. The sample groups were placed at various angles relative to the incident deutron beam and the distance between the sample and neutron source was 3–5 cm. The exposure time lasted to about 50 hours. After irradiation, the activities of the samples and monitors were determined by a well calibrated Ge(Li) spectrometer. Because neutron fluence is rather low during the irradiation;half–life of redionucler ^{22}Na is relatively long (2.602 y) and large distance between sample and detector (15.5 cm) was taken to exclude the seriously effect of sum peak by β^+, the ^{22}Na activity for some samples was too weak to count.So a calibrated ^{22}Na source was used to determine the effect efficiency in close distance (~ 0.5 cm). The measured time was about 100–150 hours per NaF sample and total peak counts of 1274 keV gamma–ray were $(0.7–3.2)\times 10^4$.

The $^{23}Na(n,2n)^{22}Na$ cross section was determined relative to the $^{93}Nb(n,2n)^{92m}Nb$ cross section, which had been accurately evaluated in previous report[15].

Corrections were made for the gamma-ray self-absorption of the ^{92m}Nb and ^{22}Na in the Nb and NaF foils, for the change of effective distance between source and detector due to thickness of foils and for the fluctuation of neutron flux during the irradiation.

The main uncertainties of the cross sections include the errors of standard cross section (1-2.7 %), efficiency of γ-ray full energy peak (1.2-1.5 %), counting statistics of activity, gamma-ray self-absorption (0.4 %) and purity of sample (0.5 %).

Table 1 Present results of cross section for $^{23}Na(n,2n)^{22}Na$ reaction

En (MeV)	σ (mb)	σ_0(mb)*
13.50 ± 0.15	5.83 ± 0.16	448.9 ± 7.4
14.10 ± 0.15	20.1 ± 0.5	456.7 ± 4.7
14.64 ± 0.21	39.5 ± 0.8	459 ± 5
14.87 ± 0.21	41.7 ± 0.9	458 ± 6
16.95 ± 0.33	89.1 ± 3.0	413 ± 11
17.98 ± 0.21	99.0 ± 4.3	388 ± 15

* $^{93}Nb(n,2n)^{92m}Nb$ reaction

The results for the $^{23}Na(n,2n)^{22}Na$ cross section are summarized in the Table 1.

Table 2 $^{23}Na(n,2n)^{22}Na$ cross section--Recommended data

Cross section		Correlation matrix
En (MeV)	XSEC (mb)	
12.5-13.0	0.50 ± 0.50	1000
13.0-13.5	2.29 ± 0.19	241 1000
13.5-14.0	9.05 ± 0.20	240 576 1000
14.0-14.5	24.3 ± 0.4	275 706 727 1000
14.5-15.0	40.4 ± 0.6	259 759 707 758 1000
15.0-15.5	51.3 ± 2.5	263 214 213 244 229 1000
15.5-16.5	68.5 ± 3.1	316 310 308 367 333 280 1000
16.5-17.5	90.7 ± 2.9	203 361 316 369 389 179 256 1000
17.5-18.5	103.1 ± 4.0	154 333 285 333 359 136 217 365 1000
18.5-19.5	115.0 ± 6.0	104 168 151 174 184 93 146 215 310 1000
19.5-20.5	119.0 ± 9.0	11 23 20 23 25 10 19 23 59 19 1000
20.5-21.5	129 ± 15	14 28 24 28 31 12 24 29 74 24 368 1000

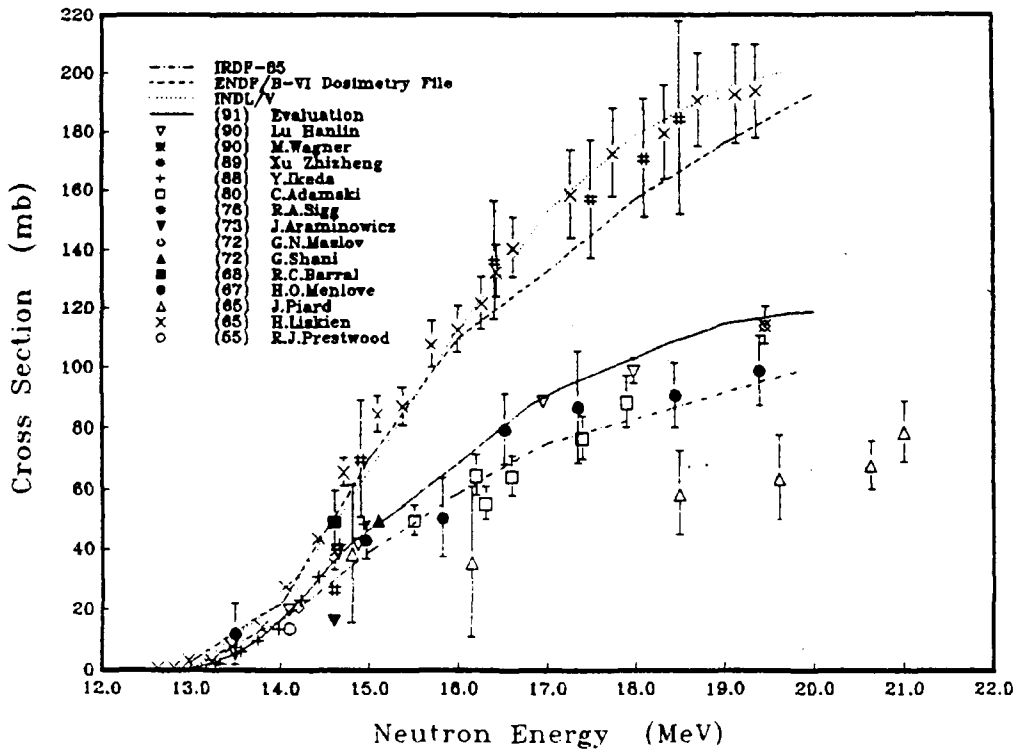

Fig.1 $^{23}Na(n,2n)^{22}Na$ Reaction

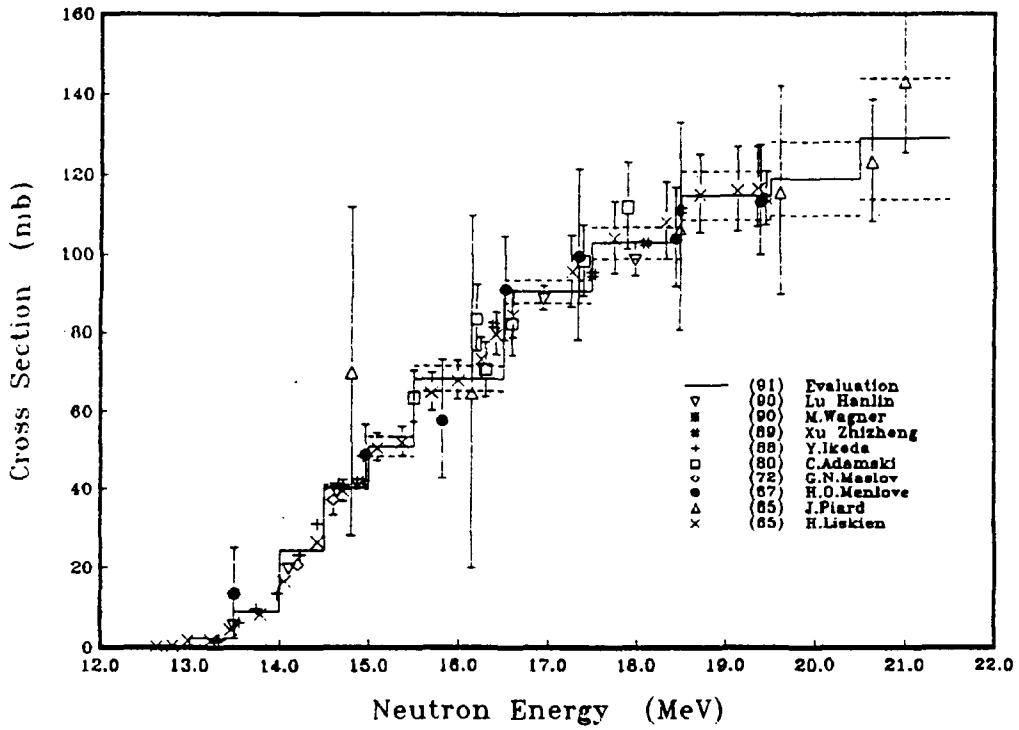

Fig.2 $^{23}Na(n,2n)^{22}Na$ Reaction

Fig.1 shows a comparison of our results with the existing data of measurements and evaluations.The present data is situated between two evaluations, ENDF/B-VI and IRDF-85. New published data of Y.Ikeda and M.Wagner are much closer to the present results which are also consistent with the

data of G.N.Maslov and Shani at 14 MeV. A new evaluation is given, based on the values of Y.Ikeda, M.Wagner, G.N.Maslov and present work and relative shapes of excitation functions given by H.Liskien, Xu Zhizheng, H.O.Menlove, J.Piard and C.Adanski. The results of this evaluation and correlation matrix are appeared in Table 2 and Fig.2.The present evaluation lies between two evaluations of ENDF / B-VI and IRDF-85, but is slightly closer to IRDF-85.

Reference

1. E.T.Cheng, NEANDC Specialists Meeting on Neutron Activation Cross Section for Fission and Fusion Energy. 13-15 Sep, 1989 Argonne U.S.A.
2. R.J.Preswood, Phys. Rev. 98,47 (1955)
3. H.Liskien and A.Paulson, Nucl Phys. 63, 393 (1965)
4. J.Picard and C.F.Williamson, Nucl. Phys. 63, 673 (1965)
5. H.O.Menlove et al., Phys. Rev. 163 1308 (1967)
6. R.C.Barrall et al, Report AFWL-TR-68-134 (1968)
7. J.Araminowicz et al., Report INR-1464 / 1 / A, 14 (1973)
8. G.N.Maslov et al., Report YF-9, 50, FEI Obninsk (1972)
9. G.Shani, Report INIS-MF-3663, 83 (1976)
10. R.A.Sigg, Thesis, Univ. of Arkansas (1976), and Diss. Abstr. B37 2237 (1976)
11. L.Adamski et al., Ann. Nucl. Energy 7, 397 (1980)
12. Y.Ikada et al., Report JAERI 1312 (1988)
13. M.Wagner et al., IRK Progress Report p-15 (1990)
14. D.Larson, Report ORNL-5662 (1980) and Nucl. Sci. Eng. 78, 324 (1981)
15. L.Adamski, Prog. Rept. INR 1809 / 1 / PL / A,(1979) and Report INDC(POL)-10 / G IAEA Vienna(1979)
16. Zhao Wenrong, INDC(CPR)-16 (1990)

Activation cross section measurement for the $^{179}Hf(n,2n)^{178m2}Hf$ reaction

Yu Weixiang, Lu Hanlin and Zhao Wenrong

(China Institute of Atomic Energy, P.O.Box 275-3,Beijing 102413)

Abstract: As an important data for a fusion reactor there are not any data for the cross section of the $^{179}Hf(n,2n)^{178m2}Hf$ reaction. So the cross section was measured in this work at neutron energy of 14 MeV. Meanwhile, we also gave the data for the cross section of the $^{180}Hf(n,2n)^{179m2}Hf$ reaction.

Key words: Long half-life, $^{179}Hf(n,2n)^{178m2}Hf$

Today the modern controlled fusion teohnique has been developed greatly. The prospect of applying the fusion reactor technique becomes more clear. However, a lot of high energy neutrons will be produced by $T(d,n)^4He$ reaction in a fusion reactor. So the cross sections of the product nuclei with a long half-life for fast neutron reactions are more important. They effect a series of problems, such as re-applying the old structure meterial of a fusion reactor; reducing its radiation background and disposing the nuclear waste, etc. But up to now, there are few data about the cross sections of the product nuclei with long half-life for the fast neutron reactions. So a CRP was carried out for them by IAEA on May, 1988. Our group is a member of the CRP. Hafnium is an important material in a fusion reactor. So the cross section value for $^{179}Hf(n,2n)^{178m2}Hf$ reaction was included in the data offered by IAEA in this CRP. We measured the cross section for $^{179}Hf(n,2n)^{178m2}Hf$ reaction by activation method at neutron energy of 14 MeV. Because the product nucleus $^{179m2}Hf$ (25.1d, 25^- / 2) for $^{180}Hf(n,2n)^{179m2}Hf$ reaction can produce $^{178m2}Hf$ by (n,2n) reaction in a fusion reactor for long time operation, we also measured the cross section for it.

The sample discs of Hf with 20 mm in diameter and 2 mm in thickness were made of natural oxide hafnium powder by pressed method, and were packed in nylon gluey type to protect the powder from losing after weighed.

The samples were irradiated at the Cockcroft-Walton accelerator of CIAE and the Intense Neutron Generator of Lanzhou University. Neutrons were produced by $T(d,n)^4He$ reaction. The $^{93}Nb(n,2n)^{92m}Nb$ reaction was used as a neutron fluence monitor, whose cross section values were taken from our evaluated data[1] and shown in table 3. Each sample was sandwiched between two Nb foils with 20 mm in diameter and 0.05 mm in thickness. Because of the long half-life of the product nuclei, the samples were placed in front of the target as close as possi-

ble so that the neutron fluence could be more intense and irradiated for long time. Meanwhile, the background sample which could determine the effect of the room background neutrons was placed in a distance of 2m from the target . But the effect wasn't seen when the background sample was measured. Table 1 and figs. 1–2 show the irradiated condition in detial.

Table 1 The irradiated condition

	Lanzhou Univ.	CIAE
Neutron energy (MeV)	14.2	14.8
Neutron flux ($cm^{-2}s^{-1}$)	3.54×10^{9}	0.88×10^{9}
Irradiated time	~7.38 h	~50 h
Distance from sample to target	~7 cm	~1.5 cm

The activities of the samples were determined by a Ge(Li) detector with a computer system. The volume of the detector is 136 cm^3. Because the activity of ^{179m2}Hf was intense, the sample was far from the surface of the detector when it was measured. Since the half-life of ^{178m2}Hf is very long, its activity was very weak, the sample was measured on the surface of the detector. The effects of sum peak is rather big. They include two parts: reduced part and increased part. The increased part is very small (< 0.5%). We only corrected for reduced part. The decay scheme of ^{178m2}Hf is shown in fig.3, which is taken from "Table of Isotopes"[2]. From fig.3 we can see that the 495 and 574 keV γ-rays are above the state of ^{178m1}Hf (4.0s) and the 325 and 426 γ-rays are below the state of ^{178m1}Hf. The effects of Kx-ray in sum peak are big for the 325 and 426 γ-rays and small for the 495 and 574 keV γ-rays. So we choose the 495 and 574 keV γ-rays to determine the activity of ^{178m2}Hf. After six monthes past irradiation we could see 495 and 574 keV γ peaks on the spectrum. However, the last data of ^{178m2}Hf activity was measured after irradiation 2 years in order to reduce the contamination of other product nuclei activities (see fig.4). The collected time of the γ-specturm was about 100–150 hours and the total counts of peak was about 10000. The characteristic γ-ray energies of the product nuclei, their intensities, half-lives and other con-

Table 2 Some Constants

Sample	Molecular Weight	Isotope	Abundance	Product Nucleus	Half-life	Er (keV)	Ir (%)
Nb	92.9064	^{93}Nb	1.00	^{92m}Nb	10.15 d	934	99.0
HfO_2	210.4888	^{179}Hf	0.13629	^{178m}Hf	31.1 y	574	83.8
						495	68.92
		^{180}Hf	0.351	^{179m2}Hf	25.1 d	454	66.0

stants were listed in table 2, which were taken from "Table of Radioactive Isotopes"[3].

Some corrections were made for the cross section values in present work, such as γ-ray self-absorption (5-8 %), sum peak effect (69% and 65% for ^{178m}Hf),fluctuation of neutron fluence (0.4-1.3 %), etc. From fig.3 we can get the corrected formula of sum peak as following:

$$(\varepsilon / \varepsilon_0)_{574} = 0.81\,(1 - T_{495})\,(1 - T_{217}) + 0.19\,(1 - T_{257})$$
$$[0.35\,(1 - T_{237})\,(1 - T_{217}) + 0.65\,(1 - T_{454})]$$
$$(\varepsilon / \varepsilon_0)_{495} = 0.9836\,(1 - T_{574})\,(1 - T_{217}) +$$
$$0.0164\,(1 - T_{277})\,(1 - T_{297}) + (1 - T_{217})]$$

In the formula,

$\varepsilon / \varepsilon_0$-- ratio of full energy peak efficiency between after and before correction;

T_x -- total efficiency of γ-ray at x energy.

The stability of the activity measurement system is very important for this work. So the error of the γ-ray activity measurement is bigger in present work. The uncertainties of the cross sections were shown in table 3.

Table 3 The uncertainties of the cross sections

main source of uncertatinty	^{179}Hf(n,2n)^{178m2}Hf	^{180}Hf(n,2n)^{179m2}Hf
standard cross section	0.9-1.1 %	1.1 %
γ-ray self-absorption	0.5 %	0.5 %
weight and purity of sample	0.5 %	0.5 %
efficiency of γ-ray full energy peak	1.5 %	1.5 %
statistics and area of γ-ray full energy peak	3.0 %	1.0 %
correction of sum peak	6.9 %	
Total	7.7-7.8 %	2.2 %

Table 4 shows the change of the values of the cross section with the measured time of the γ-spectrum. The sample was bombarded on April,14,1989.

Table 4 The values of the cross section (mb)

measured date	Oct.,27,89	Feb.,7,90	Aug.,15,90	Apr.,6,91
495 keV	10.31	8.75	8.13	8.00
574 keV	7.74	8.07	8.13	8.07

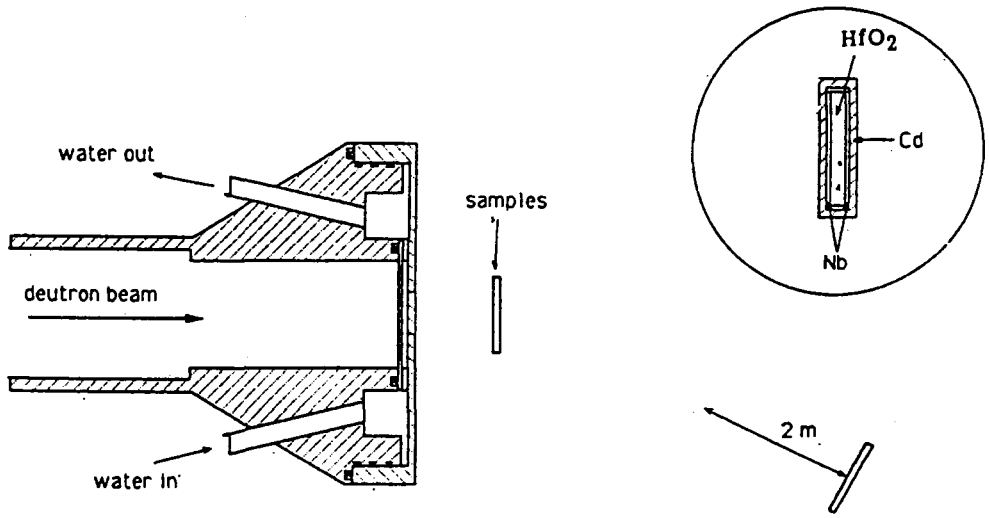

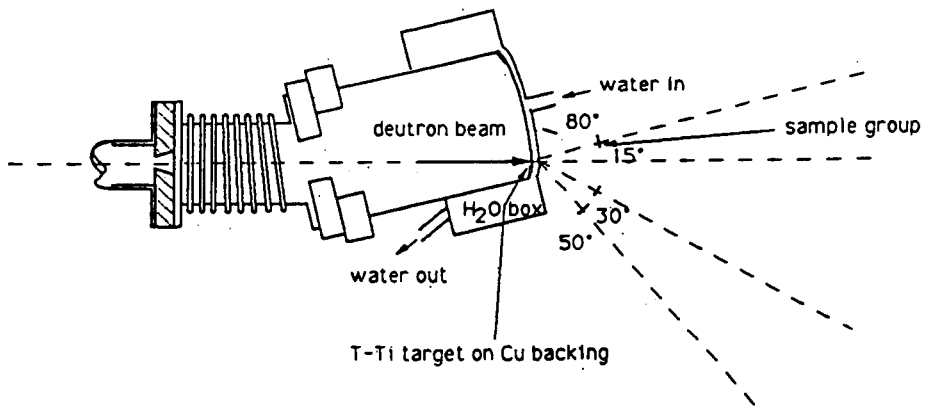

Fig. 1 Fig. 2 The irradiated condition

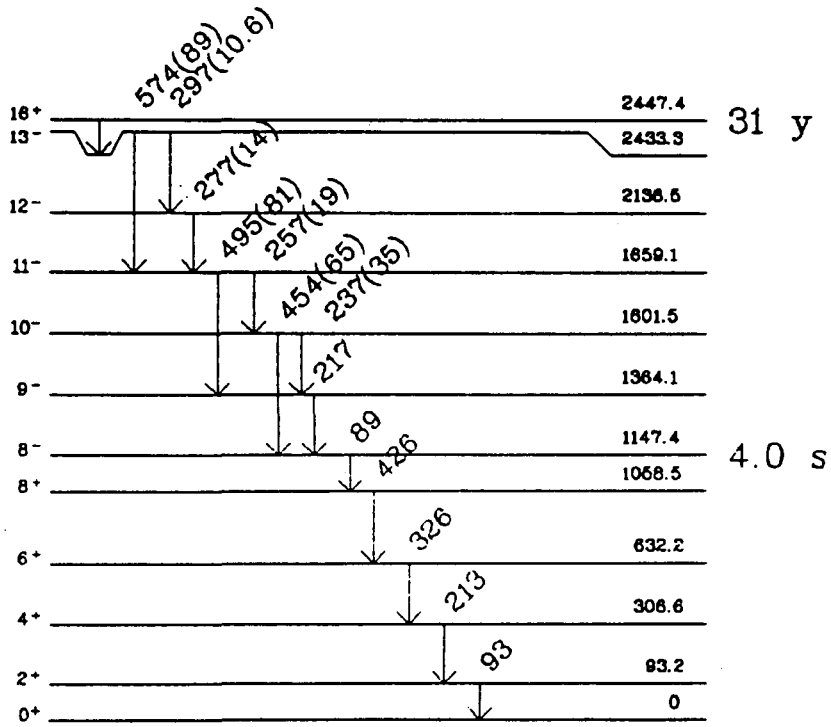

Fig.3 The decay scheme of Hf-178m2

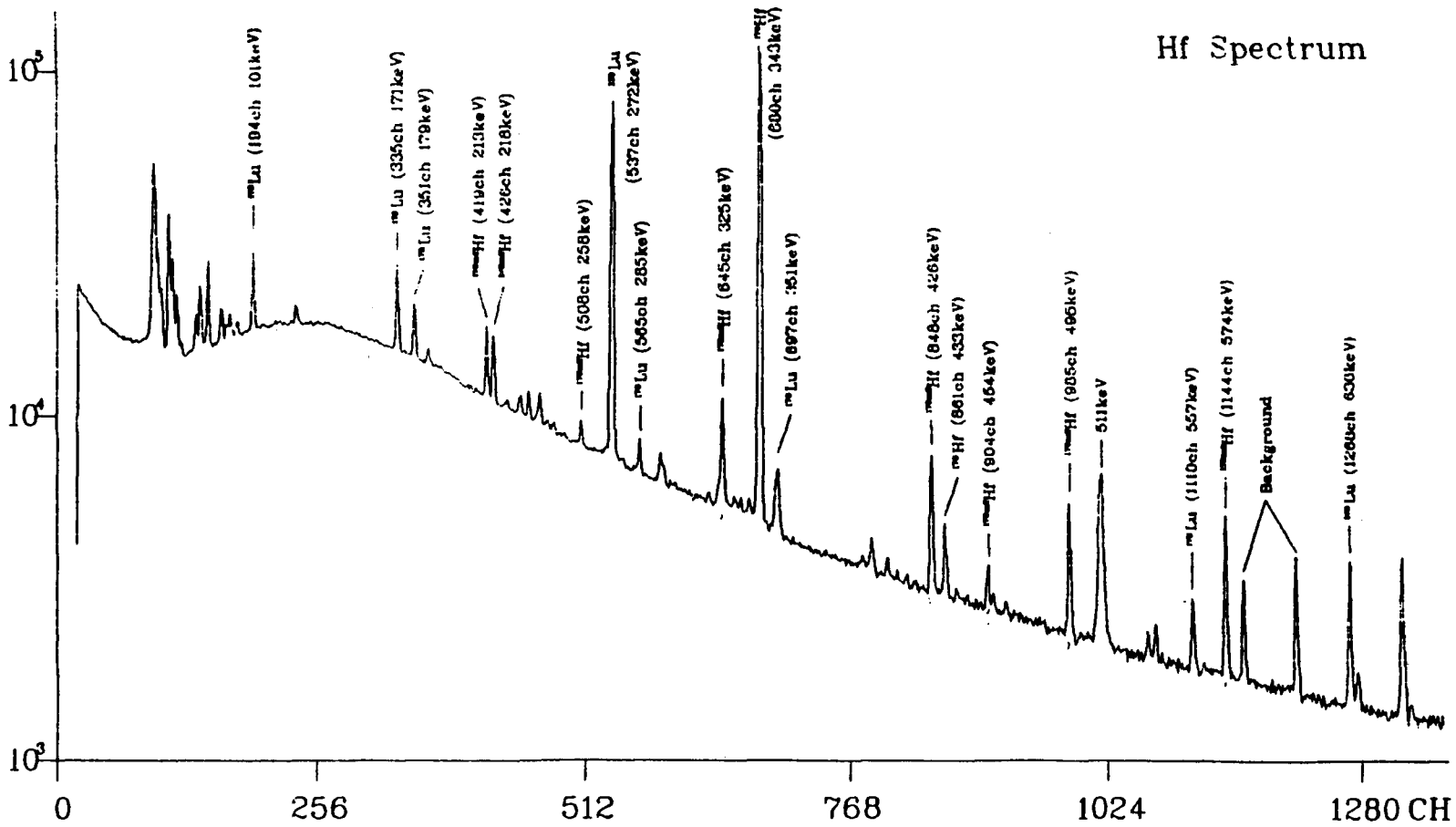

Fig. 4 Hf fiel spectrum taken 2 years after irradiation

From table 4 we know there was interference in 495 keV peak. It is the sum-peak effect of 433 keV γ-ray (1.52%) and two Kx-rays of 61 (15%) and 63 keV (4%) of ^{175}Hf.

The results of this work were shown in table 5 and the Patrick's data[4] published at the Argonne meeting were also listed in the same table.

Table 5 The measured results (mb)

	En (MeV)	^{179}Hf(n,2n)^{178m2}Hf	^{180}Hf(n,2n)^{179m2}Hf	^{93}Nb(n,2n)^{92m}Nb *
Present work	14.19 ± 0.23	7.4 ± 0.6		457.6 ± 4.5
	14.77 ± 0.48	8.0 ± 0.6	25.1 ± 0.5	458.9 ± 5.6
Patrick	15.4 (Exp.)	5.91 ± 0.64	29.5 ± 3.4	
Chadwick[5]	14 (Theo.)	2.9	13.1 * *	

* the standard cross section

* * ^{179}Hf(n,n')+^{180}Hf(n,2n)

Reference

1. Zhao Wenrong, INDC(CPR)-16 1990

2. C.M.Lederer and V.S.Shirley, Table of Isotopes, 7th edition, 1978

3. E.Browne and R.B.Firestone, V.S.Shirley, Table of Radioactive Isotopes, 1986

4. Patrick et al., INDC(NDS)-232 / L

5. M.B.Chadwick and P.G.Young, LA-UR-89-3068, 1989

MEASUREMENT AND ANALYSIS OF $^{165}Ho(n,\gamma)^{166m}Ho$ REACTION CROSS SECTION

Xia Yijun, Wang Chunhao, Long Xianguan, Yang Jingfu
He Fuging, Yang Zhihua, Peng Xiufeng ,Liu Mantian
Luo Xiaobing

Institute of Nuclear Science and Technology,Sichuan University
Chengdu 610064 P. R. China

Lu Hanlin

Institute of Atomic Energy, P. O. Box 275(3), Beijing 102413
P, R. China

Abstract: The cross sections of the $^{165}Ho(n,r)^{166m}Ho$ reaction have been studied in the energy range from 29 to 1100 kev , using Au as a standard. The upper limits of the reaction cross section in the energy region were estimated. The capture cross section of Ho to 1200 y isomeric state has been determined at 676 ± 114 kev neutron energy. The result is 2.92 ± 0.60 mb.

Introduction

Along with the development of fusion research, more capture cross section data for the generation of long-lived radionuclides are needed for estimation of radioactive waste and selection of materials leading to low-level activities. $^{165}Ho(n,r)^{166m}Ho$ reaction is one of the important reactions. Up to now, There were no reliable cross sections for the $^{165}Ho(n,\gamma)^{166m}Ho$ reaction reported in literature.

Experiment

The detailed description of experimental measurement is given in Ref(1). Therefore, only a brief description is given here.

The proton beam collimated to a diameter of < 8 mm was incident on the target producing neutron. The target cooling was achieved by compressed air. The sample of Ho was prepared by pressing 99.9% pure Ho_2O_3 powder into a thin disk. The diameter of Ho and Au samples were 20 mm. The purity of the Au samples were 99.999%.

Two irradiation runs were carried out. In the first run,the samples were sandwiched between two glod foils with thickness o.1mm and were wrapped in 0.3 mm thickness cadmium foils. A group of samples mounted on the surface of Al ring (88 mm daimeter) centered at the neutron source were irradiated simultaneously at 0° , 30° , 60° , 90° , and 120° degrees with respect to the incident proton beam. Therefore neutrons between 29 and 230 KeV were produced by the $^{7}Li(p,n)^{7}Be$ reaction, and 215 and 1100 KeV by the $T(p,n)^{3}He$ reaction. The proton beam currents were generally 8 to 14 μA and the durations of irradiation was 70 hours.

In the second run, the cross section of the $^{165}Ho(n,\gamma)^{166m}Ho$ reaction has been measured at 676±114keV neutron energy. Neutrons were produced via the $T(p,n)^{3}He$ reaction. The protom beam currents were 16 to 20 uA and the durations of irradiation was 110 hours. Ho sample was placed at 0 degree with respect to the incident proton beam. The distance betbetween the samples and target was 10 mm. In this way, the total neutron flux on the sample was 18 times larger than the first run experiment.

In order to detect the induced γ-ray activity of the samples under study and the corresponding gold reference foils , an ORTEC GEM-30195

HPGe detector was used for the γ-ray spectrum mersurement in a low background environment. The energy resolution (FWHM) of the detector was 2.1 kev at the 1332 keV ^{60}Co peak. The photopeak efficiency of the detector system was calibrated with the ^{241}Am, ^{109}Cd, ^{57}Co, ^{54}Mn, ^{65}Zn, ^{152}Eu, ^{60}Co and ^{22}Na standard sources at different source to detector distance. The coincidence sum effect at short source to detector distance was considered.

Analysis and results

The decay parameters of the reaction product in ^{165}Ho(n,γ)^{166m}Ho reaction are given in Table 1.

Table 1. Decay parameters of the produced nuclide in the ^{165}Ho(n,γ)^{166m}Ho reaction

products	Half-life (years)	-ray energy (kev)	absolute intensity (%)
^{166m}Ho	1200	184.4	73.9
		711.7	59.3
		810.3	63.3

The cross section for ^{165}Ho(n,γ)^{166m}Ho reaction can be determined by measurimg the characteristic γ-rays of 184.4, 711.7 and 810.3 keV in the decay of ^{166m}Ho. Because there are two peaks with energies of 185 (^{235}U, ^{226}Ra) and 810.8 (^{58}Co contamination) keV respectively in the background spectrum. In the calculation of the cross sections, γ-rays with energy 711.7 keV was chosen as the characteristic γ-ray for reaction product ^{166m}Ho.

In the first run, the samples were cooled for 2 months after irradiation, then to analyse each samples. The distance of sample to surface of the detector was 1.2mm. The counting time of -ray spectrum was about 153 to 216 hours. however, the net counts corresponding the 711.7kev peak were less than the lower detecting limit of the detector system which presented by the following formula:

$$L_D = 2K\sqrt{2N_b}$$

Where N_b is the background counts correponding the 711.7kev peak, and K is the confidence factor. Thus, we did not detect any characteristic γ-ray of product nuclide ^{166m}Ho in these samples.

Nevertheless,from the lower detect limit we can determing the lower limit of the nuclide ^{166m}Ho activity for the samples by the following formula:

$$A_D = \frac{2.83\ k\sqrt{N_b}}{a \cdot \varepsilon \cdot T_b}$$

Where a is absolute intensity of γ-ray, ε is the detecting efficiency of the γ-ray and T_b is the caunting time. From the lower limit of the nuclide activity for the samples, the upper limits of the reaction cross section were estimated as 68 to 150 mb in the energy range from 29 to 1100 kev.

In the second run, the sample was cooled for 57 days, and the counting time of the γ- ray spectrum was 432 hours. The net counts corresponding 711.7 kev peak was 705. Then the cross section rate relative to that of gold at the neutron energy of 676kev can be determined. The cross section has been converted to absolute cross section using the gold cross section recommended by ENDF/B-VI. The result is 2.92 $\pm$ 0.60 mb.

The main uncertainties came from the statistics of the activity measurement, the glod cross section, the decay scheme, absolute activity determination, various correction etc. The main error are listed in Table 2.

Table 2. Error sources

Error source	Error (%)
Au standard cross section	3.5
Error in decay scheme	4.0
HPGe detector efficiency	< 1.5
Statistics	19.6
Irradiation history	< 2.0
Correction for neutron scattering and attenuation	1.0
background	1.0
Gamma self absorption in the sample	1.0
Weighing error of sample	0.5
Total error	20.5

Note that our result is only preliminary . The further analysis will be considered .

The authors thank the International Atomic Energy Agency and Chinese Nuclear Data Center for encouragment and financail support.

REFERENCES

1. Xia Yijun et al., Measurement and Analysis of $^{98}Mo(n,\gamma)^{99}Mo$ reaction cross section
2. Evaluated Neutron data file for ^{197}Au. ENDF/B-VI, 1990.

Excitation Functions of $^{151}Eu(n,2n)^{150m}Eu$ and $^{159}Tb(n,2n)^{158}Tb$ Reactions

S.M. Qaim[1], F. Cserpák[1,2] and J. Csikai[2]

[1]Institut für Chemie 1 (Nuklearchemie), Forschungszentrum Jülich GmbH, 5170 Jülich, Germany
[2]Institute of Experimental Physics, Kossuth University, 4001 Debrecen, Hungary

Cross sections were measured for the formation of long-lived activation products ^{150m}Eu and ^{158}Tb in (n,2n) reactions on ^{151}Eu and ^{159}Tb, respectively, over the neutron energy range of 8.7 to 10.7 MeV.

About 10 g Tb_4O_7 or 5 g Eu_2O_3 powder (both of purity > 99.99 %) was filled in a polyethylene tube (1.6 cm Ø x 4.3 cm) and Al monitor foils were attached at the front and back of the tube. Irradiations were done in the 0° direction for 10-20 h with quasi-monoenergetic neutrons produced via the $^2H(d,n)^3He$ reaction on a deuterium gas target at the variable energy compact cyclotron CV28 at Jülich.

The average neutron energies and the relative neutron flux density distribution within the sample were calculated. The absolute neutron flux density was obtained by normalization to the $^{27}Al(n,\alpha)^{24}Na$ monitor reaction. The error in neutron flux density was estimated to be ~ 8 %.

The radioactivity of each investigated product was determined via Ge(Li) detector γ-ray spectroscopy about two years after the end of irradiation. Due to the large dimensions of the samples and the inhomogeneous distribution of the activity, counting was done by placing the samples on the detector both horizontally and vertically. A careful calibration of the detector with respect to extended sources allowed the determination of the absolute activity of the product within an error of 10 %.

For calculation of cross sections following decay data were used: ^{150m}Eu ($T_{1/2}$ = 35.8 y; E_γ = 334 keV; I_γ = 94 %), ^{158}Tb ($T_{1/2}$ = 150.3 y; E_γ = 944 keV; I_γ = 43 %). The total errors in cross sections were estimated to be 10-15 %.

The excitation functions of the $^{151}Eu(n,2n)^{150m}Eu$ and $^{159}Tb(n,2n)^{158}Tb$ reactions are shown in Fig. 1. Our data describe the first results near the

thresholds of the two reactions. Around 14 MeV sufficient information existed. The transition from the present low energy data to the available cross section values around 14 MeV appears to be smooth.

A detailed paper dealing with our measurements is in preparation.

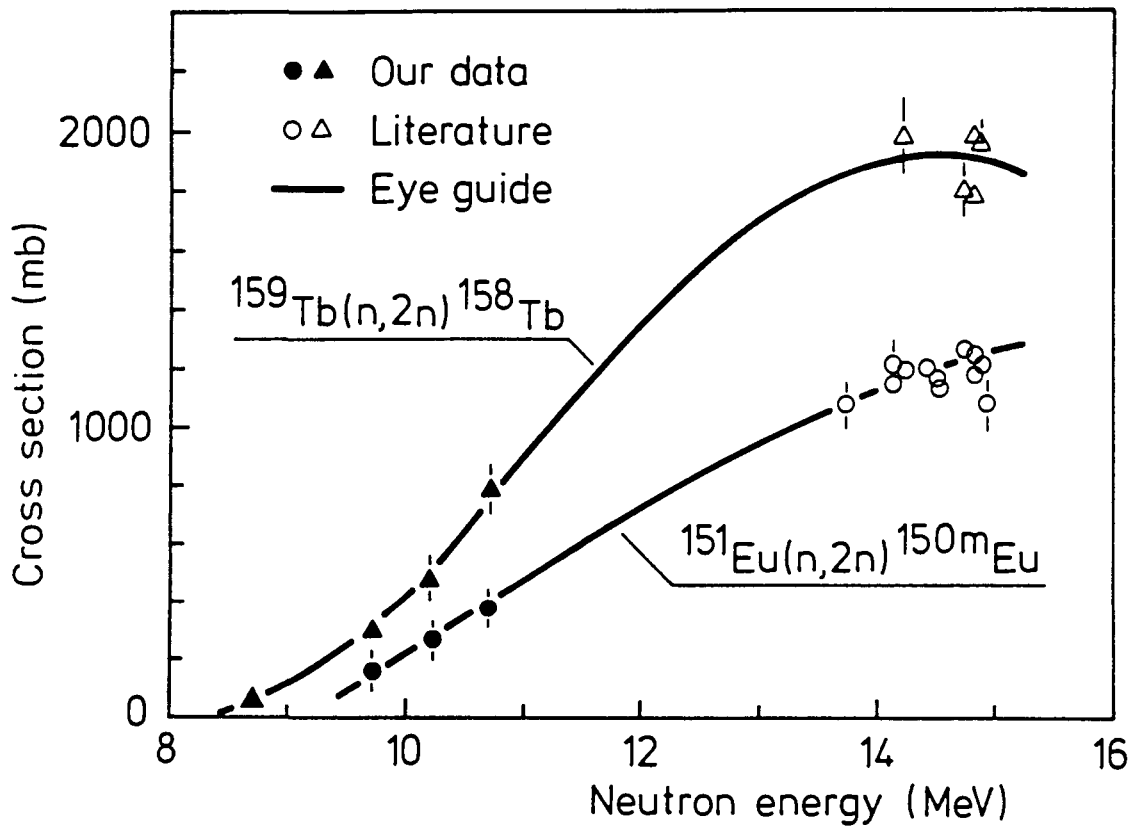

Fig. 1 Excitation functions of $^{151}Eu(n,2n)^{150m}Eu$ and $^{159}Tb(n,2n)^{158}Tb$ reactions measured by the activation technique.

MEASUREMENTS AND CALCULATIONS OF SOME ACTIVATION CROSS SECTIONS FOR GENERATION OF LONG-LIVED RADIONUCLIDES *

J. Csikai

Institute of Experimental Physics, Kossuth University,
Debrecen 4001, Pf. 105, Hungary

Abstract: Activation cross sections have been measured for $^{109}Ag(n,2n)^{108m}Ag$, $^{63}Cu(n,\alpha)^{60}Co$, $^{134}Ba(n,2n)^{133}Ba$, $^{134}Ba(n,p)^{134}Cs$ and $^{137}Ba(n,p)^{137}Cs$ reactions at 14.5 MeV. Excitation functions of $^{58}Ni(n,p)^{58m,g}Co$, $^{115}In(n,2n)^{114m,g}In$ and $^{115}In(n,n')^{115m}In$ dosimetry reactions were also measured in the 2.1 and 14.8 MeV interval. Results were compared with existing data and calculations using the STAPRE and EXIFON codes. Cross section curves were calculated around 14 MeV by the EXIFON code for a number of reactions resulting long-lived ($T_{1/2}$ > 10 y) radionuclides.

1. Introduction

Measurements and calculations of activation cross sections for production of long-lived isotopes at around 14 MeV neutron energy are of primary importance for radioactive waste estimates as well as for testing nuclear reaction models. Cross section data available for such reactions are very scarce and contradictory even in the vicinity of 14 MeV. The excitation functions of the dosimetry reactions require more precise data especially between 5 and 12 MeV. A systematic investigation has been started to complete the experimental data between 2 and 15 MeV and for testing the different reaction model codes.

2. Experimental procedure

High-purity samples were irradiated by the home-made neutron generator of the Institute of Experimental Physics in the 2.15 - 2.94 MeV and 13.44 - 14.84 MeV ranges, at (14.5 ± 0.3) MeV by the KORONA generator of the GKSS, Geesthacht and in the 5.4 - 12.3 MeV interval by the MGC-20 cyclotron of the ATOMKI, Debrecen. The $^{238}U(n,f)$, $^{27}Al(n,\alpha)$, $^{56}Fe(n,p)$ and $^{93}Nb(n,2n)^{92m}Nb$ reactions were used as fluence monitors.

* This work was performed under the "14 MeV Coordinated Research Programme" organized by the International Atomic Energy Agency, Vienna and supported in part by the Hungarian Research Foundation (Contract No. 1734/91).

Background from break up reaction and D-D self-target was taken into account. Details of the irradiation and measuring procedures have been described elsewhere [1,2,3,4,5].

3. Results and discussion

Measured and calculated cross sections obtained in the 13.4 - 15.0 MeV energy range for the reactions resulting long-lived radionuclides are summarized in Table 1. An analysis of the data indicates the followings: a) There are no measured data for a number of reactions. b) The data are consistent for the $^{109}Ag(n,2n)^{108m}Ag$, $^{209}Bi(n,2n)$, $^{40}Ca(n,p)$, $^{63}Cu(n,\alpha)$, $^{39}K(n,\alpha)$, $^{92}Mo(n,p)$ and $^{93}Nb(n,p)$ reactions, while large discrepances exist in the cross sections of the $^{50}Cr(n,p)$, $^{39}K(n,p)$, $^{14}N(n,p)$ and $^{60}Ni(n,2n)$ reactions. c) The simple EXIFON code [6,7,8] gives reasonable results especially for the (n,2n) cross sections around 14 MeV. In some cases (^{139}La, ^{60}Ni, ^{80}Se, ^{51}V) significant changes exist in the (n,2n) cross sections around 14 MeV, therefore, the precise energy determination is indispensable.

Measured, evaluated and calculated data shown in Figs. 1,2 and 3 demonstrate the necessity of more precise cross section measurements.

The excitation functions of $^{63}Cu(n,p)^{63}Ni$ reaction calculated from the thereshold to 18 MeV by the STAPRE and the EXIFON codes deviate significantly from each other (see Fig.4.). A large spread exists also in the measured data available only around 14 MeV. Copper samples have been irradiated in Debrecen at 12 different energies between 5.4 and 12.3 MeV, in addition to the 14.5 MeV point. The activity measurements are in progress at these samples to determine the real shape of the cross section curve of the $^{63}Cu(n,p)^{63}Ni$ reaction.

Further measurements are needed also for the $^{94}Mo(n,p)^{94}Nb$ reaction for testing the cross section curves perdicted by different models (see Fig.5).

Precise cross section curves have been measured for the $^{115}In(n,2n)^{114}In$ and $^{115}In(n,n')^{115m,g}In$ around 14 MeV. Calculated curve using the STAPRE code are in good agreement with the experimental data if the nonelastic cross sections are taken from either the semi-classical optical model [9,10] or the evaluation of the measured values. The measured σ_{NE} data at 14 MeV can be well approximated by the following expression:

$$\lg \sigma_{NE}(b) = -0.68283 + 0.47011 \lg A$$

The general expression for the mass and energy dependence of σ_{NE} is the following:

$$\sigma_{NE}(b) = \left[r_o(A)A^{1/3} + t_o + \lambda\!\!\!^{-}\right]^2 (1-\rho^2)\cdot 10^{-2},$$

where $\lambda\!\!\!^{-} = \dfrac{4.55}{\sqrt{E_n(MeV)}} \cdot \dfrac{(A+1)}{A}$ fm, $t_0 = 0.97 \pm 0.05$ fm and

$$r_0(A) = 1.133 + 0.55\,A^{-2/3} - 5.37A^{-4/3} \text{ fm}.$$

Table 1. Measured and calculated cross sections.

REACTION	$T_{1/2}$	σ(mb) meas. (13.4-15.0 MeV)	σ(mb) calc. (13.4-15.0 MeV) (EXIFON)
$^{109}Ag(n,2n)^{108m}Ag$	418 y	724, 757, 671, 866 ± 66*	-
$^{27}Al(n,2n)^{26}Al$	7.5 10^6 y	0.62	0-75.2
$^{134}Ba(n,2n)^{133}Ba$	10.54 y	1556 ± 95*	-
$^{134}Ba(n,p)^{134}Cs$	2.06 y	6 ± 2*	-
$^{137}Ba(n,p)^{137}Cs$	30 y	5 ± 1*	8.2 - 13.3
$^{209}Bi(n,2n)^{208}Bi$	$3\cdot10^4$y	2197, 2147, 2750, 1800, 2250, 2420, 2520, 2250, 2260	2118.2 - 2159.9
$^{79}Br(n,p)^{79}Se$	$6.5\cdot10^4$y	-	40.7 - 42.8
$^{40}Ca(n,p)^{40}K$	$1.28\cdot10^9$y	470, 492, 471	485 - 456
$^{42}Ca(n,\alpha)^{39}Ar$	269y	90	138.1 - 147.9
$^{63}Cu(n,p)^{63}Ni$	100y	54	78.4 - 87.4
$^{63}Cu(n,\alpha)^{60}Co$	5.27y	51, 45 ± 2*	61.4 - 73
$^{50}Cr(n,p)^{50}V$	$0.25\cdot10^{14}$y	830, 357	521.6 - 496.4
$^{113}In(n,p)^{113}Cd$	$9\cdot10^{15}$y 14.6 y	-	9.1 - 12.1
$^{39}K(n,p)^{39}Ar$	269y	195, 162, 314, 354	108.9 - 114.3
$^{39}K(n,\alpha)^{36}Cl$	$3\cdot10^5$y	110, 120, 109	310.4 - 308.5
$^{139}La(n,2n)^{138}La$	$1.1\cdot10^{11}$y	-	1496.7 - 1700.2
$^{92}Mo(n,p)^{92}Nb$	$1.7\cdot10^8$y	60, 64	197 - 206.4
$^{94}Mo(n,p)^{94}Nb$	$2\cdot10^4$y	55	45.8 - 55.7
$^{14}N(n,p)^{15}C$	5736y	77, 38	18.9 - 24.4
$^{93}Nb(n,p)^{93}Zr$	$1.5\cdot10^6$y	51, 42	23 - 30
$^{60}Ni(n,2n)^{59}Ni$	$7.5\cdot10^4$y	325, 391, 104	246.3 - 557.5
$^{64}Ni(n,2n)^{63}Ni$	125y	958	916 - 1120.2
$^{17}O(n,\alpha)^{14}C$	5736y	-	154.4 - 155.4
$^{141}Pr(n,\alpha)^{138}La$	$1.3\cdot10^{11}$y	3, 3	0.6 - 1.1
$^{80}Se(n,2n)^{79}Se$	$7\cdot10^4$y	-	855 - 1133,9
$^{116}Sn(n,\alpha)^{113}Cd$	$9\cdot10^{15}$y 14.6 y	-	2.2 - 4.4
$^{99}Tc(n,2n)^{98}Tc$	$1.5\cdot10^6$y	1227	1231.5 - 1368.3
$^{51}V(n,2n)^{50}V$	$4.8\cdot10^{14}$y	-	388.9 - 751.4
$^{180}W(n,p)^{180}Ta$	$2\cdot10^{13}$y	1	5.6 - 6.7
$^{66}Zn(n,\alpha)^{63}Ni$	100y	-	18.4 - 27.7
$^{93}Zr(n,\alpha)^{90}Sr$	29y	-	12 - 13.1
$^{94}Zr(n,2n)^{93}Zr$	$9\cdot10^5$y	-	1459.3 - 15O1.8

*Present experiment

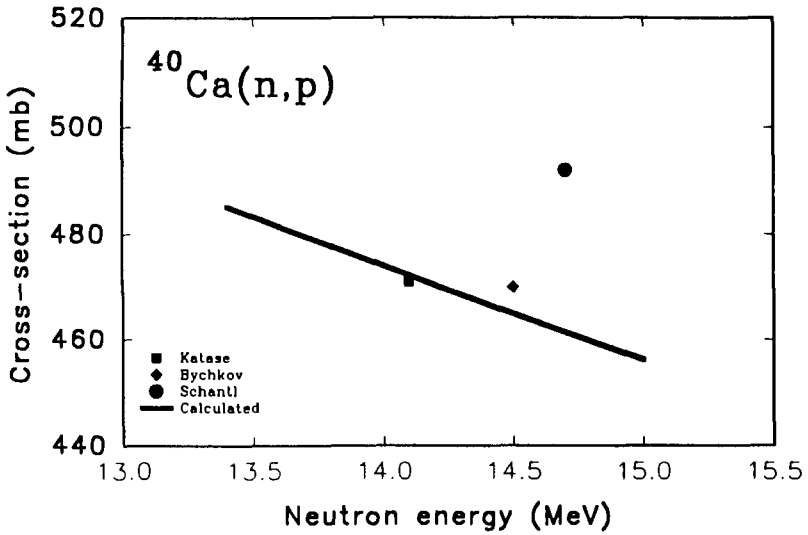

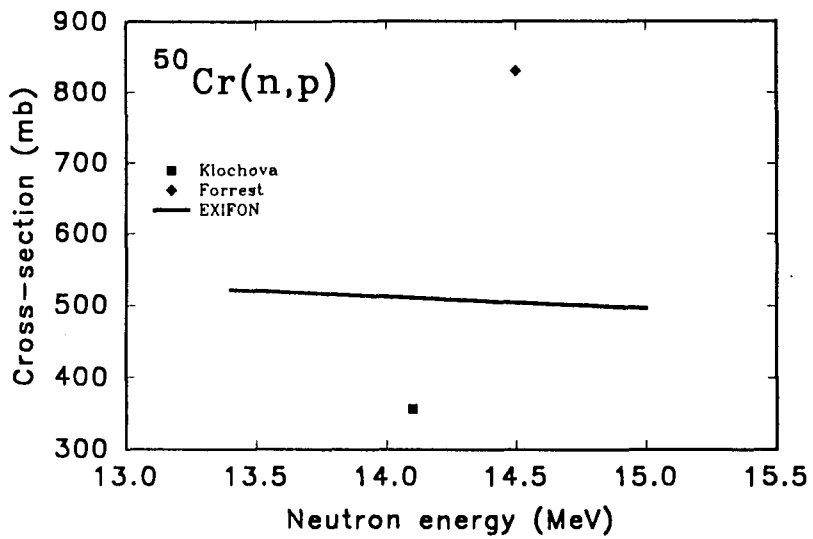

Fig. 1. Excitation functions of $^{40}Ca(n,p)^{40}K$ and $^{50}Cr(n,p)^{50}V$ reactions.

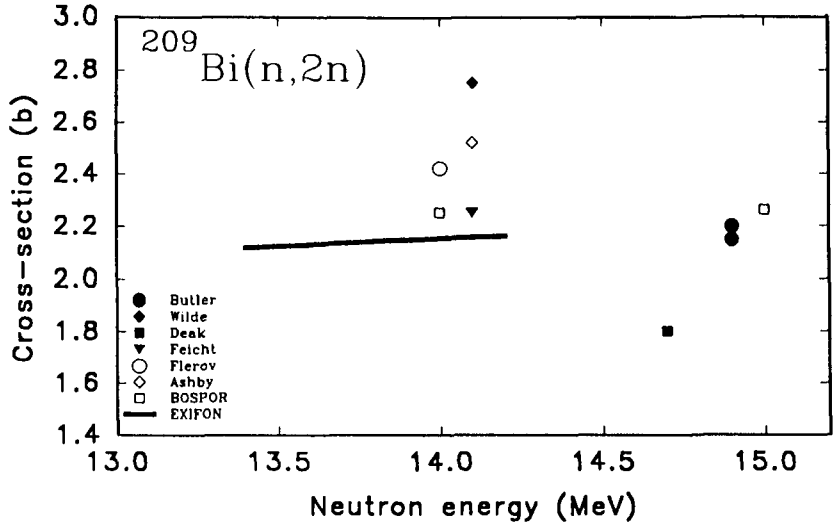

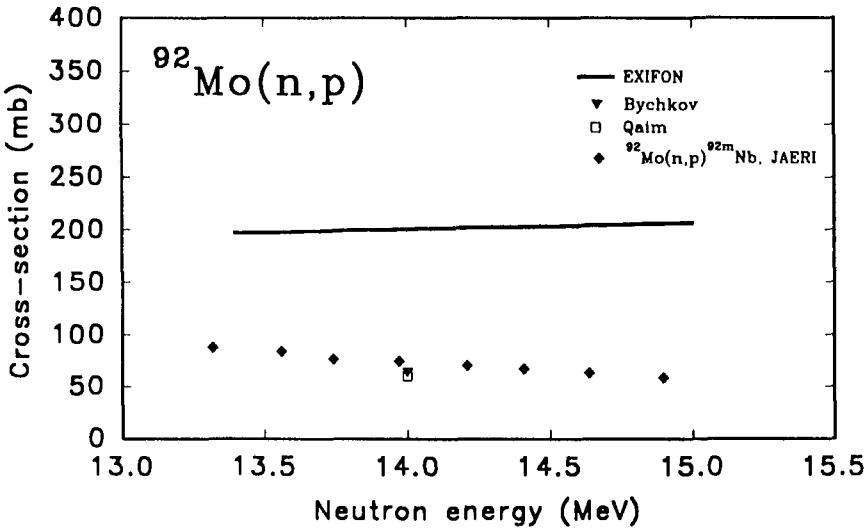

Fig.2. Excitation functions of $^{209}Bi(n,2n)^{208}B$ and $^{92}Mo(n,p)^{92}Nb$ reactions.

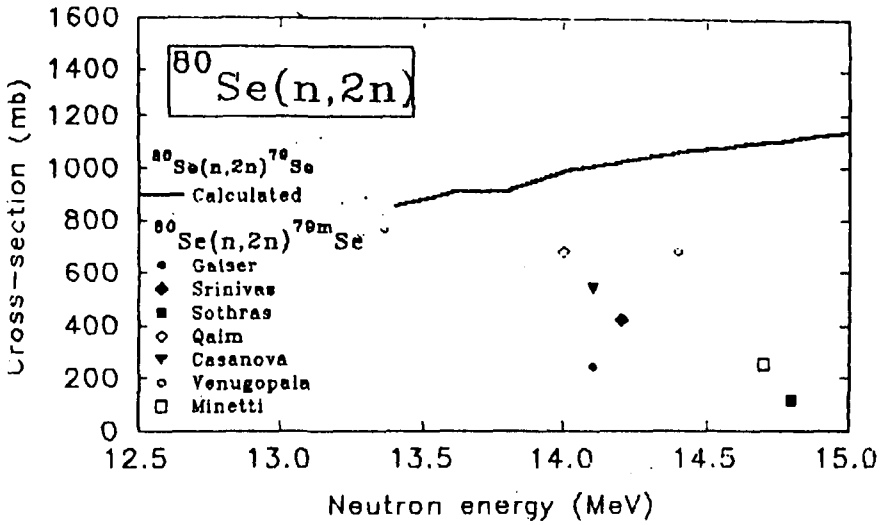

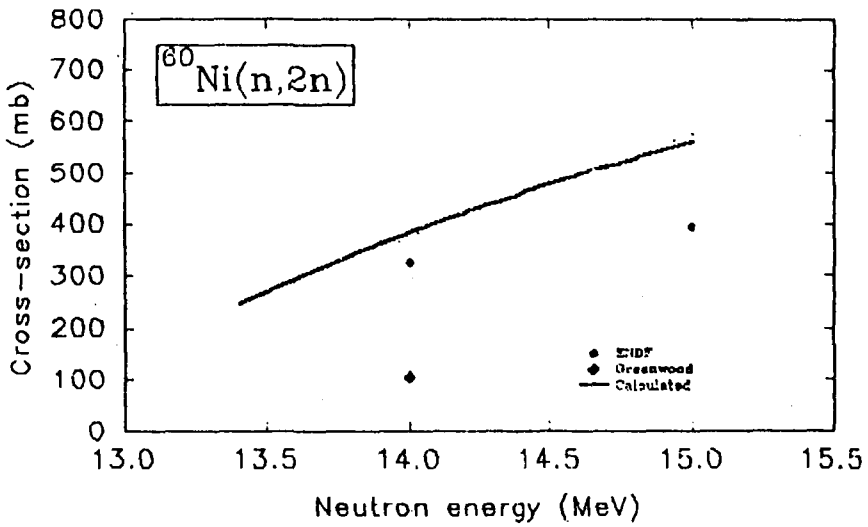

Fig.3. Excitation functions of $^{80}Se(n,2n)^{79}Se$ and $^{60}Ni(n,2n)^{59}Ni$ reactions.

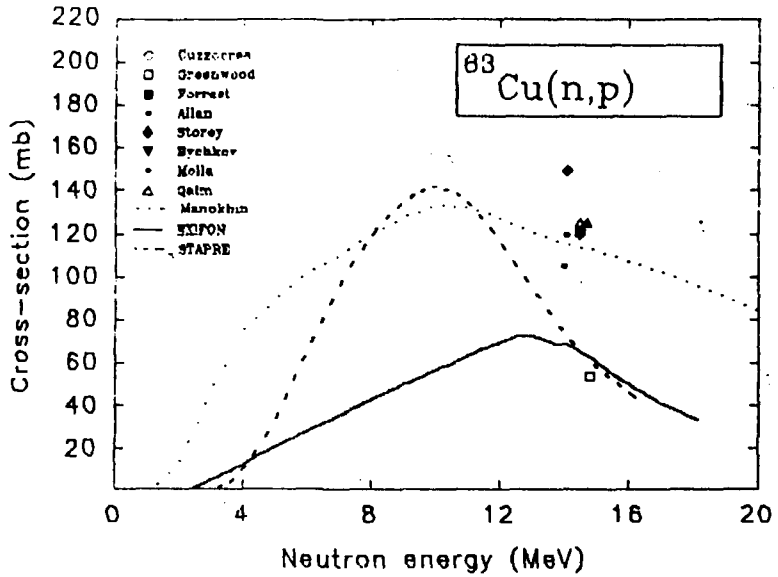

Fig.4. Excitation function of $^{63}Cu(n,p)^{63}Ni$ reaction.

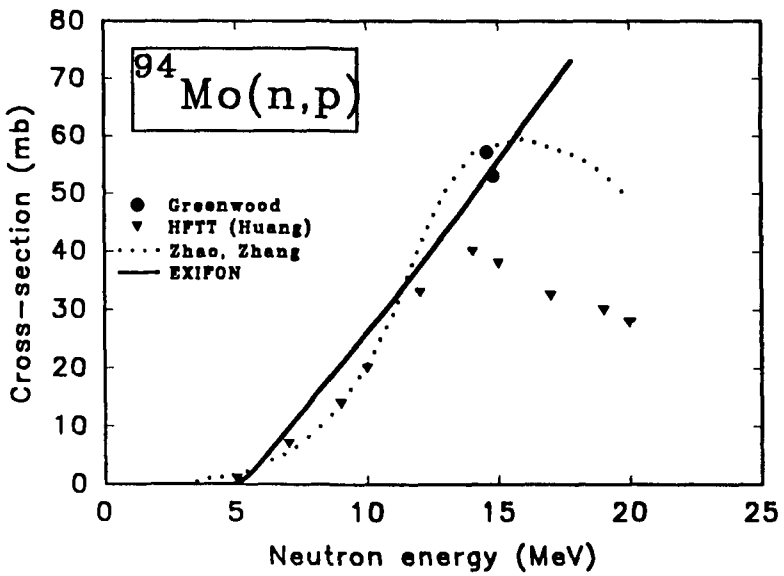

Fig. 5. Excitation function of $^{94}Mo(n,p)^{94}Nb$ reaction.

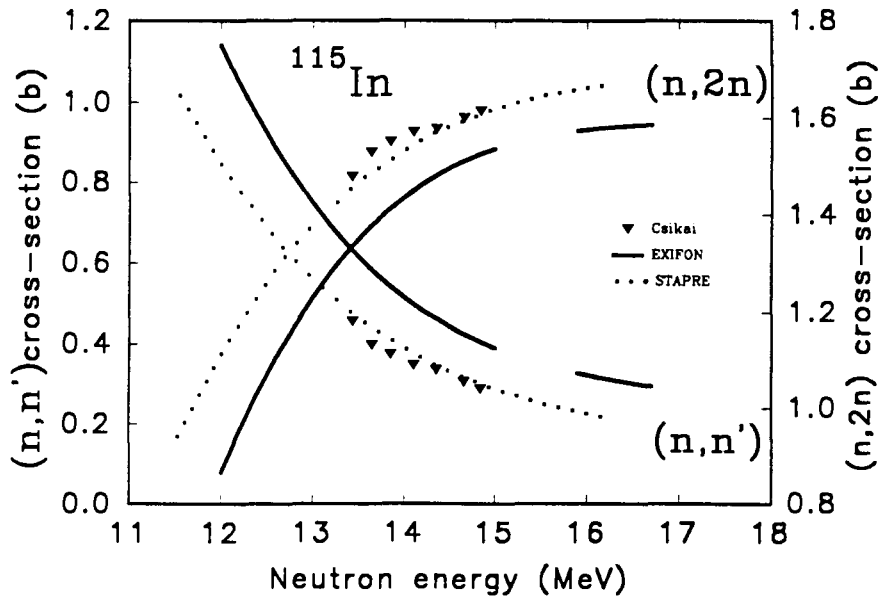

Fig.6. Excitation functions of $^{115}In(n,n')^{115}In$ and $^{115}In(n,2n)^{114}In$ reactions.

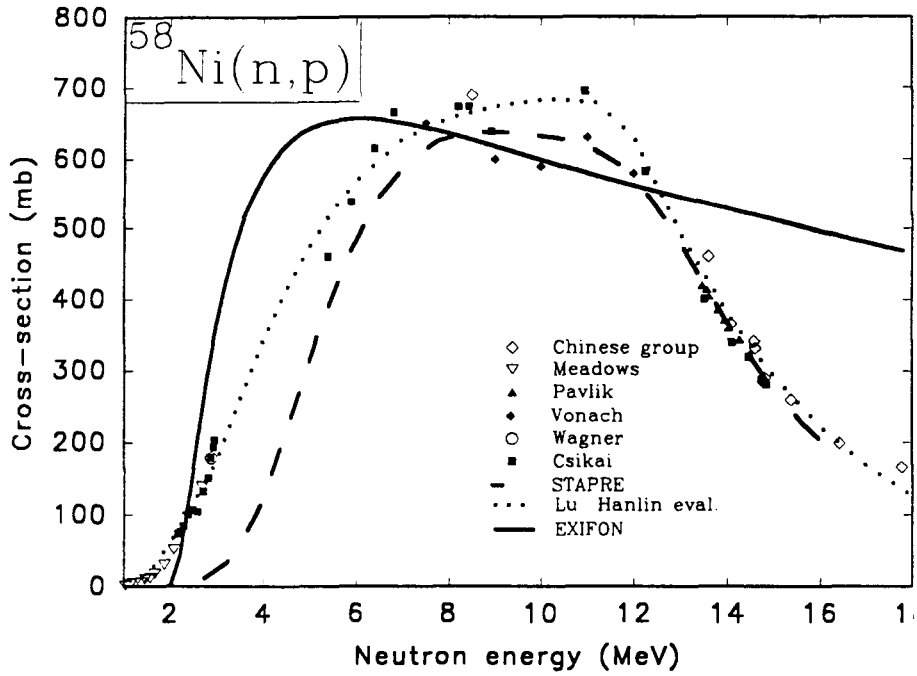

Fig.7. Excitation function of $^{58}Ni(n,p)^{58}Co$ reaction.

The shapes of the (n,n') and (n,2n) excitation functions obtained by the EXIFON code agree with the STAPRE calculations (see. Fig.6). The deviations are caused the differences in the accepted nonelastic cross sections. The $\sigma^{g}_{n,n'}$ values were deduced from the σ_{NE}-$\sum\sigma_{n,i}$ data.

Recent experimental data obtained in Debrecen for the $^{58}Ni(n,p)^{58}Co$ reaction between 2.15 and 14.84 MeV prove the conclusion of the Chinese group [11]. As it can be seen in Fig. 7 neither the STAPRE nor the EXIFON can give a good approximation for the description of the evaluated excitation function.

REFERENCES

[1] J. Csikai, Cs.M.Buczkó, R.Pepelnik and H.M.Agrawal, Ann.nucl.Energy 18 (1991) 1.

[2] M.Wagner, G.Winkler, H.Vonach, Cs.M.Buczkó and J. Csikai, INDC(NDS)-232/L, IAEA Vienna (1990) p.17.

[3] J.Csikai, Zs.Lantos, Cs.M.Buczkó and S.Sudár, Z. f. Phys. A - Atomic Nuclei 337 (1990) 39.

[4] P.Raics, S.Nagy, S.Szegedi, N.V.Kornilov and A.B.Kagalenko, in Proc. Int. Conf. on Nuclear Data for Science and Technology, 13-17 May 1991, Jülich (in press).

[5] M.Wagner, G.Winkler, H.Vonach and G.Pető, Ann.nucl.Energy 15 (1988) 363

[6] H.Kalka, M.Torjman and D.Seeliger, Phys. Rev. C40 (1989) 1619.

[7] H.Kalka, M.Torjman, H.N.Lien, R.Lopez and D.Seeliger, Z. f. Phys. A335 (1990) 163.

[8] H.Kalka, Int. Conf. on Nuclear Data for Science and Technology, 13-17 May 1991, Jülich, Book of Abstracts, p. 96.

[9] I.Angeli, J.Csikai and P.Nagy, Nucl.Sci.Eng. 55 (1974) 418.

[10] J.Csikai, Nucl.Instrm. Meth. A280 (1989) 233.

[11] Zhao Wenrong, Lu Hanlin, Yu Weixiang and Yuan Xialin, INDC(CPR)-16, IAEA, Vienna (1989).

Measurements of Long-Lived Activation Cross Sections at 14.7 MeV in the Inter-Laboratory Collaboration with ANL/LANL/JAERI

Yujiro Ikeda, Chikara Konno and Donald L. Smith*
Japan Atomic Energy Research Institute
*Argonne National Laboratory

Abstract : Six long-live activation cross sections at 14.7 MeV have been measured by using the FNS facility in order to provide experimental data meeting the requirement in the radioactive wastes disposal assessment in the D-T fusion reactor. The measurements were conducted under an inter-laboratory collaboration with ANL/LANL/JAERI. Measured data were compared with data available in the literature and discussed in terms of accuracy needed for the requirement.

1. Introduction

An endeavor to arrive at sufficient accuracy in the nuclear data for long-lived activation cross section have been initiated a few years ago as the IAEA-CRP1) to satiety the nuclear data needs from radioactivity waste disposal assessment. Since at the time, significant effects have been devoted on the experimental measurement, the theoretical prediction and the evaluation. An experimental program as an inter-laboratory collaboration[2] was proposed by Dr. D. L. Smith at ANL under a support by the IAEA-CRP, which included different neutron sources, d-Be at ANL[3], T-p at LANL[4] and D-t at FNS, JAERI[5]. In this collaboration, it was expected that cross sections of concerned cover the neutron energy range from several MeV to 14 MeV. ANL was responsible to deliver the sample package to other facilities and to measure the activities after irradiation. The measurement of cross sections at 14 MeV was carried out at FNS, JAERI as a part of this collaboration : the package with an identical set of samples were irradiated along with the other package which had been sent to back to ANL for counting there.

This report describes the experiments at FNS in some detail and gives results so far of some cross sections at 14 MeV, reactions of which include $^{63}Cu(n,\alpha)^{60}C$ o, $^{109}Ag(n,2n)^{108m}Ag$, $^{151}Eu(n,2n)^{150m}Eu$, $^{153}Eu(n,2n)^{152m}Eu$, $^{159}Tb(n,2n)^{158m}Tb$ and $^{179}Hf(n,2n)^{178m2}Hf$.

2. Experiment

2.1 Long-lived activity production reactions invesigated

The reactions, half-lives of products, natural abundances, γ-ray - branching ratios, atomic mass are given in Table 1. Decay data were taken from the Table of Isotopes.[6] The long-lived radioactivities with half-lives from 5 to 150 years were concerned in this experiments. And also the radioactivities which associate the γ-ray emission were the objects in this measurements. The other β-emitter or 63Ni and 49V are subjected in the future task.

Table 1 Objecttive Reactions and Associated Decay Data of Products

Reaction	Half-Life (year)	Abundance (%)	γ-ray Energy (keV)	γ-ray Branching (%)
$^{63}Cu(n,\alpha)^{60m+g}Co$	5.271± 0.001	69.17±0.02	1332.50	99.9824
$^{109}Ag(n,2n)^{108m}Ag$	127±21	48.161±0.005	433.93	90.5±0.6
$^{151}Eu(n,2n)^{150m}Eu$	35.8±1.0	47.8±0.5	333.93	94±2
$^{153}Eu(n,2n)^{152m2+g}Eu$	13.33±0.04	52.2±0.5	344.3	26.6±0.5
$^{159}Tb(n,2n)^{158m+g}Tb$	150±30	100	944.2	43±2
$^{179}Hf(n,2n)^{178m2}Hf$	31±1	13.629±0.005	325.56	94.1±0.3

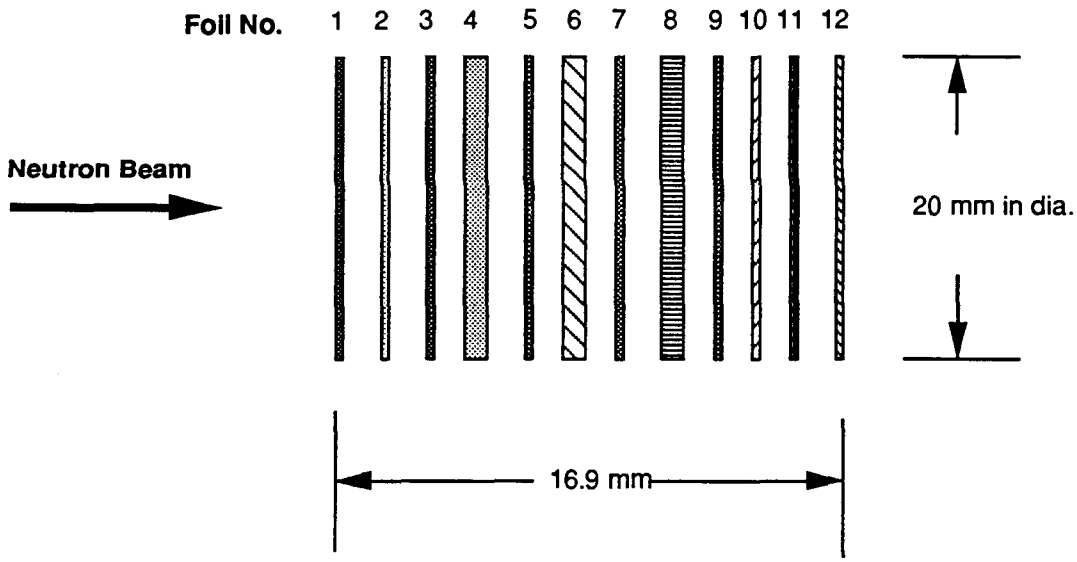

No.	Foil Name	Thickness(mm)	Weight(gram)
1	Ni-1	0.2541	1.132
2	Ag	0.5083	2.742
3	Ni-2	0.2541	1.142
4	HfO2	4.7015	2.879
5	Ni-3	0.2541	1.145
6	Tb4O7	4.7015	2.498
7	Ni-4	0.2541	1.143
8	Eu2O3	4.7015	1.223
9	Ni-5	0.2541	1.136
10	Cu	0.2541	1.163
11	Fe	0.5083	1.910
12	Ti	0.2541	0.545

Fig. 1 Sample arrangement and their weight

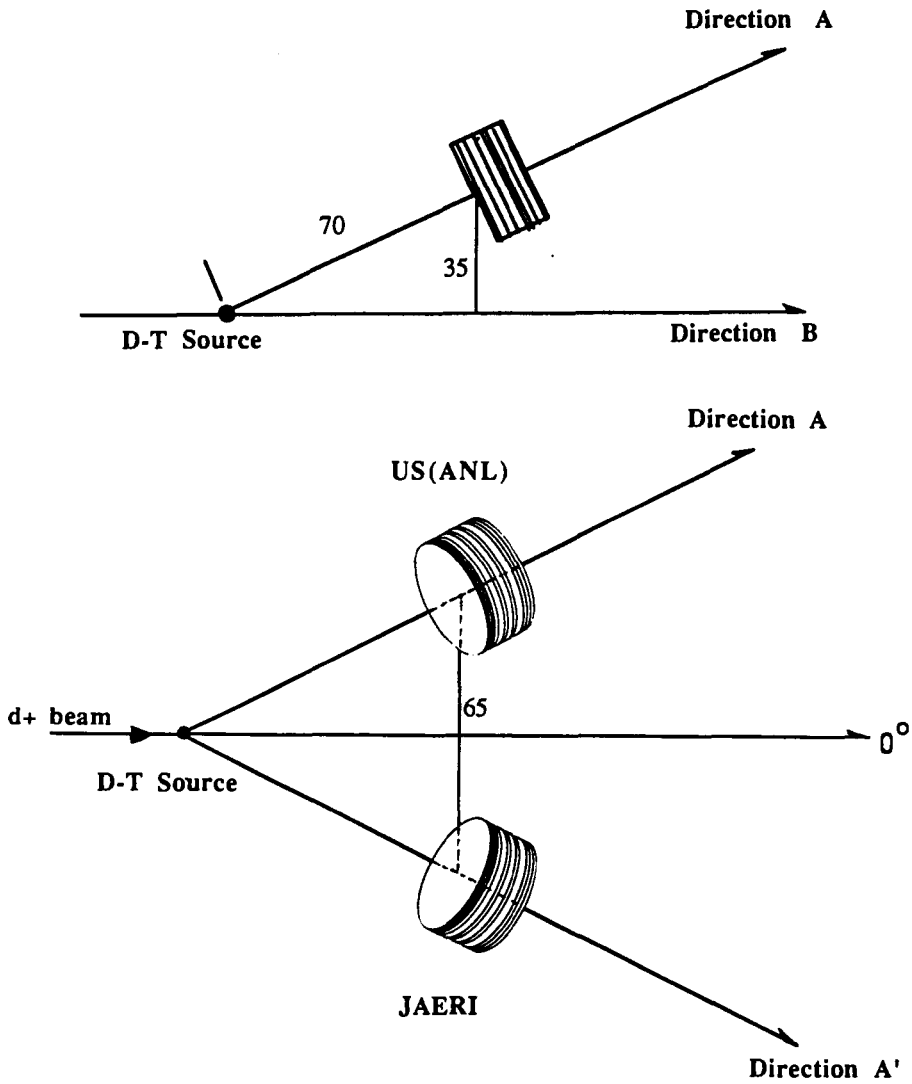

Fig. 2 Schematic irradiation configuration

2.2 Irradiation configuration

The two sample packages for the inter-laboratory collaboration with ANL/LANL/FNS-JAERI were placed at identical positions of 7 cm distances from D-T source. A schematic sample configuration is shown in Fig. 2. Samples were irradiated with 14 MeV neutrons for 4 days (8 hours irradiation per a day). It resulted in 1.73×10^{17} neutrons of total neutron yield at the DT target. The irradiation history is given in Fig. 3. The nominal fluence on the irradiated sample was about 2×10^{14} n/cm2. This fluence was much less than that expected because of poor tritium target performance. Neutron fluence in the sample package was monitor by some dosimetry foils of Ni reaction, $^{58}Ni(n,p)^{58}Co$ ($T_{1/2}$=70.8d). However, this reaction has rather low threshold energy around 1.0 MeV so that large contribution of low energy neutrons to the total reaction rate seemed very significant. In such a case, well defined neutron spectrum should be known to correct that low energy contribution. For this purpose, analytical calculation of the spectrum was separately carried out. In order to assure the neutron fluence determination with Ni foil, Nb foils were attached on both front and rear surfaces of the package. Since cross

Table 2 Neutron flux monitor

Sample Name	Neutron Flux(/sec/cm^2) $^{58}Ni(n,p)^{58m+g}Co$ *	$^{93}Nb(n,2n)^{92m}Nb$ **	Ratio
Ag	7.127E+8	7.22E+8	1.030
Hf	6.775E+8	6.69E+8	1.057
Tb	5.967E+8	5.77E+8	1.080
Eu	5.119E+8	4.87E+8	1.097
Cu	4.985E+8	4.78E+8	1.043

* Low energy contributions to the reaction rates ranged 8 to 10 %, depending on sample positions. The cross section of 292±7 mb was assumed for this reaction. Uncertainties of the reaction rates were within ± 5 %.

** The data were deduced by interpolating data at front and rear surface of the sample package. The cross section of 455±7 mb was assumed for this reaction.

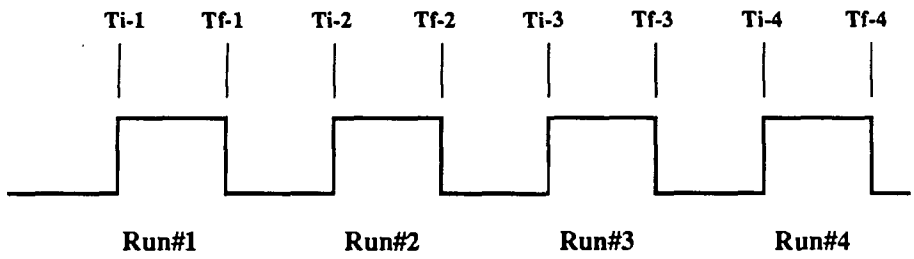

Run#	Ti	Tf	dT	Neutron Yield
	(June 20, 1989)			
Run#1	10:54	18:54	8 h	3.627E+16
	(June 21, 1989)			
Run#2	9:50	17:50	8 h	3.730E+16
	(June 22, 1989)			
Run#3	9:40	17:41	8 h 1m	3.119E+16
	(June 23, 1989)			
Run#4	9:44	17:55	8 h 11m	2.621E+16
			Total Yn:	1.310E+17

Fig. 3 Irradiation history

section of $^{93}Nb(n,2n)^{92m}Nb$ has threshold energy around 10 MeV, quite accurate flux of 14 MeV was derived. The results of neutron flux derived from the both nethod are shown in Table 2. In the present data processing, the values taken by Ni(n,p) reaction were adopted.

2.3 Gamma-ray counting

More than 2 years after irradiation, γ-ray counting has started by using a high detection efficiency Ge detector[EG&G ORTEC] (115 % relative to 3N × 3N NaI(Tl)). Gamma-ray spectrum was analysed by GENIE code system provided by CANBERRA. The detector efficiency was calibrated by standard γ-ray sources. The uncertainty of data for efficiency is about 2 % at present moment although it was very tentative one. The data associated with g-ray counting are given in Table 3.

Table 3 Data of gamma-ray measurement

Reaction	γ-ray counts(*)	Efficiency	Cooling time	Collection time	Reaction rate
$^{63}Cu(n,\alpha)^{60m+g}Co$	45,773(0.5)	1.098E-2	7.0558456E+7	3.2183E+4	1.360E-16( )
$^{109}Ag(n,2n)^{108m}Ag$	30,164(0.9)	2.165E-2	6.9779504E+7	3.1550E+4	1.912E-17( )
$^{151}Eu(n,2n)^{150m+g}Eu$	52,646(0.5)	2.508E-2	6.9542568E+7	1.1189E+4	5.962E-16( )
$^{153}Eu(n,2n)^{152m}Eu$	69,422(0.4)	2.465E-2	6.9542568E+7	1.1189E+4	1.0044E-15( )
$^{159}Tb(n,2n)^{158m}Tb$	64,568(0.4)	1.326E-2	6.9953440E+7	3.3483E+4	1.0189E-15( )
$^{179}Hf(n,2n)^{178m2}Hf$	5,438(5.8)	2.540E-2	7.0224784E+7	2.47319E+5	4.27E-18( )

3. Results

From Summary peak counts, reaction rates of concern were derived with necessary corrections, e. g. decay constant, cooling time, collection time, detector efficiency, natural abundance of the target material, γ -ray branching ratio, sample weight, self-absorption of γ -ray, neutron flux fluctuation during irradiation, and so forth. In Table 4, experimental errors are sammaraized.

The cross section were obtained from the reaction rates divided by neutron flux determined by $^{58}Ni(n,p)^{58}Co$ reaction rate. In Table 5. present data are summarized along with data available.

3.1 63Cu(n,a)60Co

3.2 $^{109}Ag(n,2n)^{108m}Ag$

No experimental data for the cross $^{109}Ag(n,2n)^{108m}Ag$ (T1/2=127y) has been reported before IAEA-CRP report. In the IAEA-CRP report three experiments and one evaluation have

Table 4 Experimental Error

Items	Range of % Error
Statistics	0.4 - 6
Efficiency	2.0
Sample Weight	< 0.1
Decay Constant	0.2 - 20
γ-ray Branching	0.1 - 4
Sum-Peak Correction	0 - 1.5
γ-ray Self-Absoption	0.1 - 0.5
Low-Energy Neutron	Not Considered
Flux Monitor : (^{58}Ni(n,p)$^{58m+g}$Co)	
Cross section	2.5 [291±7 mb at 14.7MeV]
Reaction Rate	3.0*
Total	4.4 - 21
	(4.4 - 8.6)**

* Including correction for low energy neutron contribution.
** When error due to decay constant is excluded.

been given ; 230 ± 7 mb at 14.77 by IAE Beijing, 263 ± 20 mb by Debrecen and 208 ± 37 mb by KRI Leningrard ; 665 ± 73 mb by IRK vienna.

As long as the half-live of 127 ± 21 years is used, the present experiment gives cross section of 191 ± 14 mb. This value is very close to the other experimental values,whereas it is three times as much as smaller them that of evaluation by IRK. This large difference between experimental data and the evaluation should be attributed to the wrong half-live data for the deduction of experimental data.

3.3 ^{151}Eu(n,2n)^{150m}Eu

The reaction of ^{151}Eu(n,2n) produces. Two isomers of 150Eu with half-lives of 35.8 years and 12.6 hours. From the decay schem of ^{150}Eu, there is no isomeric transition so that activities are treated as independent reaction products. In this study, we to used on the cross section of production for 150Eu with 35.8y half-live.

Only two cross section data has been reported previonsely by Qaim 8) and Nethaway 9). They gave cross sections of 1,270 ± 149 b and 1,180 ± 150 b at 14.7 and 14.8 MeV, respectively. Recent summary of IAEA-CRP showed available in the report 1); 1,209 ± 28 at 14.77 MeV measured by IEA Beijing, 1,090 ± 84 at 14.9 MeV by KRI Leningrard. These data showed somewhat cowerfgency around 1,200 barns.

The present data of 1,162 ± 66 mb at 14.7 MeV gives a good agreement with those reported within experimental errors. Meanwhile we have carried out the measurement using separated isotopes (enriched 151Eu samples) before. This measurement gave cross sections rauging from

Table 5 Cross Sections Measured

Reaction	Present Work at 14.7 ± 3 MeV (mb)	References E_n(MeV)	Cross Section(mb)	
$^{63}Cu(n,\alpha)^{60m+g}Co$	40.0±1.6	14.8	40.1±1.2	7)
		14.8	40.4±2.3	11)
		14.5	43.8±2.5	11)
$^{109}Ag(n,2n)^{108m}Ag$	191±14	14.77	230±7	*-1)
		14.56	263±20	*-2)
		14 - 15	665±73	*-3)
		14.9	208±37	*-4)
		14.8	212±11	11)
$^{151}Eu(n,2n)^{150m}Eu$	1162±66	14.77	1219±28	*-1)
		14 - 15	1325±94	*-3)
		14.9	1090±84	*-4)
		14.7	1270±149	8)
		14.8	1180±150	9)
		14.8	1276±64	11)
		14.5	1170± 59	11)
		14.1	1215±53	11)
$^{153}Eu(n,2n)^{152m+g}Eu$	1970±95	14.77	1544±42	*-1)
		14 - 15	1442±60	*-3)
		14.9	1740±145	*-4)
		14.7	1542±138	8)
		14.8	1659±83	11)
		14.5	1533±77	11)
		14.1	1326±75	11)
$^{159}Tb(n,2n)^{158m+g}Tb$	1708±85	14.77	1968±56	*-1)
		14 - 15	1930±49	*-3)
		14.7	1801	8)
		14.8	1930	10)
		14.8	1775±88	11)
$^{179}Hf(n,2n)^{178m2}Hf$	6.3±0.5	14.8	5.9±0.6	*-5)
		14	2.9	*-6)
		14.8	6.3±0.6	11)

* Measurement, evaluation or calculation performed for IAEA-CRP:

*-1); IAE Beijing
*-2); Debrecen
*-3); IRK, Vienna
*-4); KRI Leningrad
*-5); Harwell
*-6); Oxford/LANL

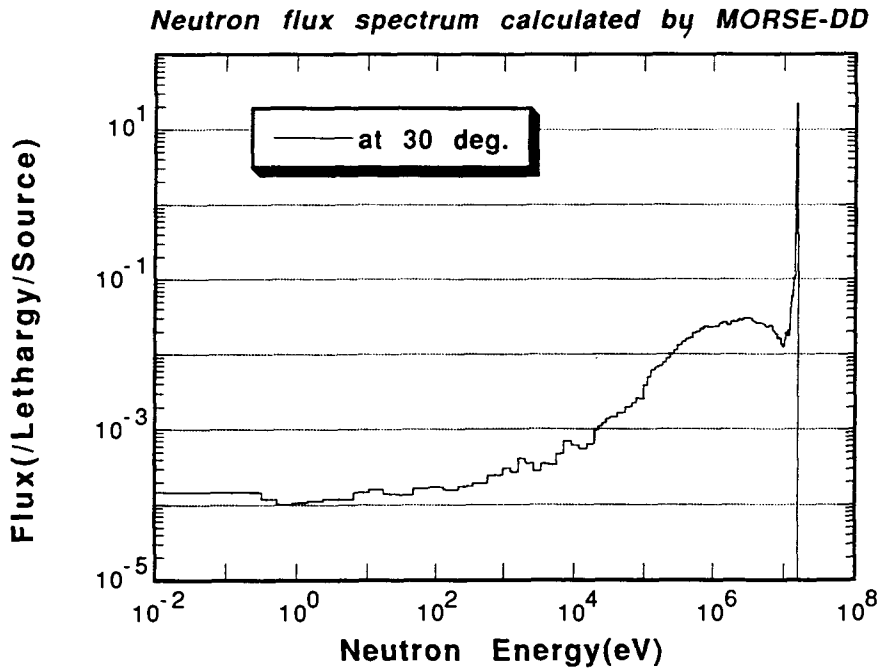

Fig. 4 Incident neutron energy spectrum

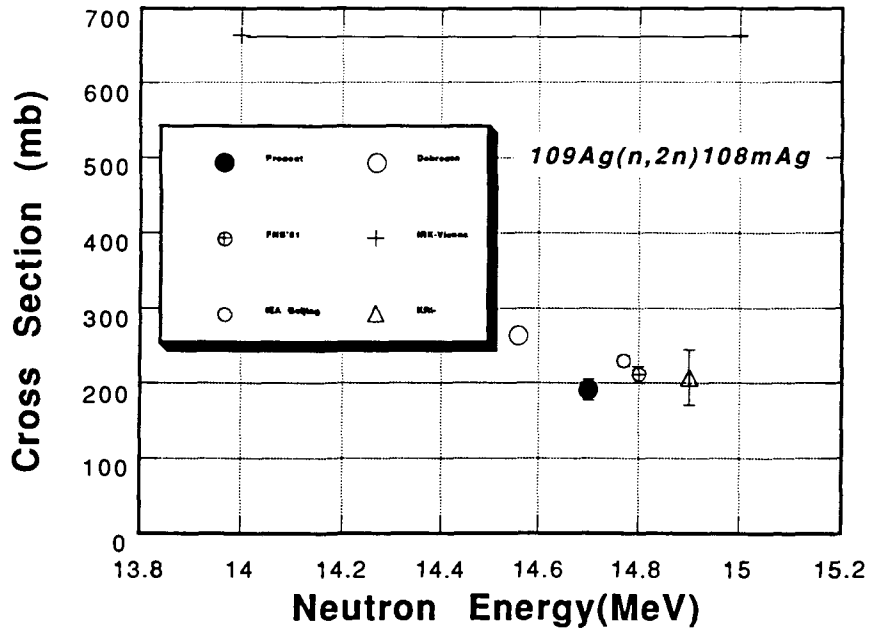

Fig. 5.1 Cross section of 109Ag(n,2n)108mAg

1,034 to 1,130 mb at the energies 13.5 to 14.9 MeV. Both experimental data are in quite good agreements each, although the sample configuration, neutron field and Ge detectors used were different.

Thus, we may conclude that the this reaction cross section data 14 - 15 MeV could be convergented in early time. One thing should be mentioned is that the IRK evaluation seems a little bit higher than those measured. Howere, if they evaluate again using how data, it would be consistent one.

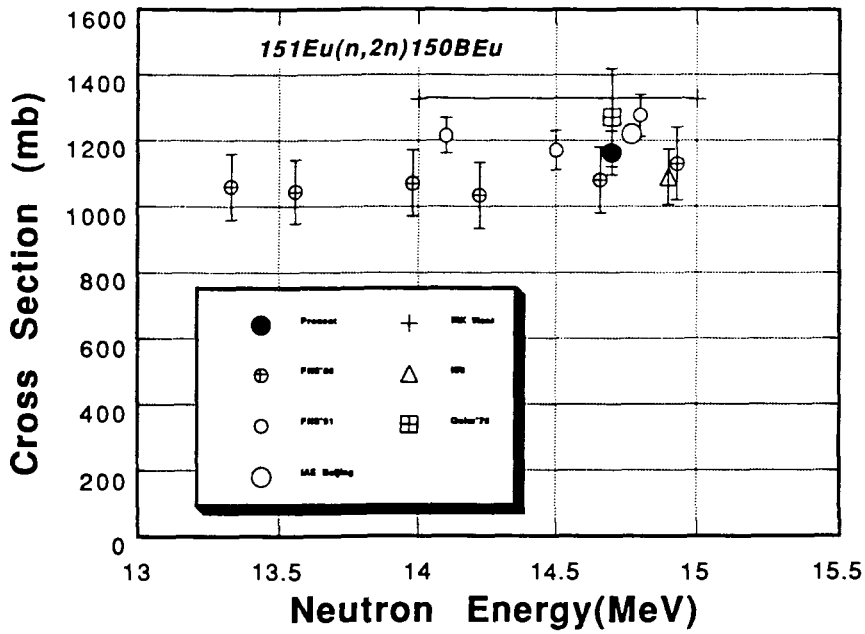

Fig. 5.2 Cross section of 151Eu(n,2n)150mEu

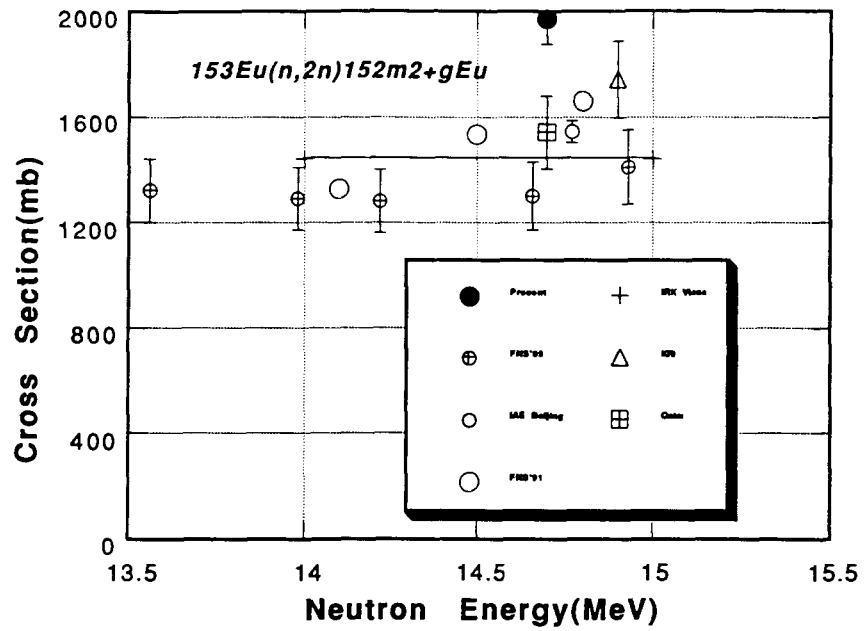

Fig. 5.3 Cross section of 153Eu(n,2n)152m2+gEu

3.4 $^{153}Eu(n,2n)^{152m}Eu$

Reaction of $^{153}Eu(n,2n)$ produce three state of ^{152}Eu ; one is isomeric state decaying to the ground state with 96 min half-live, the other isomer with half-life of 9.3h which disintegrates to both ^{152}Sm and ^{152}Gd and the other is the ground state with half-live of 13.2 years which disintegrates to the ^{152}Gd with β decay.

Since the isomeric state of 96 min de excites with 100 % isomeric transitions to the ground state the cross section has bean obtained for the $^{153}Eu(n,2n)^{152m1+g}Eu$; Although there have

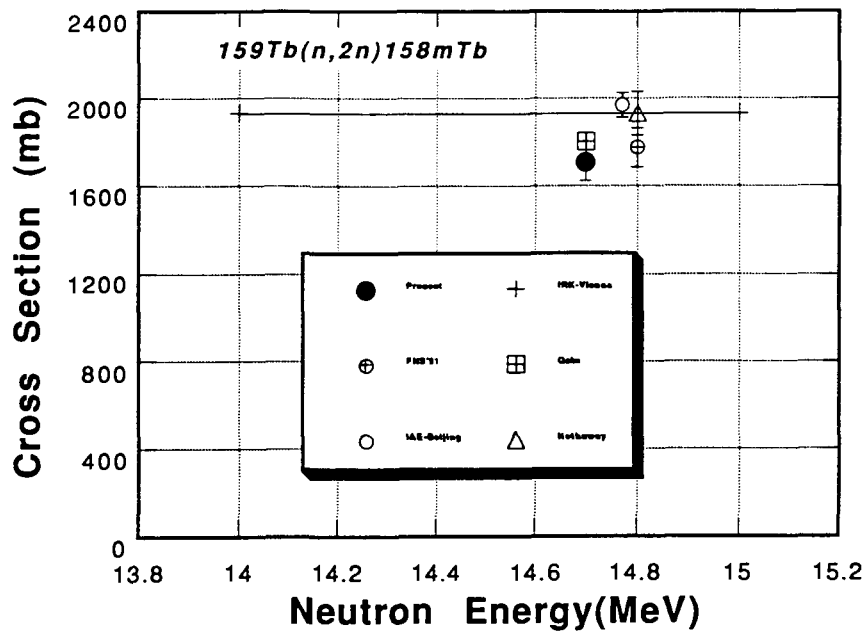

Fig. 5.4 Cross section of 159Tb(n,2n)158mTb

been a lot of cross section measurements for the products of 96 min and 9.3 hr, only one data was avaireble for the 13.2 years production by Qaim [8] before IAEA-CRP report has appeared. It gave 1,542 ± 138 mb.

In the summary report of IAEA-CRP, we found the data of 1,544 mb at 14.77 MeV by Beijing ; 1,740 mb at 14.7 MeV by KRI Leningrad. IRK vienna gave evaluation of 1,442 mb 14 - 15 MeV. These are rether scattered around 1,500 mb. Meanwhile, at FNS, we measured cross section by using enriched sample of ^{153}Eu, resulted in from 1,300 to 1,410 mb around 14 MeV.

Note that the natural Europium has as mentioned two isotopes with mass number of 151 and 153, so that we have to be careful in the correction for the (n, γ) contribution for the 152Eu production. Natural abundance of ^{151}Eu is so high 48 % that you can not neglect the (n, γ) contribution when you use the natural Eu sample. The case is in the present measurement giving 1,970 ± 95 mb at 14.7 MeV without any correction for the (n, γ) contribution. Apparently considerbl amount of (n,g) reaction suffered the reaction rate determination. An attempted was made to correct (n, γ) fraction on the 152Eu production. Using the neutron spectrum calculated by the MORSE-DD code and 151Eu(n, γ)152Eu reaction cross section taken from JENDL-3 dosimetry file, contribution was deduced to be 40 % to the total reaction rate. However, we have to considered the self-shielding effects for the very large capture g reaction in the sample. The fraction of 40 % seems too high to be used as the correction factor. It is complicated that it is very hard to arrive at reasonably accurate corrections for the ^{152}Eu production cross section. Concludiegly, the use of enriched ^{153}Eu sample is highly recommended.

The status of the cross section seems a little bit controvertial, because of , as mentioned, rather scattered experimental data.

3.4 ^{159}Tb(n,2n)$^{158m+g}$Tb

Terbium-158 has two states, one isomeric state deexciting through 100 % isomeric transition with half-life of 10.5 sec and the ground state decaying with 150 year half-life. The isomer is so

short life that cross section is given as ^{159}Tb(n,2n) $^{158m+g}$Tb. Natural abundance of ^{159}Tb is 100 % so that there is no interference (n, γ) contribution to ^{158}Tb products.

Two experimental data have been reported by Qaim [8] and Prestwood [10] befor IAEA-CRP report. They are 1,801 mb at 14.7 MeV and 1,930 mb at 14.8 MeV, respectively.In the IAEA-CRP report, one experimental data and one evaluation are given by IAE Beijing to be 1,968 mb at 14.77 MeV and by IRK Vienna to be 1,930 mb at 14 - 15 MeV. Those data seem very close each other. The present data gives a cross section of 1,708 mb at 14.7 MeV. The value is in good agreement with data at FNS[11], but is rather lower than those previously reported even though the experimental errors are taken into account.

3.5 ^{179}Hf(n,2n)^{178m2}Hf

Abundances of ^{179}Hf and ^{177}Hf are 13.7 % and 18.6 %, respectively. In general it is expected that ^{177}Hf(n,γ) reaction contributes to produce ^{178}Hf. However, the state of 178m2Hf of interest in this study is a high spin state (16+), so that capture reaction to this state must be very inhibited. We assume that contribution of the (n,γ) reaction is negligible.

No data has been reported so far before IAEA-CRP summary. Only Harwell reported an experimental data ; 5.9 $\pm$0.6 mb at 14.8 MeV. One calculation has been given by Oxford/LANL to be 2.9 mb at 14 MeV.

Present measurement showed the value of 6.3 $\pm$0.5 mb at 14.9 MeV very close to that of Harwell.

4. Present Summary

In this report, the preliminary cross section data for six reactions of ^{63}Cu(n,α)^{60}Co, ^{109}Ag(n,2n)^{108m}Ag, ^{151}Eu(n,2n)^{150m}Eu, ^{153}Eu(n,2n)$^{152m+g}$Eu, ^{159}Tb(n,2n)^{158m}Tb and ^{179}Hf(n,2n)^{178m2}Hf are given.

Aknowledements

Author would like to express their sincere thank to the members of the FNS facility for their opperation of accelerator.

References

1. INDC(NDS)-232/L, "Activation Cross Sections for the Generation of Long-Lived Radionuclides of Importance in Fusion Reactor Technology", Proc. of an IAEA Consultant's Meeting, Argonne National Laboratory, 11th - 12th. Sept 1989
2. T. Nakamura, et al.;" Present Status of the Fusion Neutron Source(FNS)," Proc. 4th Symp. on Accelerator Sci. Technol., RIKEN, Saitama, 24 - 26 November 1982, pp 155 - 156.

3. J. W. Meadows, et. al. "A Search for Activation Produced by Fast-Neutron Irradiations of Copper, Silver, Europium, Terbium and Hafnium", Proc. of an IAEA Consultants' Meeting, Argonne National Laboratory, 11th - 12th. Sept 1989.
4. D. L. Smith and J. W. Meadows; ANL/NDM-95, Argonne National Laboratory (986).
5. R. C. Haight "Activation with an Intense Source of Monoenergetic Neutrons in the Range 8-14 MeV", Proc. of a Specialists' Meeting on "Neutron Activation Cross Section for Fission and Fusion Energy Applications", Argonne National Lab.,
6. C. M. Ledere and V. S. Shirley;" Table of Isotopes," 7th edition, John Wiley & Sons, Inc., New York (1978).
7. L. R. Greenwood, "Recent Research in Neutron Dosimetry and Damage Analysis for Materials Irradiations", Proc. Symp. on theEffects of Radiation on Materials, June 23-25, 1986 Seattle, Washington, U.S.A.
8. S. M. Qaim, Nucl. Phys. A 224, 319(1974).
9. D. R. Nethaway, Nucl. Phys. A 190, 635(1972).
10. R. J. Prestwood, D. B. Curtis, D. J. Rokop, D. R. Nethaway and N. L. Smith, Phys. Rev. C 30, 823(1984).
11. Y. Ikeda, A. Kumar and C. Konno, " Measurements of Long-Lived Activation Cross Sections by 14 MeV Neutrons at FNS", Proc. on Nucl. Data, May 13 -17, 1991, Kfa Julich, Germany.

MEASURED FAST-NEUTRON ACTIVATION CROSS SECTIONS OF AG, CU, EU, FE, HF, NI, TB AND TI AT 10.3 AND 14.8 MEV AND FOR THE CONTINUUM NEUTRON SPECTRUM PRODUCED BY 7-MEV DEUTERONS ON A THICK BE-METAL TARGET*

J.W. Meadows and D.L. Smith, Engineering Physics Division
L.R. Greenwood**, Chemical Technology Division
Argonne National Laboratory
Argonne, Illinois 60439, U.S.A.

R.C. Haight, Physics Division
Los Alamos National Laboratory
Los Alamos, New Mexico 87545, U.S.A.

Y. Ikeda and C. Konno, Reactor Engineering Department
Japan Atomic Energy Research Institute
Tokai-mura, Naka-gun, Ibaraki-ken 319-11, Japan

ABSTRACT

Four identical sample packets containing elemental Ag, Cu, Eu, Fe, Hf, Ni, Tb and Ti have been irradiated in three distinct accelerator neutron fields, at Argonne National Laboratory and Los Alamos National Laboratory, U.S.A., and Japan Atomic Energy Research Institute, Tokai, Japan, under the auspices of an International Atomic Energy Agency Coordinated Research Program to investigate the production of long-lived radionuclides for fusion waste disposal applications. Final experimental results are presented here for 13 distinct reactions which ultimately lead to production of the following activities: Ag-106m,108m; Co-60g; Cr-51; Eu-150g,-152g; Hf-175,-179m2; Mn-54; Sc-46g,-47,-48; Tb-158g. The neutron fluence standard used was Ni-58(n,p)Co-58. The measured data include differential cross section values at 10.3 and 14.8 MeV, and integral cross sections for the continuum neutron spectrum produced by 7-MeV deuterons incident on a thick Be-metal target. The U-238(n,f) cross section was also measured at 10.3 MeV as a consistency check on the experimental technique. Some of the results of this study are compared with corresponding values from earlier work at Argonne and from ENDF/B-VI.

1. INTRODUCTION

1.1 Background and Objectives

A recommendation was made at the 16th Meeting of the International Nuclear Data Committee (INDC), held in Beijing, People's Republic of China, 12-16 October 1987, to establish an International Atomic Energy Agency (IAEA) Coordinated Research Program (CRP) entitled "Measurements and Calculations of Activation Cross Sections for Long-lived Radionuclides Important for Radioactive Waste Estimates in Fusion Reactor Technology". This action followed from an earlier

---

* Work sponsored by the U.S. Department of Energy, Energy Research Programs (Contracts W-31-109-Eng-38 and W-7405-Eng-36) and the International Atomic Energy Agency, Vienna (Agreement No. 5064/CF).
** Present address: Battelle Pacific Northwest Laboratories, Richland, Washington 99352.

suggestion made by E. Cheng at the 1986 Gaussig Advisory Meeting on Nuclear Data for Fusion Reactor Technology [Che88]. According to Cheng, the contemporary fusion reactor design studies call for operation at a very low rate of production of long-lived radionuclides, in order to minimize the problems of reactor maintenance, low-level waste disposal and, ultimately, reactor decommissioning. In order to meet these stringent requirements, cross section data are needed for activation reactions, not only for all the major structural constituents of fusion reactors, but also for the probable impurities. Consequently, the list of activation data needs spans nearly the entire periodic table. While some of these data requirements are familiar from fission-reactor technology, many are new because of the significant differences in these technologies, e.g. the higher average neutron energies that will be encountered in fusion machines. Current knowledge of the important cross sections varies from adequate to essentially unknown.

The IAEA concluded that formation of this CRP would provide a strong motivation to bring together the available technical resources required for addressing the problem. In order to provide a focus, the list of reactions to be considered by this CRP was limited to about a dozen. Argonne National Laboratory (ANL) was approached to participate in the project, along with various other organizations around the world. It was evident at the outset that intense sources of neutrons in the energy range of interest (< 15 MeV) would be needed in order to investigate these reactions experimentally. Such sources are generally limited to fission reactors (which are inappropriate for the present purposes), intense 14-MeV generators (not available at ANL), accelerator thick-target reactions such as Be(d,n), and certain other special-purpose intense monoenergetic sources (e.g., the Los Alamos National Laboratory gas-target facility which employs the H(t,n) reaction). ANL originally planned to conduct it's investigations solely at the ANL FNG accelerator facility [CH71], employing the Be(d,n) source [SMG85,SM86,Mea91] for its irradiations. It was suggested that this source, which provides an intense, continuum spectrum of neutrons with energies < 12 MeV, would provide useful cross section data at energies below 14 MeV, to complement the 14-MeV studies which were proposed by some of the other participants in the CRP. In particular, these data could shed light on the threshold regions for high-threshold reactions such as (n,2n) processes. Subsequently, ANL decided to solicit a collaboration with the Japan Atomic Energy Research Institute (JAERI) at Tokai, Japan (YI and CK). This laboratory had not been approached initially by the IAEA, but JAERI later expressed a strong interest in contributing the formidable JAERI experimental resources (in particular the FNS 14-MeV neutron source facility) to this effort. Finally, Los Alamos National Laboratory (LANL) also expressed a desire to participate in this work (RH), thereby bringing to the project it's unique capability for producing intense, monoenergetic neutrons in the 5-13 MeV energy range via the H(t,n) gas-target neutron source [HG90] at the LANL tandem accelerator facility [WMH74]. The LANL irradiations were performed at 10.3-MeV neutron energy for the present investigation.

A report on the progress of this investigation up to 1989 was presented at the first meeting of the CRP which was held at ANL in September 1989 [Mea+90]. Subsequently, a summary progress report on the activities of all participants in the CRP was presented at the Juelich Conference by Vonach [Von91]. The purpose of the present communication is to report some numerical results from the ANL/JAERI/LANL collaboration effort to date.

1.2 Scope of the Present Work

A careful review of the experimental resources available to the partners in this collaboration led us to decide to confine the investigation to certain activities which can be produced by neutron irradiation of the elements Ag, Eu, Hf and Tb. In addition, the elements Cu, Fe, Ni and Ti were included in the program because the cross sections for several reactions associated with these materials are reasonably well known and, therefore, afforded a check on the experimental procedures. Furthermore, these materials are also of interest for fusion applications. The neutron fluence standard chosen for the experiment was Ni-58(n,p)Co-58, a well-known dosimetry reaction. Table 1 lists the reactions specifically examined in this project. Table 2 provides essential decay parameters for the relevant

Table 1: Reactions Considered in the Present Work

Reaction	Target Isotopic Abundance (%)[a]	Q-value (MeV)[a]
Ag-107(n,2n)Ag-106m	51.839±0.005	-9.637
Ag-109(n,2n)Ag-108m	48.161±0.005	-9.300
Cu-63(n,α)Co-60g+m	69.17±0.02	1.715,1.656*
Eu-151(n,2n)Eu-150g	47.8±0.5	-7.965
Eu-153(n,2n)Eu-152g+m2	52.2±0.5	-8.551,-8.699*
Fe-54(n,p)Mn-54†	5.9±0.2	0.086
Fe-54(n,α)Cr-51†	5.9±0.2	0.843
Hf-176(n,2n)Hf-175†	5.206±0.004	-8.091
Hf-180(n,2n)Hf-179m2	35.100±0.006	-8.495
Tb-159(n,2n)Tb-158g+m	100	-8.132,-8.242*
Ni-58(n,p)Co-58g+m§	68.077±0.005	0.402,0.377*
Ti-46(n,p)Sc-46g+m	8.0±0.1	-1.584,-1.727*
Ti-47(n,p)Sc-47†	7.3±0.1	0.182
Ti-48(n,p)Sc-48†	73.8±0.1	-3.207
U-238(n,f)	Enriched deposit#	NA‡

---

* Multiple Q-values correspond to the ground state and those indicated isomeric levels which are included in the measured cross section.
† There are no isomeric states in this nucleus.
§ Reaction cross-section standard for this experiment.
# See Section 2.2 of the text.
‡ NA = Not applicable.
[a] Ref. Tul90.

Table 2: Decay Properties of the Radioactive Nuclei Involved in the Present Work

Activity	Jπ	Excitation Energy (MeV)	Half Life*	Decay Mode#	Measured γ Ray (MeV)	Relevant γ Branch (%)
Ag-106m[a]	6+	0.090	8.46±0.10 d	EC,(β+)	0.512	87.7±0.5
Ag-108m[b]	6+	0.109	418±12 y[o]	EC,β+,IT	0.434	90.5±0.6
Co-58g[c]	2+	g.s.	70.82±0.03 d	EC,β+	0.811	99.448±0.008
Co-58m‡[c]	5+	0.025	9.15±0.10 h	IT	NA†	NA
Co-60g[d]	5+	g.s.	5.2714±0.0005 y	β-	1.333	99.982±0.001
Co-60m‡[d]	2+	0.059	10.47±0.04 m	IT,(β-)	NA	NA
Cr-51§[e]	7/2-	g.s.	27.702±0.004 d	EC,(β+)	0.320	10.08±0.23
Eu-150g[f]	5-	g.s.	35.8±1.0 y	EC,(β+)	0.334	96±3
Eu-152g[g]	3-	g.s	13.542±0.010 y	EC,β+,β-	0.344	27.6±0.3
Eu-152m2‡[g]	8-	0.148	96±1 m	IT,(β-)	NA	NA
Hf-175§[h]	5/2-	g.s.	70±2 d	EC	0.343	87.0±0.5
Hf-179m2[i]	25/2-	1.106	25.1±0.3 d	IT	0.454	68.6±3.6
Mn-54§[j]	3+	g.s.	312.12±0.10 d	EC,(β+)	0.835	99.976±0.001
Sc-46g[k]	4+	g.s.	83.810±0.010 d	β-	0.889	99.984±0.001
Sc-46m[k]	1-	0.143	18.75±0.04 s	IT	NA	NA
Sc-47§[l]	7/2-	g.s.	3.345±0.003 d	β-	0.159	67.9±1.5
Sc-48§[m]	6+	g.s.	43.7±0.1 m	β-	0.984	100
Tb-158g[n]	3-	g.s.	180±11 y	EC,β+,β-	0.944	43.9±1.3
Tb-158m[n]	0-	0.110	10.5±0.2 s	IT	NA	NA

---

* s (second), m (minute), h (hour), d (day), y (year).
\# Decay branches marked by (...) are negligibly weak.
‡ Isomeric activity not measured directly in this investigation. Decay contributes indirectly to the measured ground state activity.
† NA: Not applicable.
§ There are no isomeric states for this nucleus.
[a] Ref. Fre88 [e] Ref. Chu91 [i] Ref. Bro88 [m] Ref. Alb85
[b] Ref. Bla91 [f] Ref. Mat86 [j] Ref. GJJ87 [n] Ref. Lee89
[c] Ref. Pek90 [g] Ref. Pek89 [k] Ref. Alb86 [o] Ref. SSD91
[d] Ref. AEL86 [h] Ref. Min76 [l] Ref. Bur86

activities associated with these processes. The choice of reactions to investigate in this work was restricted by limitations inherent to the experimental resources of the collaborators. In particular, certain longer-lived radionuclides of interest to the CRP could not be investigated because of insufficient available time (to date) to adequately eliminate the interference from shorter-lived components and/or insufficient neutron doses to the irradiated samples.

Some brief comments on the individual reactions from Table 1 are in order. First, no attempt was made to determine any cross sections for (n,γ) reactions. Interpretations of such data are very sensitive to detailed knowledge of the low-energy neutron spectra of the irradiation environments (see Section 3.2). Thus, the present work addresses only fast-neutron energies and threshold reactions. In fact, no specific effort was made to quantitatively examine any activities produced mainly by lower-energy neutrons other than what was required to apply corrections to the primary reaction data of this study. For Ag, both Ag-106g and Ag-106m are involved in the (n,2n) reaction on Ag-107. Ag-106g was not investigated because of its short half life. Ag-106m decays to Pd-106, not to Ag-106g. Consequently, the measured cross section accounts only for excitation of the isomer and those energetically accessible levels which feed it. A similar situation exists in the formation of Ag-108. Both Co-60g and Co-60m are involved in the (n,α) reaction on Cu-63. Since Co-60m decays with a moderately short half life to Co-60g, the present experiment yields a cross section for excitation of all energetically accessible levels in Co-60. Similar comments can be made for Sc-46 and Co-58, which are produced by (n,p) reactions on Ti and Ni, respectively, and for Tb-158 which is generated by the (n,2n) reaction on Tb-159. Eu-150g and Eu-150m are produced by the (n,2n) reaction on Eu-151. However, the isomer decays with a relatively short half life to adjacent nuclei. There are no isomeric transitions to Eu-150g. Consequently, the present experiment measures only the excitation of Eu-150g and those levels which feed it. For Eu-152, the situation is more complicated. The ground state and two isomers are involved. However, the first isomer (m1) is isolated owing to a relatively short half life and a decay scheme which precludes transitions to Eu-152g. The second isomer (m2) feeds only Eu-152g by isomeric transitions, bypassing the first isomer. Therefore, the cross section measured in this work includes only levels which feed the ground state or m2. For Hf-179, the ground state is stable so its direct formation rate by the (n,2n) reaction is not measurable by activation. There are two isomers involved. The first isomeric state (m1) has a very short half life and was not measured. Furthermore, the second isomer (m2) decays ultimately to the ground state, bypassing m1. Consequently, only the yield of m2 and those levels which feed it is measured in this experiment. Finally, there are no isomeric levels involved in Cr-51, Hf-175, Mn-54, Sc-47 and Sc-48 so the present measurements include the strength for all energetically-accessible levels in these nuclei.

2. EXPERIMENTAL PROCEDURES

2.1 Samples

It was essential for the success of this experiment to accumulate the maximum possible neutron doses for each of the sample materials within the available irradiation times. Therefore, it was decided to

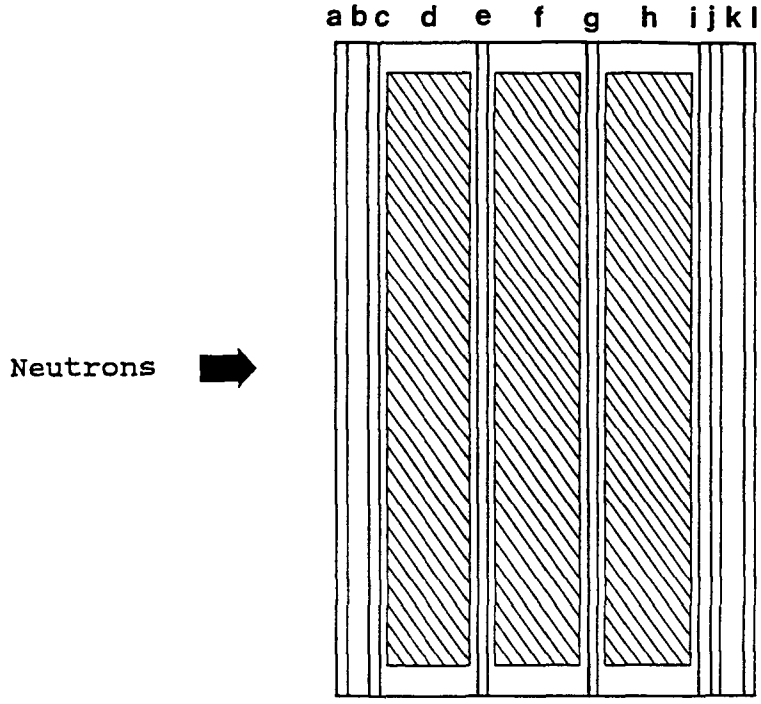

Fig. 1: Schematic diagram for the identical sample packets used in each of the neutron irradiations. The sample materials are as follows: a = Ni(#1), b = Ag, c = Ni(#2), d = HfO_2, e = Ni(#3), f = Tb_4O_7, g = Ni(#4), h = Eu_2O_3, i = Ni(#5), j = Cu, k = Fe, l = Ti. The oxide samples (indicated by the shaded regions) are contained in plastic capsules.

employ sample packets that included all of the materials of interest for this work. Several identical sample packets of this nature were assembled for the experiment, as shown in Fig. 1. These packets were nominally 2.54 cm in diameter and $\leq$ 2 cm thick. The Eu, Hf and Tb samples were represented in the form of oxides, since these rare-earth elements are quite reactive in the natural state. The oxides were encapsulated in sealed plastic containers which defined the sample geometries and prevented any loss of material. All the other sample materials were in the form of metal foils. The chemical purity of all samples was > 99.9% and the isotopic abundances were standard elemental (see Table 1). Table 3 lists some of the other important sample parameters. Five Ni foils were included in each sample packet to measure the total neutron fluences and associated fluence gradients in the irradiation environments seen by these packets (see Fig. 1).

2.2 Irradiation Procedures

The irradiation at ANL was carried out using the Be(d,n) thick-target neutron spectrum [SMG85,SM86,Mea91] produced by 7-MeV deuterons from the ANL FNG accelerator [CH71] incident on a thick Be-metal target. The neutron spectrum is a continuum ranging from < 0.1 MeV up to about 11.4 MeV. The sample packet occupied a position on the beam line (zero deg) in the range 5 - 7 cm from the Be target. This experiment was entirely passive in the sense that no data were recorded in real time with instrumented radiation detectors. The neutron fluences were deduced solely from Co-58 activity measurements performed for each of the five Ni monitor foils contained in the

Table 3: Properties of Sample Materials in the Irradiation Packets

Element	Chemical Form	Mass (gram)†	Nominal Sample Dimensions (cm)‡
Ag	Element (metal)	2.715-2.742	2.54 dia x 0.0508 thick
Cu	Element (metal)	1.1630-1.1744	2.54 dia x 0.0254 thick
Eu	Oxide (powder)	1.057-1.223	2.06 dia x 0.3175 thick§
Fe	Element (metal)	1.9101-2.0316	2.54 dia x 0.0508 thick
Hf	Oxide (powder)	2.879-3.184	2.06 dia x 0.3175 thick§
Ni	Element (metal)	1.1319-1.1471	2.54 dia x 0.0254 thick
Tb	Oxide (powder)	1.864-2.498	2.06 dia x 0.3175 thick§
Ti	Element (metal)	0.5455-0.5761	2.54 dia x 0.0254 thick

† Range of masses encountered for individual samples of this type.
‡ Exact dimensions vary somewhat from sample to sample.
§ These are the approximate dimensions of the oxide region itself. The overall dimensions of the sample, including the encapsulating material, are approximately 2.54 dia x 0.476 cm thick. See Fig. 1.

sample packet, thereby utilizing the Ni-58(n,p)Co-58 reaction as a standard (see Table 1.). The irradiation consisted of about 110 hours of cumulative exposure, occurring over a period of nearly a month during November and December 1988. The accumulated neutron fluence at the sample position was ~ 1-2 x 10^{15} n/cm^2.

The measurement at LANL utilized a 15.75-MeV triton beam from the tandem accelerator [WMH74] and a rotating hydrogen-gas-target assembly [HG90] to produce neutrons via the H(t,n) source reaction. The gas volume of this target extended 4.6-cm along the beam line (zero deg). The sample packet used in this irradiation occupied a position on the beam line which was stated to be in the range 4 - 6 cm from the gas target. However, in subsequent analysis of the data, it was found that an effective distance of 5 - 7 cm had to be assumed in order to obtain consistent results for the Ni monitor foils (see Section 3.1). This arrangement yielded a calculated mean neutron energy of 10.3 MeV with a corresponding resolution of about 0.4 MeV. A fission chamber was also employed during these irradiations as an auxiliary neutron monitor. This detector contained a uranium deposit (identified as U-238-26 in Ref. Mea90) with a total mass of 950 ± 60 μg of material. Its isotopic composition was: U-238 (99.585%), U-235 (0.415%). Other uranium isotopes were negligible. About 14 hours of total beam time were devoted to this experiment, occuring during two irradiation periods in October and November 1988. The accumulated neutron fluence at the sample position was ~ 2-3 x 10^{13} n/cm^2.

Two sample packets were irradiated in June 1989 at the JAERI FNS accelerator facility [Nak+82]. These were placed at two symmetric positions located at 43 deg relative to the incident beam line and 7

cm from the target. The mean energy for the neutrons impinging on each sample was 14.8 MeV with a resolution of about 0.5 MeV. A total of 32 hours (divided into four 8-hour intervals) of beam time was allocated to the experiment. The accumulated neutron fluence at the sample position was $\sim$ 1-2 x 10^{14} n/cm^2. Like the ANL experiment, this irradiation was passive and relied on the Ni dosimeter foils for determination of neutron fluences. One of the sample packets was retained at JAERI for activity counting and subsequent data analysis. The results of this investigation are reported elsewhere [Ike+91]. The present communication deals only with results derived from the sample packet which was sent back to ANL after the irradiation at JAERI, for counting and analysis.

2.3 Activity Measurements

With the exception of one sample packet which remained at JAERI, all the irradiated samples were counted at ANL. In each instance, the gamma-ray activities were measured with germanium detectors whose efficiencies had been calibrated by conventional techniques (e.g., Ref. MS84) using standard gamma-ray sources (e.g., from the National Institute of Standards and Technology). Full-energy peak yields were determined from recorded gamma-ray spectra. At early counting times following the irradiations, these spectra were dominated by shorter-lived components. Peaks corresponding to longer-lived activities could only be measured after the passage of many months following the irradiations. Some activities which might ultimately be measurable in these samples remain to be investigated. Several years will be needed to arrive at the proper counting conditions, so this work will have to be deferred to a later date. Table 2 provides a summary of the important parameters associated with various activities which have been studied up to the present time. This information was derived from the available documented compilations and/or evaluations of such data (e.g., the Nuclear Data Sheets), as indicated in the footnotes to Table 2. In some cases, several gamma-ray lines attributed to the same decay activity were analyzed. For compactness, Table 2 provides information only on the dominant transition in these instances.

3. DATA ANALYSIS

3.1 Procedures and Data Corrections

The raw activation data were processed using conventional experimental techniques (e.g., see Refs. SM73, SMB85, GSM89, Smi+91). The numbers of target atoms in each of the samples were determined from the known sample masses, atomic masses, isotopic abundances (see Table 1), and chemical compositions of the irradiated materials. The gamma-ray counting data were converted to reaction product yields using calibrated detector efficiencies, decay branching parameters (see Table 2), and activity-decay factors based on tabulated half lives (see Table 2). Other corrections to the counting data were applied as needed (e.g., geometry factors, coincidence summing, etc.). The fission detector events which were recorded during the LANL experiment were corrected for spectrum extrapolation and fission-deposit thickness losses. The data from LANL were also corrected for empty cell contributions to the fission detector counts and sample activities. These latter corrections were calculated from

Table 4: Experimental Cross Sections Obtained from this Investigation

Reaction	Cross Section (millibarn)* Be(d,n)†	10.3 MeV#	14.8 MeV@
Ag-107(n,2n)Ag-106m	1.03 (± 4.9%)	11.6 (± 4.4%)	NA‡
Ag-109(n,2n)Ag-108m	NA‡	40.8 (± 8.5%)	734 (± 3.9%)
Cu-63(n,α)Co-60g+m	2.01 (± 2.2%)	29.1 (± 4.7%)	43.5 (± 2.2%)
Eu-151(n,2n)Eu-150g	15.7 (± 5.8%)	198 (± 7.9%)	1282 (± 5.8%)
Eu-153(n,2n)Eu-152g+m2	NA‡	NA‡	1909 (± 7.4%)
Fe-54(n,p)Mn-54	185 (± 2.4%)	447 (± 3.1%)	306 (± 2.9%)
Fe-54(n,α)Cr-51	3.43 (± 2.5%)	40.8 (± 4.9%)	92.8 (± 2.5%)
Hf-176(n,2n)Hf-175	39.6 (± 5.0%)	1139 (± 7.2%)	2100 (± 5.0%)
Hf-180(n,2n)Hf-179m2	2.63 (± 7.7%)	24.7 (± 8.5%)	24.9 (± 7.1%)
Tb-159(n,2n)Tb-158g+m	28.0 (± 9.6%)	536 (± 9.8%)	2110 (± 7.9%)
Ti-46(n,p)Sc-46g+m	37.7 (± 2.2%)	255 (± 5.2%)	321 (± 2.2%)
Ti-47(n,p)Sc-47	34.8 (± 6.1%)	NA‡	NA‡
Ti-48(n,p)Sc-48	1.50 (± 7.1%)	NA‡	NA‡
U-238(n,f)	NA‡	1064 (± 6.5%)§	NA‡

---

* Absolute cross sections are derived from the following standard cross section values for the Ni-58(n,p)Co-58g+m reaction: Be(d,n) - 240 millibarn; 10.3 MeV - 589 millibarn; 14.8 MeV - 320 millibarn [ENDF90]. The errors are obtained from Tables 5-7. Errors in the applicable standard cross sections are not included.

† ANL irradiation (Section 2.2). Standard integral cross section value based on the Be(d,n) spectrum representation from Meadows [Mea91].

LANL irradiation (Section 2.2).

@ JAERI irradiation (Section 2.2).

‡ NA = Not measured in the present investigation.

§ Includes a 6.3% fission-deposit mass error [Mea90] in addition to the error obtained from Table 6.

available spectral data and differential cross sections, since empty-cell measurements were not explicitly performed in this investigation. Finally, corrections were applied to all the data to account for irradiation geometry effects, neutron source properties, neutron absorption and neutron multiple scattering. It is interesting to note that the activation data for the five Ni monitor foils included in each sample packet were very consistent after application of all these corrections. The standard deviations for the five individual foils relative to the mean were as follows for the three irradiations of this experiment: ANL, Be(d,n) - 1.6%; LANL, 10.3 MeV - 0.7%; JAERI, 14.8 MeV - 0.6%. As mentioned in Section 2.2, a change

Table 5: Examined Error Sources for the Be(d,n) Spectrum Measurements

Reaction	Estimated Error Component (%)								Total Error
	γ Yield	Half Life	γ Branch	Activ. Decay	Geom.	Neut. Trans.	Mult. Scat.	(n,γ)*	
Ag-107(n,2n)	2.3	0.1	0.6	4.2	0.1	0.1	0.6	NA†	4.9
Ag-109(n,2n)	--- NA ---								
Cu-63(n,α)	2.2	Neg‡	Neg	0.1	Neg	0.1	0.3	NA	2.2
Eu-151(n,2n)	4.0	2.8	3.1	Neg	0.3	0.1	0.4	NA	5.8
Eu-153(n,2n)	--- NA ---								
Fe-54(n,p)	2.0	Neg	Neg	0.5	Neg	0.1	1.2	Neg	2.4
Fe-54(n,α)	2.5	Neg	Neg	1.4	Neg	0.1	0.3	NA	2.9
Hf-176(n,2n)	2.1	2.9	0.6	Neg	0.3	0.1	0.3	3.4	5.0
Hf-180(n,2n)	5.5	1.2	5.2	1.0	0.3	0.1	0.3	Neg	7.7
Tb-159(n,2n)	6.8	6.1	3.0	Neg	0.3	0.1	0.4	NA	9.6
Ti-46(n,p)	2.1	Neg	Neg	0.1	Neg	0.1	0.6	NA	2.2
Ti-47(n,p)	2.2	0.1	1.2	5.4	Neg	0.1	1.3	NA	6.1
Ti-48(n,p)	2.6	0.2	Neg	6.6	Neg	0.1	0.2	NA	7.1
U-238(n,f)	--- NA ---								

* See Section 3.2.
† NA = Not applicable.
‡ Neg = Negligible (< 0.1%).

had to be made in the assumed distance of the sample from the gas target in the LANL measurements (from 4 - 6 cm to 5 - 7 cm) in order to achieve the consistency quoted above. No other plausible explanation could be found to explain the discrepancy which would have existed otherwise. Cross section ratios relative to the Ni-58(n,p)Co-58 standard reaction were obtained from the adjusted results and, ultimately, experimental cross sections were derived using appropriate values for the Ni-58(n,p)Co-58 cross section. In the case of the Be(d,n) spectrum irradiations at ANL, it was necessary to calculate a value for the spectrum-averaged Ni-58(n,p)Co-58 standard cross section from the ENDF/B-VI differential cross section values and an appropriate representation of the Be(d,n) continuum neutron spectrum. Recent results from Meadows [Mea91] were employed for the spectrum representation in this analysis.

3.2 Interfering Activities

Interpretation of the measured data for four of the (n,2n) reactions considered in this work was complicated by interference from

Table 6: Examined Error Sources for the 10.3-MeV Measurements

Reaction	Estimated Error Component (%)									
	γ Yield	Half Life	γ Branch	Activ Decay	Geom	Neut Trans	Mult Scat	(n,γ)*	Empty Cell	Total Error
Ag-107(n,2n)	2.6	0.1	0.6	2.1	0.1	0.1	0.5	NA†	2.7	4.4
Ag-109(n,2n)	7.4	2.9	0.6	0.7	0.1	0.1	0.5	1.2	2.7	8.5
Cu-63(n,α)	2.2	Neg‡	Neg	Neg	0.1	0.1	0.7	NA	4.1	4.7
Eu-151(n,2n)	2.8	2.8	3.1	0.7	3.3	0.1	0.8	NA	5.0	7.9
Eu-153(n,2n)				--- NA ---						
Fe-54(n,p)	2.1	Neg	Neg	0.5	0.1	0.1	0.3	NA	2.2	3.1
Fe-54(n,α)	2.7	Neg	Neg	0.8	0.1	0.1	0.7	NA	3.9	4.9
Hf-176(n,2n)	2.2	2.9	0.6	0.7	3.3	0.1	0.3	0.4	5.2	7.2
Hf-180(n,2n)	2.4	1.2	5.2	0.9	3.3	0.1	0.3	Neg	5.2	8.5
Tb-159(n,2n)	3.1	6.1	3.0	0.7	3.3	0.1	0.3	NA	5.4	9.8
Ti-46(n,p)	2.3	Neg	Neg	3.8	0.2	0.1	0.8	NA	2.5	5.2
Ti-47(n,p)				--- NA ---						
Ti-48(n,p)				--- NA ---						
U-238(n,f)	NA	NA	NA	NA	Neg	0.1	1.2	Neg	1.2	1.7

* See Section 3.2.
† NA = Not applicable.
‡ Neg = Negligible (< 0.1%).

(n,γ) capture-activation processes on other target isotopes in the elemental samples. These (n,γ) reactions could produce sample activities which were indistinguishable from those generated by the primary (n,2n) processes. The (n,γ) cross section is quite small in the MeV region so this process usually causes no serious problems in the measurement of the much larger (n,2n) cross sections for fast neutrons. However, in the radiation environments of the present investigation, particularly those at ANL and LANL, there were room-return neutrons present at thermal and epithermal energies which, in spite of their relatively modest numbers, were troublesome because the afflicted materials have rather large thermal capture cross sections and resonance capture integrals. Fortunately, there were other activities present in some of the samples which could be attributed only to neutron capture reactions, and these could be used to estimate corrections to the other data for (n,γ) events. For the purpose of evaluating these needed corrections, estimates were made of the thermal and resonance-region neutron fluences from the observed yields of the activities produced solely by neutron capture. These deduced effective neutron fluences were then used to compute required

Table 7: Examined Error Sources for the 14.8-MeV Measurements

Reaction	Estimated Error Component (%) γ Yield	Half Life	γ Branch	Activ. Decay	Geom.	Neut. Trans.	Mult. Scat.	(n,γ)*	Total Error
Ag-107(n,2n)	--- NA† ---								
Ag-109(n,2n)	2.2	2.9	0.6	0.2	1.3	0.1	0.4	Neg‡	3.9
Cu-63(n,α)	2.2	Neg	Neg	0.2	0.1	0.1	0.4	NA	2.2
Eu-151(n,2n)	2.1	2.8	3.1	0.2	3.4	0.1	0.7	NA	5.8
Eu-153(n,2n)	2.3	0.1	1.1	0.2	3.4	0.1	0.7	6.0	7.4
Fe-54(n,p)	2.2	Neg	Neg	0.2	0.1	0.1	0.4	NA	2.2
Fe-54(n,α)	2.5	Neg	Neg	0.2	0.1	0.1	0.2	NA	2.5
Hf-176(n,2n)	2.1	2.9	0.6	0.6	3.4	0.1	0.3	Neg	5.0
Hf-180(n,2n)	3.1	1.2	5.2	0.5	3.4	0.1	0.3	Neg	7.1
Tb-159(n,2n)	2.1	6.1	3.0	0.2	3.4	0.1	0.5	NA	7.9
Ti-46(n,p)	2.1	Neg	Neg	0.3	0.2	0.1	0.7	NA	2.2
Ti-47(n,p)	--- NA ---								
Ti-48(n,p)	--- NA ---								
U-238(n,f)	--- NA ---								

* See Section 3.2.
† NA = Not applicable.
‡ Neg = Negligible (< 0.1%).

corrections to the (n,2n) data for (n,γ) interferences by means of the thin-absorber approximation. The samples involved are by no means thin, but fairly consistent results were obtained. Since this entire procedure is not a very exact one, it was decided not to report explicitly any experimental (n,γ) cross sections from the present investigation (see Section 1.2). The capture-activation correction was largest for Eu-153(n,2n)Eu-152g+m2. That activity specifically due to Eu-151(n,γ) amounted to about 12% for the JAERI irradiations and, in the case of the ANL and LANL exposures, substantially exceeded the primary contributions from the (n,2n) reaction. In fact, these latter corrections were so large that the (n,2n) cross section values we deduced for these two irradiation environments are quite speculative at best. Therefore, we decided not to report them here. In contrast, the corrections for Ag-109(n,2n)Ag-108m and Hf-176(n,2n)Hf-175, due to Ag-107(n,γ) and Hf-177(n,γ), respectively, were quite modest (< 7%), and that for Hf-180(n,2n)Hf-179m2 due to Hf(n,γ) was essentially negligible.

Table 8: Comparison of Present Results with Previously Reported Experimental Values from ANL for Selected Be(d,n) Integral Cross Sections

Reaction	Integral Cross Section (millibarn)* Present†	Previous Work[a]	Ratio
Cu-63(n,α)Co-60g+m	2.01 (± 2.2%)	1.90 (± 7.3%)	1.06
Fe-54(n,p)Mn-54	185 (± 2.4%)	193 (± 4.8%)	0.96
Fe-54(n,α)Cr-51	3.43 (± 2.9%)	3.23 (± 10.5%)	1.06
Ti-46(n,p)Sc-46g+m	37.7 (± 2.2%)	34.0 (± 4.6%)	1.11
Ti-47(n,p)Sc-47	34.8 (± 6.1%)	40.4 (± 6.7%)	0.86
Ti-48(n,p)Sc-48	1.50 (± 7.1%)	1.16 (± 6.5%)	1.29

* Errors are those appearing in the original cross-section tables.
† ANL irradiation (Section 2.2). Standard integral cross section value based on the Be(d,n) spectrum representation from Meadows [Mea91]. See Table 4.
[a] Ref. SMG90.

Table 9: Comparison of Selected Present Cross Section Results with Corresponding Evaluated Values from ENDF/B-VI

Reaction	Cross Section (millibarn) Be(d,n)# Exp.*	Eval.†	Rat.‡	10.3 MeV Exp.	Eval.	Rat.	14.8 MeV Exp.	Eval.	Rat.
Cu-63(n,α)	2.01	1.77	1.14	29.1	32.5	0.90	43.5	38.8	1.12
Fe-54(n,p)	185	184	1.01	447	471	0.95	306	306	1.00
Fe-54(n,α)	3.43	3.06	1.12	40.8	56.8	0.72	92.8	87.5	1.06
Ti-46(n,p)	37.7	33.1	1.14	255	249	1.02	321	250	1.28
Ti-47(n,p)	34.8	45.9	0.76	NA§	134	---	NA	112	---
Ti-48(n,p)	1.50	1.08	1.39	NA	33.7	---	NA	63.0	---
U-238(n,f)	NA	461[a]	---	1064	989	1.08	NA	1176	---

ANL irradiation (Section 2.2). Standard integral cross section value based on the Be(d,n) spectrum representation from Meadows [Mea91].
* See Table 4.
† Ref. ENDF90.
‡ Ratio = experimental cross section ÷ evaluated cross section
§ NA = Not available.
[a] Obtained from SMG90.

4. RESULTS AND DISCUSSION

4.1 Experimental Cross Sections

The cross sections obtained from the present experiment are presented in Table 4. The obvious deficiencies of this table are attributable to specific circumstances relating to activity decay, interfering activities, etc., which made it impossible to determine reliable cross section values. Estimates were made of the contributions from various conventional sources of error in these measurements. These errors are listed in Tables 5 - 7. The composite errors also appear in Table 4. We believe that these quoted errors are essentially lower bounds on the total experimental error, and they do explicitly exclude the standard cross section errors. In the case of the Be(d,n) measurements, it was necessary to include a representation of the continuum neutron spectrum in the analysis in order to provide a value for the standard integral cross section for Ni-58(n,p)Co-58. The spectral representation from Meadows [Mea91] was employed for this purpose. All references to Ni-58(n,p)Co-58 differential cross sections are based on ENDF/B-VI [ENDF90].

4.2 Comparisons with Other Corresponding Available Results

The main purpose of this communication is to thoroughly document the results from our work so that they can be properly compared with other results from the CRP project. Up to this point, we have not undertaken a comprehensive search of the relevant literature for reactions leading to long-lived radionuclides because we believe that it would be premature to do so before all the other data from the CRP are available. However, it is of interest to compare the present results for the better known reactions with some other recent values from the literature, in order to assess the reliability of our experimental procedures. To this end, we have compared certain Be(d,n) results with corresponding values obtained from earlier work at ANL [SMG90]. The outcome is documented in Table 8. We find that the agreement is generally pretty good for the Cu and Fe reactions but not as good, overall, for the Ti reactions. There is a good reason why the quality of the present results for Ti-47,48(n,p) should be inferior to the corresponding earlier ANL results. As indicated in Section 2.2, the exposure time for the irradiated sample packet amounted to nearly a month. We undertook as long an exposure time as the circumstances allowed in order to enhance the yield of the sought-after long-lived activities. This irradiation period exceeded the half lives for Sc-47 and Sc-48 by at least an order of magnitude. The decay corrections that had to be applied to these data to obtain cross sections were very large and, consequently, the results are quite sensitive to the exact details of the irradiation history. This lends considerable uncertainty to the resultant cross sections for these reactions, which is probably only partially reflected in the quoted errors.

A comparison was also made of some of the present results with corresponding evaluated values based on ENDF/B-VI [ENDF90], as shown in Table 9. As mentioned above, the Be(d,n) spectrum representation from Meadows [Mea91] was employed in comparing the integral results. Once again, the overall agreement is fairly good for Cu and Fe and not as good for Ti. A probable reason for Ti-47,48(n,p) has already been discussed in the preceding paragraph. However, it is not clear at this time as to why there is a discrepancy for the 14.8-MeV cross section of Ti-48(n,p).

4.3 Future work

There remains the possibility that data can eventually be acquired for the Cu-63(n,p)Ni-63 (100.1 y) and Hf-179(n,2n)Hf-178 (31 y) reactions. These two reactions appeared in the original CRP list but have not been addressed in the present work. In the case of Ni-63, it will be necessary to rely on alternative counting procedures since there are no gamma rays associated with Ni-63 decay. For us, it is mainly a matter of finding support for this work, or finding a willing collaborator who is already equipped to perform the necessary activity measurements. In the case of Hf, we intend to recount the samples in the near future to see if it will be possible to observe and measure the 31-y activity which was previously masked by shorter-lived components.

REFERENCES

AEL86 P. Andersson, L.P. Ekstrom and J. Lyttkens, Nuclear Data Sheets 48, 251 (1986).

Alb85 D.E. Alburger, Nuclear Data Sheets 45, 557 (1985).

Alb86 D.E. Alburger, Nuclear Data Sheets 49, 237 (1986).

Bla91 Jean Blachot, Nuclear Data Sheets 62, 803 (1991). See also: R.L. Haese, F.E. Bertrand, B. Harmatz and N.M. Martin, Nuclear Data Sheets 37, 289 (1982).

Bro+88 E. Browne, Nuclear Data Sheets, 55, 483 (1988).

Bur86 T.W. Burrows, Nuclear Data Sheets 48, 1 (1986).

CH71 S.A. Cox and P.R. Hanley, IEEE Transactions on Nuclear Science NS-18, No. 3, 108 (1971).

Che88 E. Cheng, Proc. IAEA Advisory Group Mtg. on Nucl. Data for Fusion Reactor Tech., Gaussig, Fed. Rep. Germany, 1-5 Dec. 1986, IAEA-TECDOC-457, International Atomic Energy Agency, Vienna, p. 16 (1988)

Chu91 Zhou Chunmei, Nuclear Data Sheets 63, 229 (1991). See also: Zhou Chunmei, Zhou Enchen, Lu Xiane and Huo Junde, Nuclear Data Sheets 48, 111 (1986).

ENDF90 "Evaluated Neutron Data File, ENDF/B-VI", National Nuclear Data Center, Brookhaven National Laboratory (1990).

Fre+88 D. De Frene, E. Jacobs, M. Verboven and G. De Smet, Nuclear Data Sheets 53, 73 (1988).

GJJ87 Wang Gongqing, Zhu Jiabi and Zhang Jingen, Nuclear Data Sheets 50, 255 (1987).

GSM89 L.P. Geraldo, D.L. Smith and J.W. Meadows, Annals of Nucl. Energy 16, 293 (1989).

HG90 R.C. Haight and J.L. Gariboldi, Nucl. Sci. Eng. 106, 296 (1990).

Ike+91 Y. Ikeda, D.L. Smith, A. Kumar and C. Konno, Proc. 1990 Symposium on Nuclear Data, eds. M. Igashira and T. Nakagawa, JAERI-M-91-032, Japan Atomic Energy Research Institute (1991). See also: Y. Ikeda, A. Kumar, C. Konno and N. Yamamuro, Proc. International Conference on Nuclear Data for Science and Technology, 13-17 May 1991, ed. S. Qaim, Juelich, Germany (to be published in 1991). Y. Ikeda et al., contribution to this conference (1991).

Lee89 M.A. Lee, Nuclear Data Sheets 56, 199 (1989).

Mat86 Edward der Mateosian, Nuclear Data Sheets 48, 345 (1986).

Mea90 J.W. Meadows, ANL/NDM-118, Argonne National Laboratory (1990).

Mea+90 J.W. Meadows, D.L. Smith, L.R. Greenwood, R.C. Haight, Y. Ikeda and C. Konno, Proc. of an IAEA Consultants' Meeting on Activation Cross Sections for the Generation of Long-lived Radionuclides of Importance in Fusion Reactor Technology, INDC(NDS)-232/L, International Atomic Energy Agency, Vienna, p. 79 (1990).

Mea91 J.W. Meadows, ANL/NDM-124, Argonne National Laboratory (1991).

Min76 M.M. Minor, Nuclear Data Sheets 18, 331 (1976). See also: C.M. Lederer et al., Table of Isotopes, 7th Edition, John Wiley and Sons, Inc., N.Y. (1978).

MS84 James W. Meadows and Donald L. Smith, ANL/NDM-60, Argonne National Laboratory (1984).

Mug84 S. Mughabghab, Neutron Cross Sections, Vol. I-Resonance Parameters, Academic Press, New York (1984).

Nak+82 T. Nakamura et al., Proc. 4th Symposium on Accelerator Sci. Technol., RIKEN, Saitama, 24-26 November 1982, pp. 155-156 (1982).

Pek89 L.K. Peker, Nuclear Data Sheets 58, 93 (1989).

Pek90 L.K. Peker, Nuclear Data Sheets 61, 189 (1990). See also: L.K. Peker, Nuclear Data Sheets 42, 457 (1984).

SM73 Donald L. Smith and James W. Meadows, ANL-7989, Argonne National Laboratory (1973).

SM86 D.L. Smith and J.W. Meadows, ANL/NDM-95, Argonne National Laboratory (1986).

SMB85 D.L. Smith, J.W. Meadows and M.M. Bretscher, ANL/NDM-93, Argonne National Laboratory (1985).

SMG85 D.L. Smith, J.W. Meadows and P.T. Guenther, ANL/NDM-90, Argonne National Laboratory (1985).

SMG90 D.L. Smith, J.W. Meadows and L.R. Greenwood, Proc. 7th ASTM-Euratom Symposium on Reactor Dosimetry, Strasbourg,

France, 27-31 August 1990, eds. R. Dierckx and W.N. McElroy (1990).

Smi+91 D.L. Smith, J.W. Meadows, H. Vonach, M. Wagner, R.C. Haight and W. Mannhart, Proc. International Conference on Nuclear Data for Science and Technology, 13-17 May 1991, ed. S. Qaim, Juelich, Germany (to be published in 1991).

SSD91 U. Schuetzig, H. Schrader and K. Debertin, Proc. International Conference on Nuclear Data for Science and Technology, 13-17 May 1991, ed. S. Qaim, Juelich, Germany (to be published in 1991).

Tul90 J.K. Tuli, "Nuclear Wallet Cards", National Nuclear Data Center, Brookhaven National Laboratory (1990).

Von91 H. Vonach, Proc. International Conference on Nuclear Data for Science and Technology, 13-17 May 1991, ed. S. Qaim, Juelich, Germany (to be published in 1991).

WMH74 R. Woods, J.L. McKibben and R.L. Henkel, Nucl. Instr. and Meth. 122, 81 (1974).

CONSISTENT ACTIVATION CROSS SECTION CALCULATIONS FOR ALL STABLE ISOTOPES OF V, Cr, Mn, Fe, Co, Ni *

M. Avrigeanu, M. Ivascu and V. Avrigeanu

Institute of Physics and Nuclear Engineering, Bucharest, Romania

Abstract: Comparison of the available experimental fast neutron reaction excitation functions on all stable isotopes of the elements V, Cr, Mn, Fe, Co, and Ni with nuclear model calculations is presented. Neutron and charged-particle emission spectra have also been analyzed in order to validate the pre-equilibrium emission model calculations (with no free internal parameters). The trial procedure involved provides confidence in the nuclear-model parameter basis used and makes possible calculations of increased accuracy for activation cross sections in this mass range, required for applications.

Nuclear model calculations carried out within IPNE to improve the methods and the calculated fast neutron cross sections, with application in the atomic mass range A=50, have achieved the following points.

(a) Consistent pre-equilibrium emission and Hauser-Feshbach statistical model calculations have been made possible by: (1) generalization of the Geometry-Dependent Hybrid (GDH) pre-equilibrium emission model through the inclusion of the **alpha-particle emission** [1] as well as of the angular momentum and parity conservation [2,3], and (2) the **unitary use of the common parameters** of the two models. The last point concerns also the Distorted Wave Born Approximation (DWBA) method used to describe the direct inelastic scattering on discrete excited nuclear states while the GDH model has been proved to describe the same process in the continuum [4].

(b) **Consistent sets of input parameters**, determined or validated by means of various independent types of experimental data, are used in these calculations. A particular attention was given to nuclear level density semi-empirical formulas [5] and gamma-ray strength functions [6]. On the other hand, a single set of two-fermion level density parameters has been used [7] to get both the exciton state densities (involved in the GDH model) and the nuclear level densities for statistical

---

* Work done in the frame of the **IAEA** Co-ordinated Research Progamme on **"Methods for the Calculation of Neutron Nuclear Data for Structural Materials of Fast and Fusion Reactors"**, and Research Contract 3802/R4/RB

model calculations. Furthermore, a **realistic nuclear level density approach** has been established by analyzing the fast neutron reaction excitation functions on the stable isotopes of Cr, Fe and Ni [1], as a direct outcome of using consistent parameter sets.

(c) **The unitary account** of a whole body of related experimental data for isotope chains of the neighbouring elements Cr, Fe and Ni has increased the predictive capability of these calculations. In a subsequent step the parameter set already established and used in analyzing the data of the above-mentioned elements has been involved in a similar analysis carried out for the isotopes ^{51}V, ^{55}Mn, and ^{59}Co. The same work is presently done for all stable isotopes of Ti, for which the (n,p) and (n,2n) reactions were previously [8] analyzed.

In the present work is summarized the large amount of (n,p), (n,α), (n,2n), (n,3n), and (n,n'p) reaction experimental data for the target nuclei ^{51}V, $^{50,52,53,54}Cr$, ^{55}Mn, $^{54,56,57,58}Fe$, ^{59}Co, $^{58,60,61,62,64}Ni$, which have been well described on the above-mentioned basis (so-called "two-step approach" of semi-classical unified nuclear reaction theory [9]). Neutron and charged-particle emission spectra have also been analyzed in order to validate the pre-equilibrium emission model calculations (with no free internal parameters [10]).

Following the above-described calculations, analysis of the trend of calculated and experimental neutron cross sections at the 14.7 MeV incident energy, against the asymmetry parameter (N-Z)/A, has been carried out with following results [11]: (**a**) good agreement with experimental data for the model prediction across the valley of stability, and (**b**) the unknown cross sections have been predicted with higher accuracy with respect to the gross systematics of the isotope effect.

The present conclusions could be completed by a comparison between semi-classical and quantum-mechanical theories, performed by using the same consistent parameter set, which has given a good agreement of the GDH and MSC cross sections at the pre-equilibrium emission energies [12]. The absence of any free parameter adjusted in the cross sections

analyses, for both theories, should be pointed out. Therefore, the present method and parameter basis could be quite useful for accurate predictions of reaction cross sections important for activation [13].

References

1. Avrigeanu M., Ivascu M., Avrigeanu V.: Z. Phys. A **335**,299(1990)
2. Ivascu M., Avrigeanu M., Avrigeanu V.: Rev. Roum. Phys. **32**,713(1987)
3. Avrigeanu M., Ivascu M., Avrigeanu V.: Z. Phys. A **329**, 177(1988)
4. Avrigeanu M., Bucurescu D., Ivascu M., Semenescu G., Avrigeanu V.: J. Phys. G: **15**,L241(1989)
5. Ivascu M., Avrigeanu M., Avrigeanu V.: Rev. Roum. Phys. **32**,697(1987)
6. Avrigeanu M., Avrigeanu V., Cata G., Ivascu M.: Rev. Roum. Phys. **32**,837(1987)
7. Avrigeanu M., Avrigeanu V.: J. Phys. G: **15**,L261(1989)
8. Avrigeanu M., Ivascu M., Avrigeanu V.: Atomkernenergie-Kerntechnik **49**,133(1987)
9. Blann M.: in Proc. IAEA AGM on Nuclear Theory for Fast Neutron Nuclear Data Evaluation, IAEA-TECDOC-483, IAEA, Vienna, 1988, p.195
10. Hodgson P.E.: in Proc. Int. Conf. on Nuclear Data for Science and Technology, May/June 1988, Mito, Japan, S. Igarasi (Ed.), Tokyo: Saikon, p. 655
11. Avrigeanu M., Avrigeanu V.: in Proc. Int. Conf. on Nuclear Data for Science and Technology, May 1991, Jülich, FRG, contribution D41
12. Avrigeanu M., Hodgson P.E.: Int. Conf. on Nuclear Reaction Mechanisms, Varenna, June 1991.
13. Forrest R.A., Sowerby M.G.: **"UK Work on Activation Related Nuclear Databases and Codes"**, IAEA Consultants'Meeting "First Results of FENDL-1 and Start of FENDL-2", Vienna, 25-28 June, 1990.

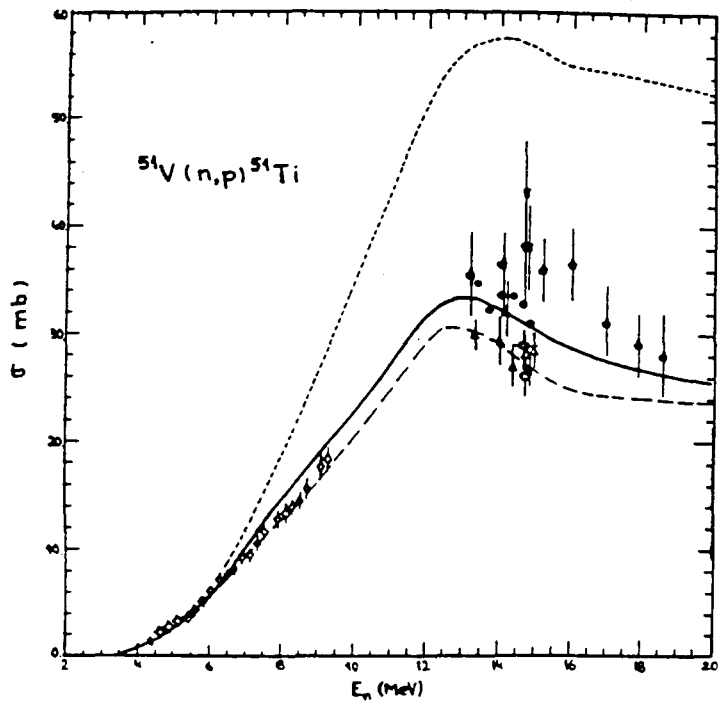

Fig. 1

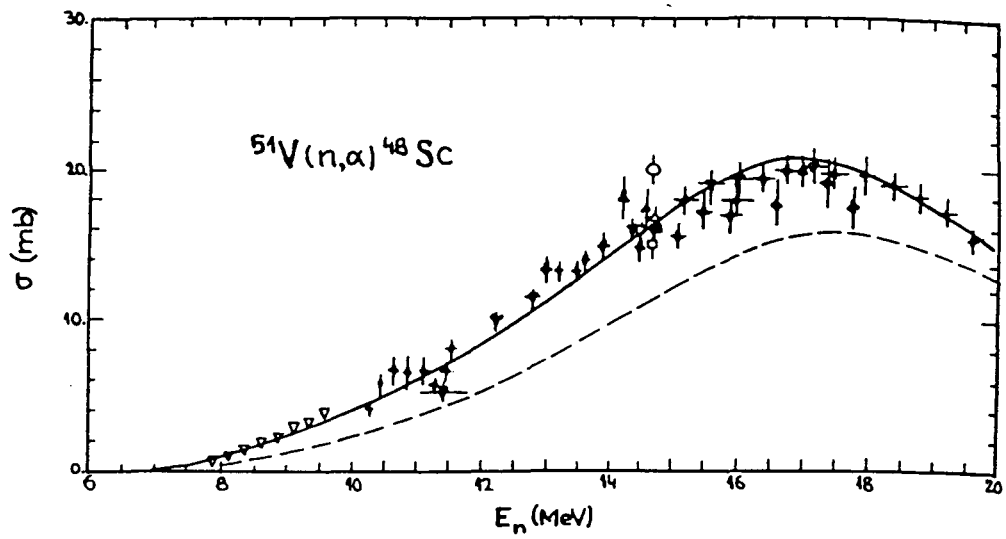

Fig. 2

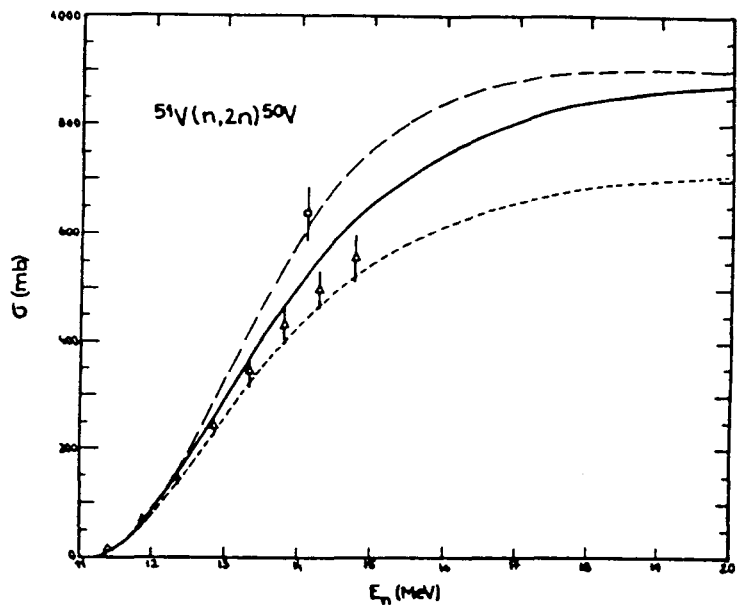

Fig. 3

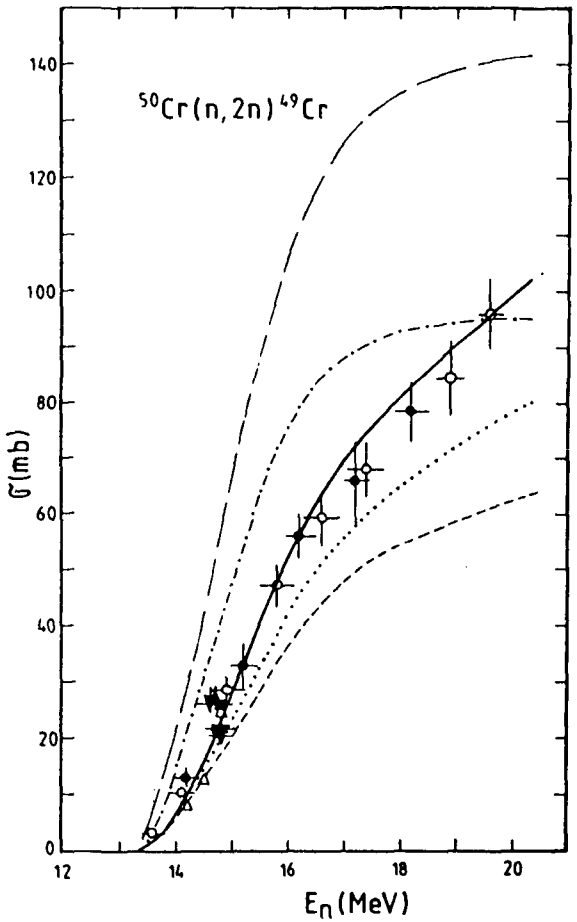

Fig. 4

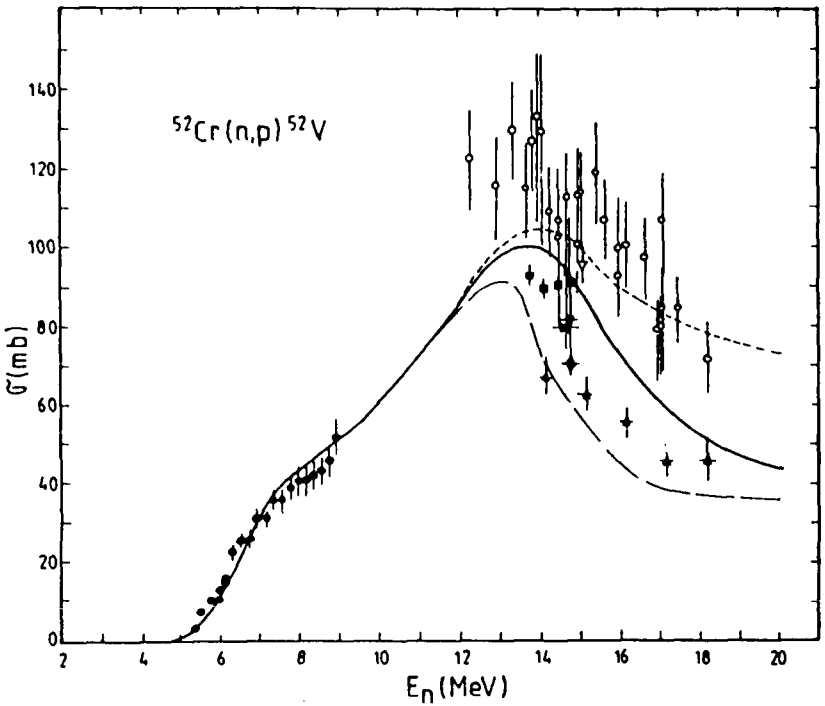

Fig. 5

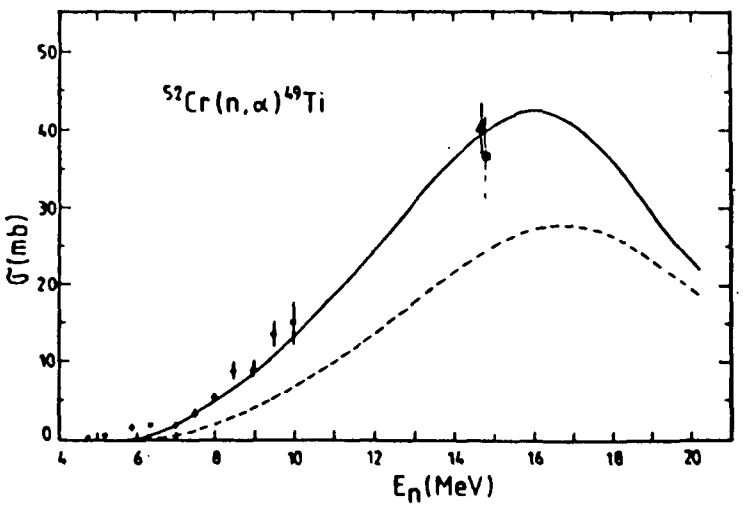

Fig. 6

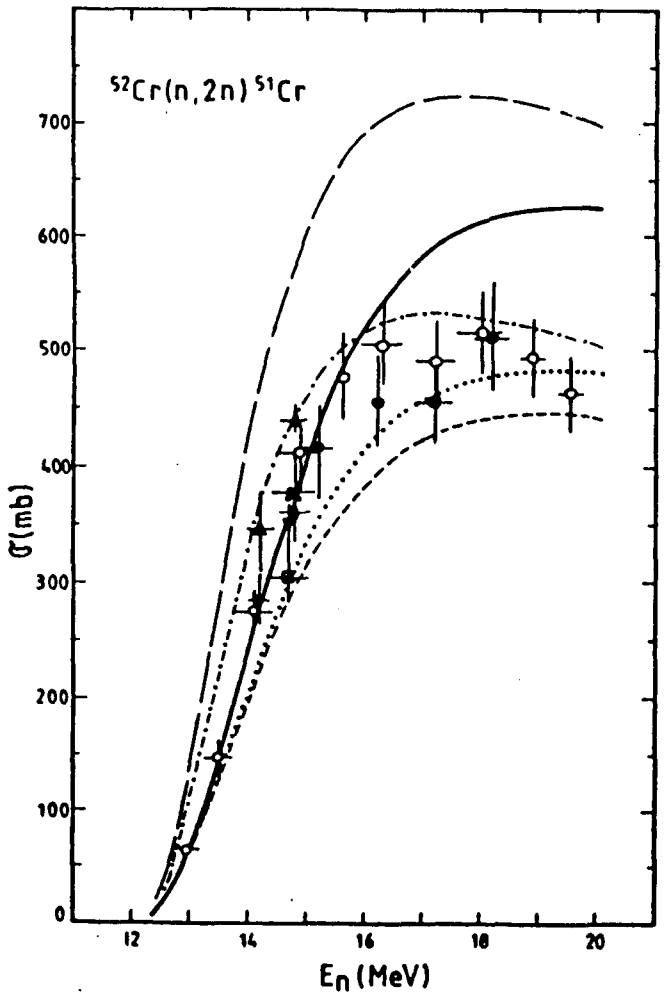

Fig. 7

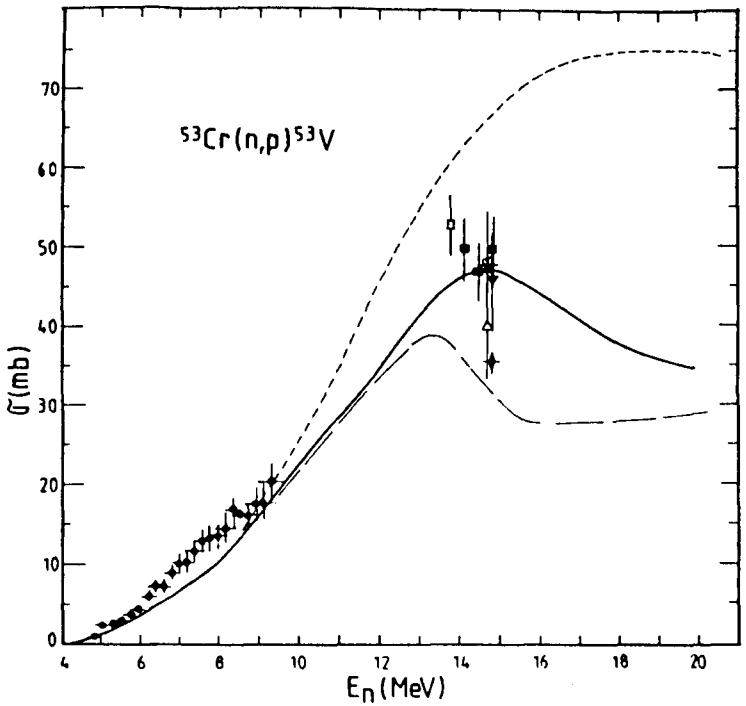

Fig. 8

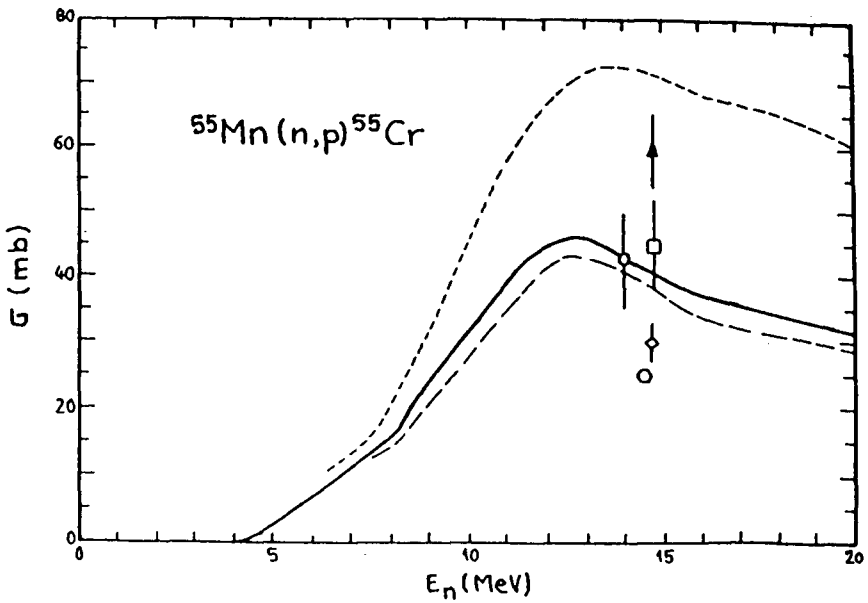

Fig. 9

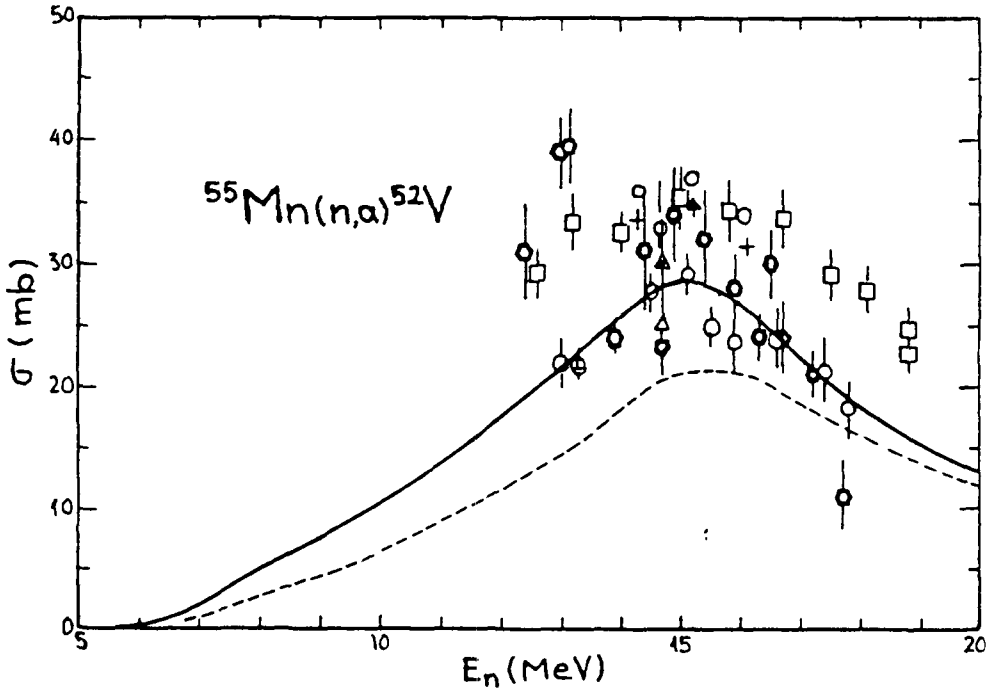

Fig. 10

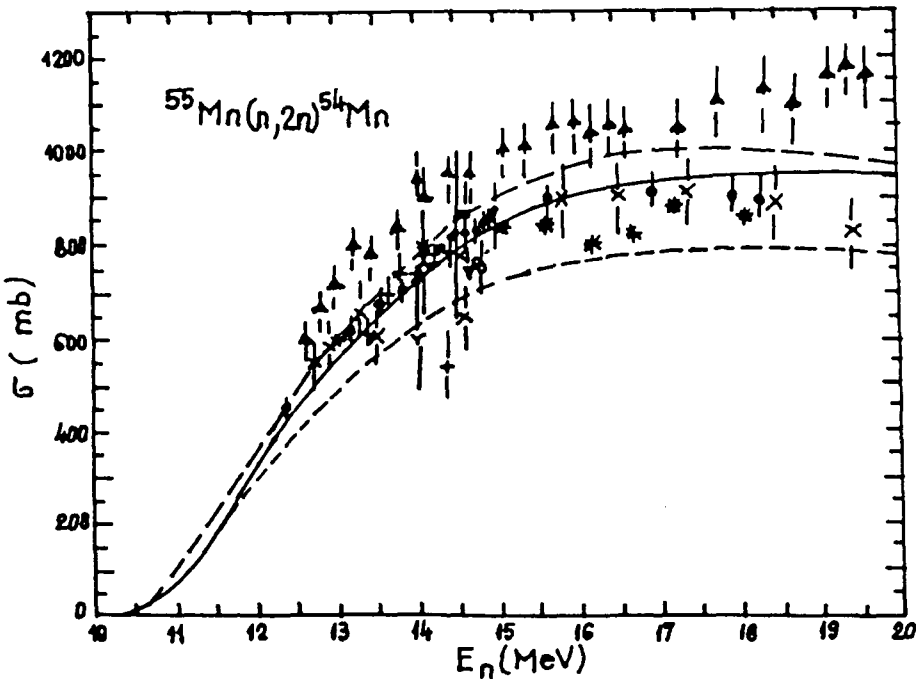

Fig. 11

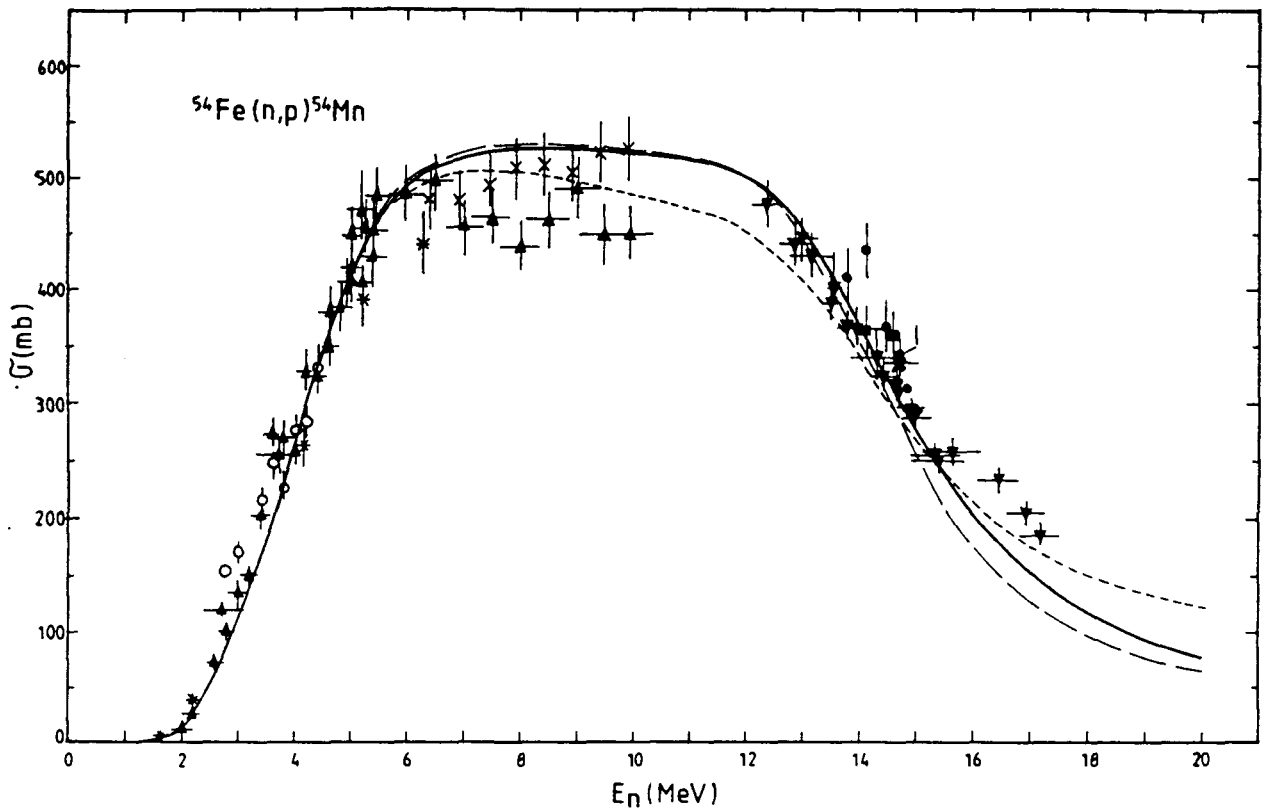

Fig. 12

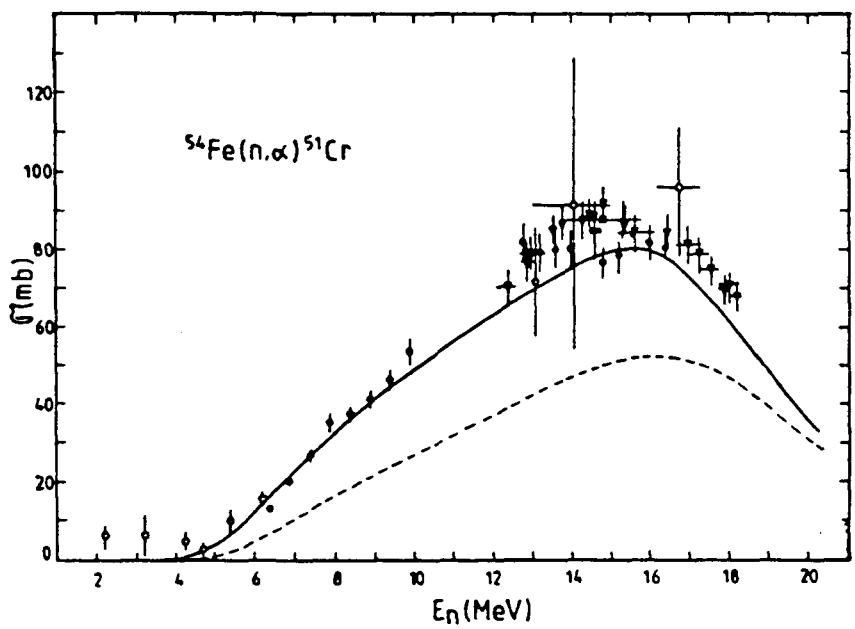

Fig. 13

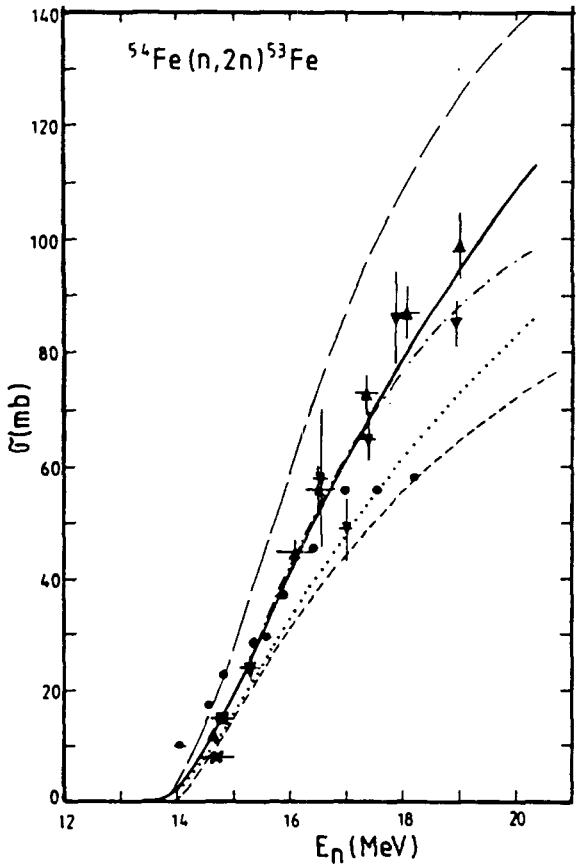

Fig. 14

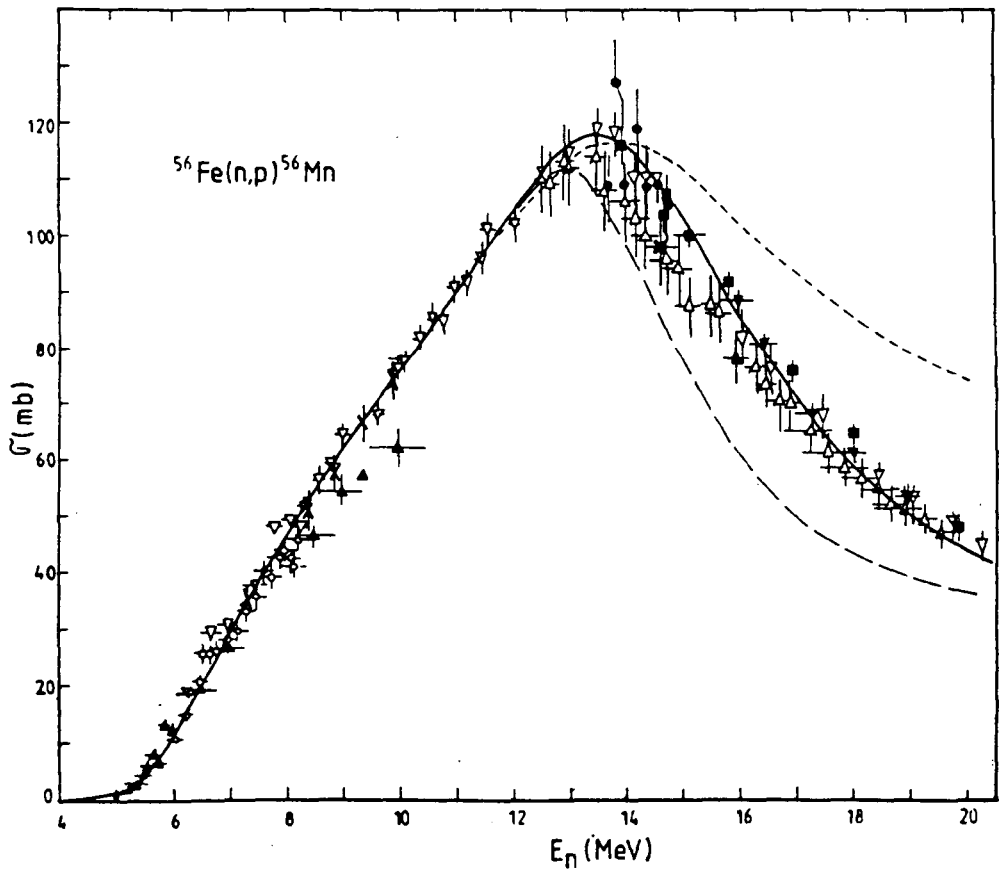

Fig. 15

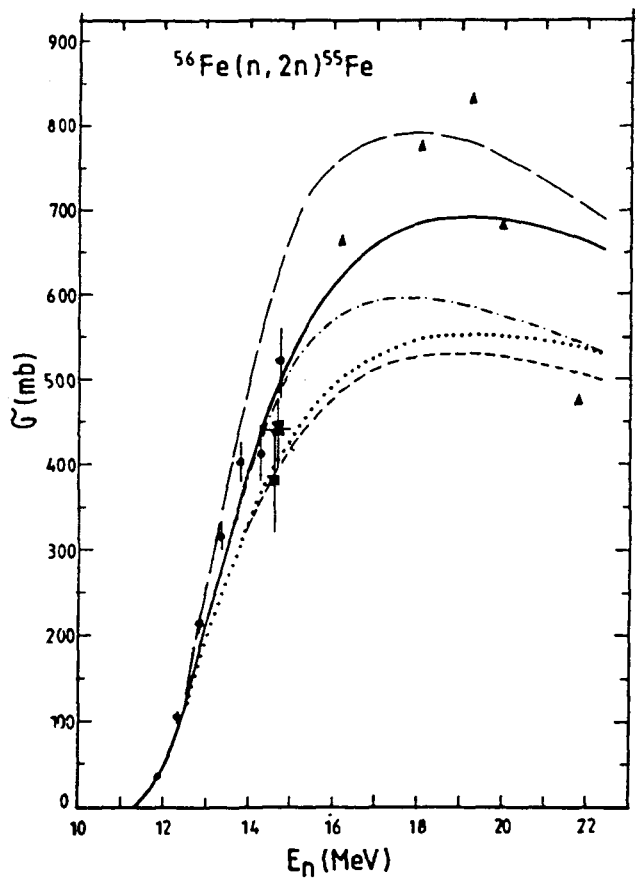

Fig. 16

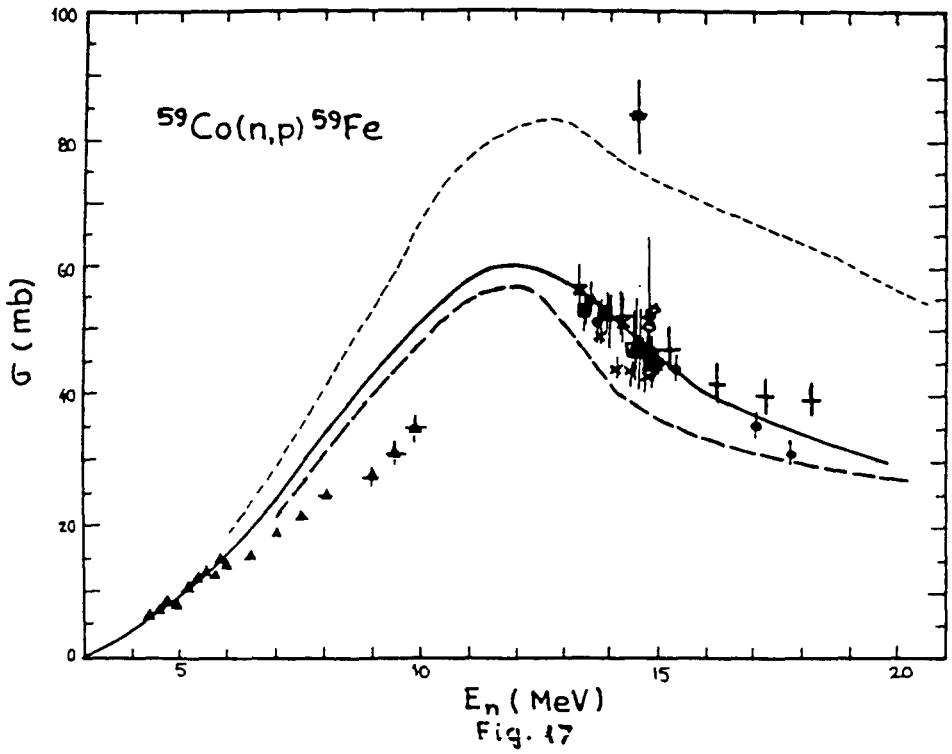

Fig. 17

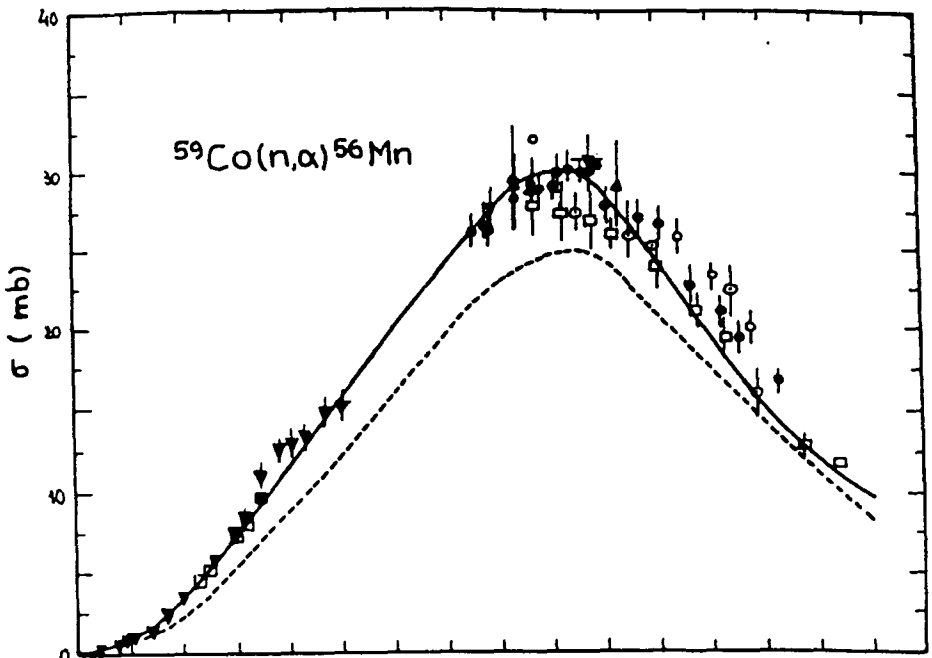
$^{59}Co(n,\alpha)^{56}Mn$
σ (mb)
E n (MeV)

Fig. 18

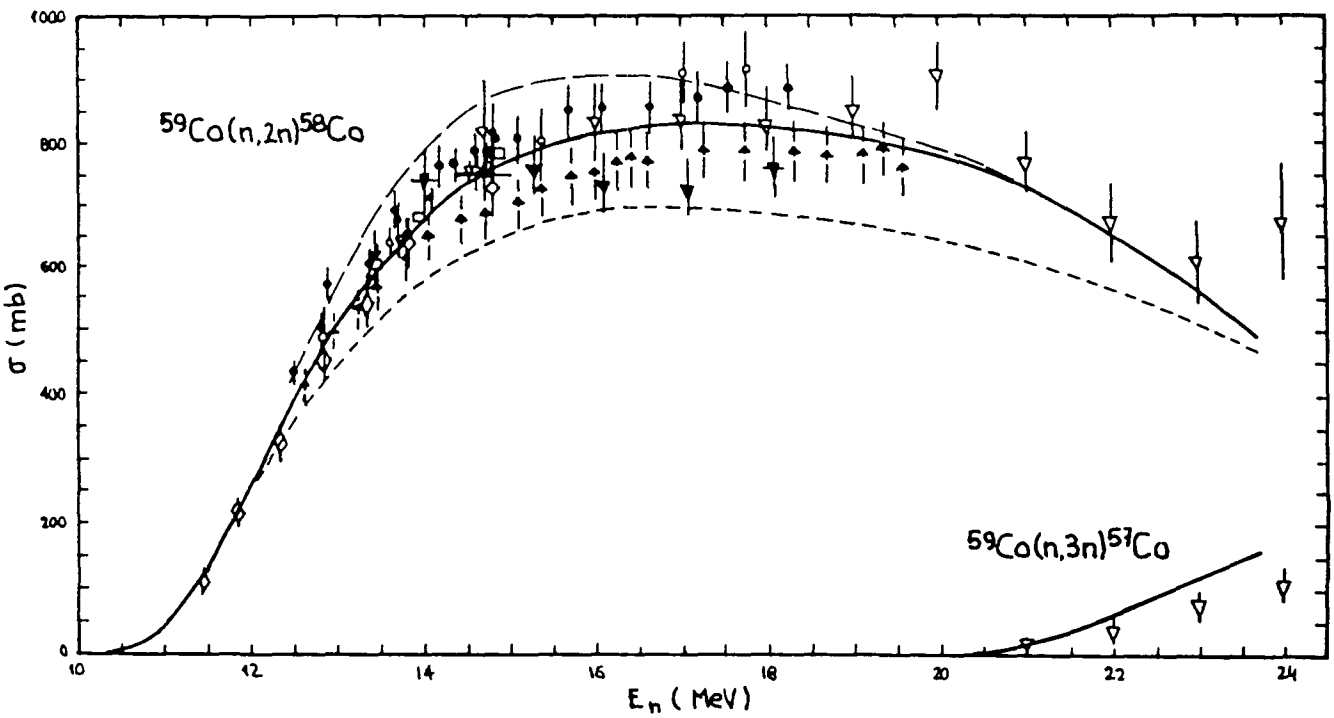
$^{59}Co(n,2n)^{58}Co$
$^{59}Co(n,3n)^{57}Co$
σ (mb)
E n (MeV)

Fig. 19

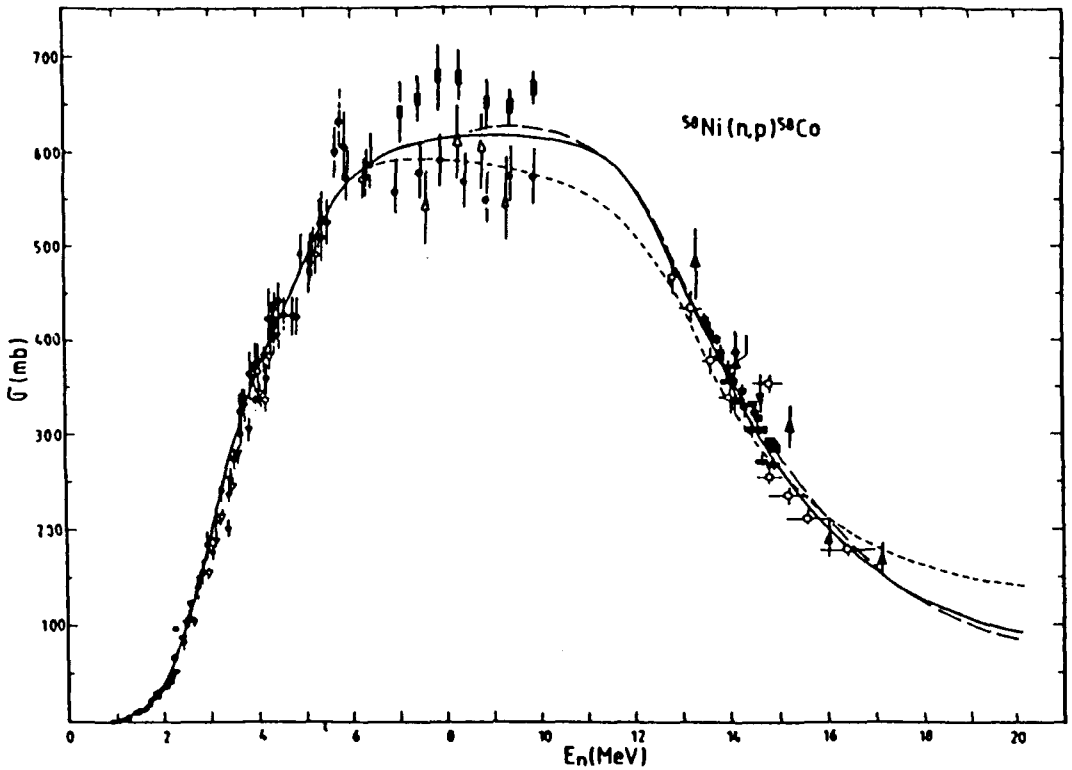

Fig. 20

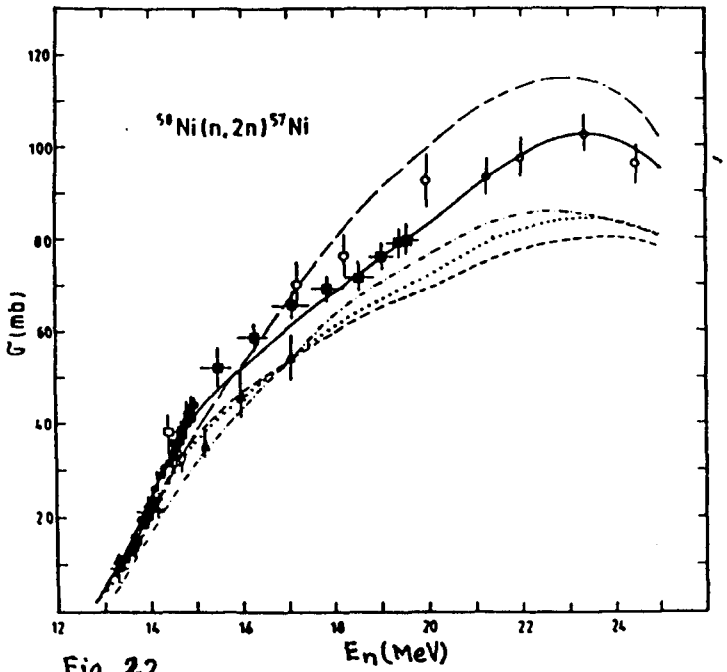

Fig. 22

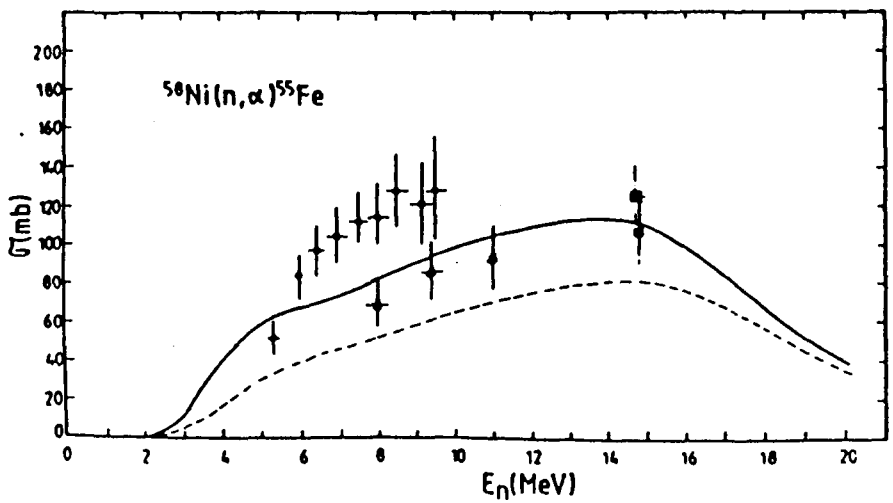

Fig. 21

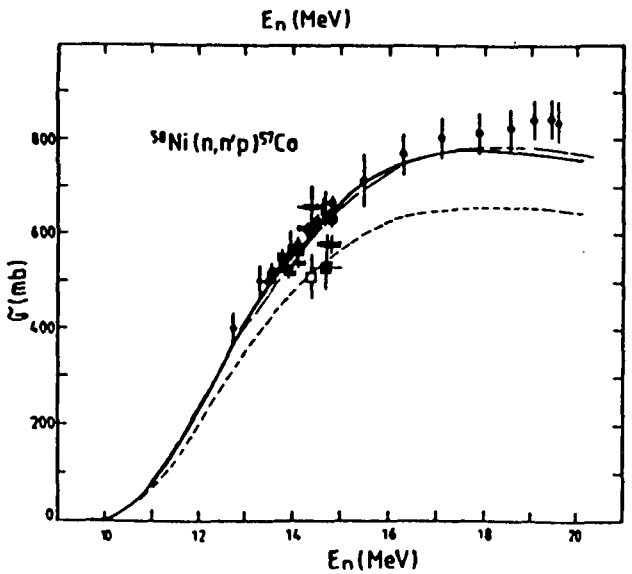

Fig. 23

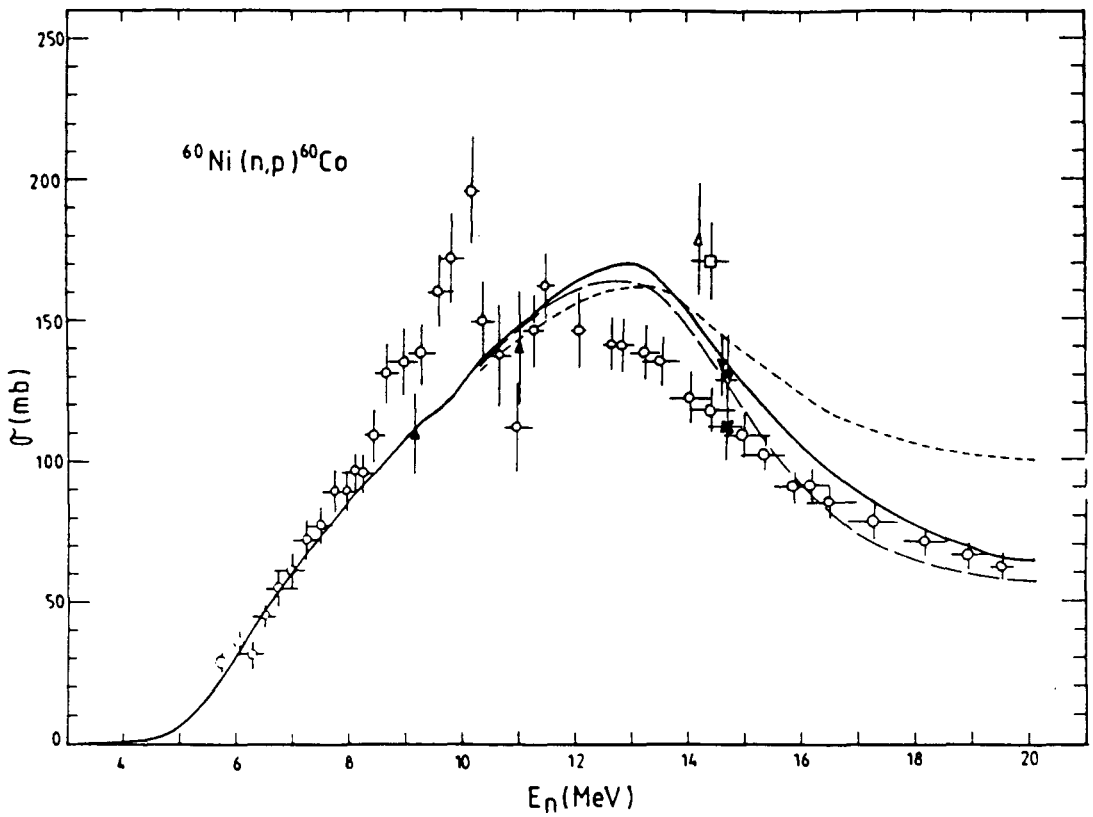

Fig. 24

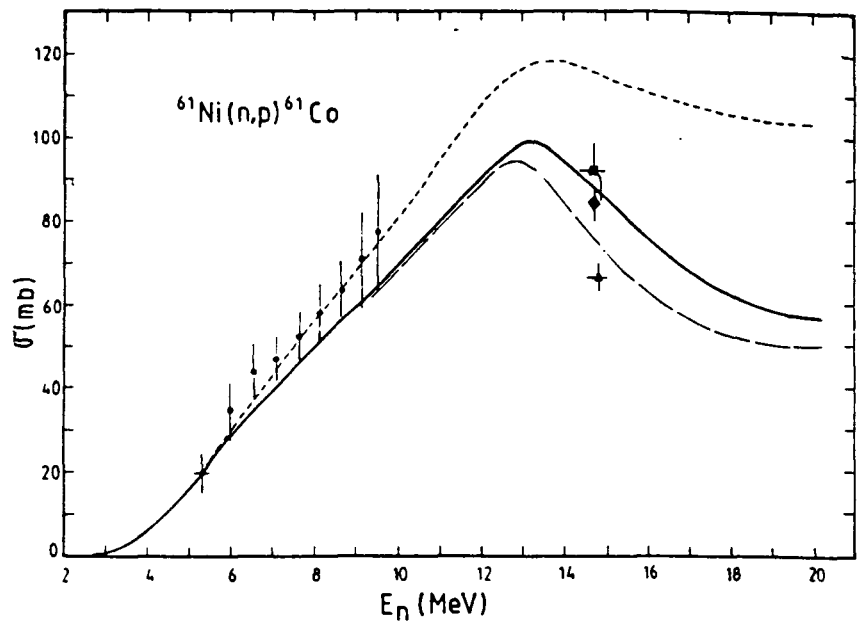

Fig. 25

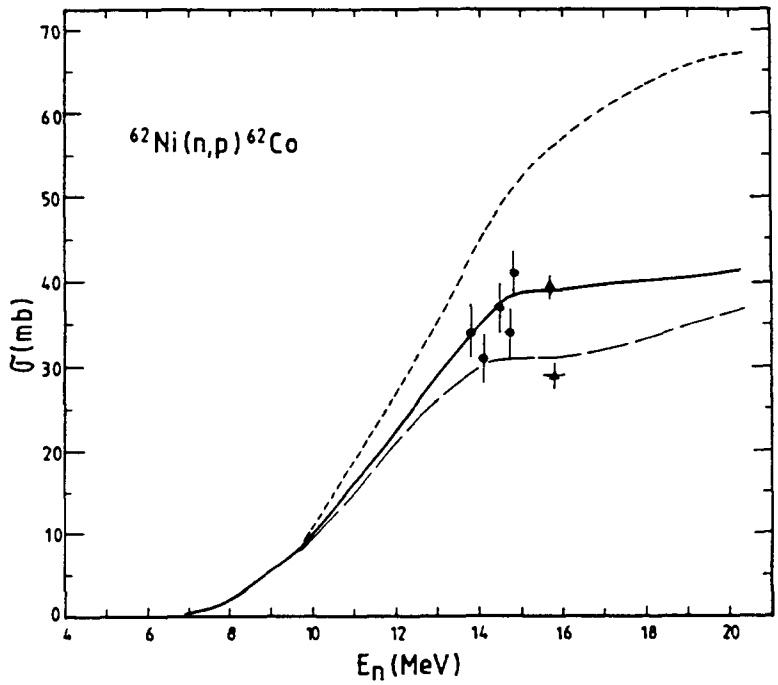

Fig. 26

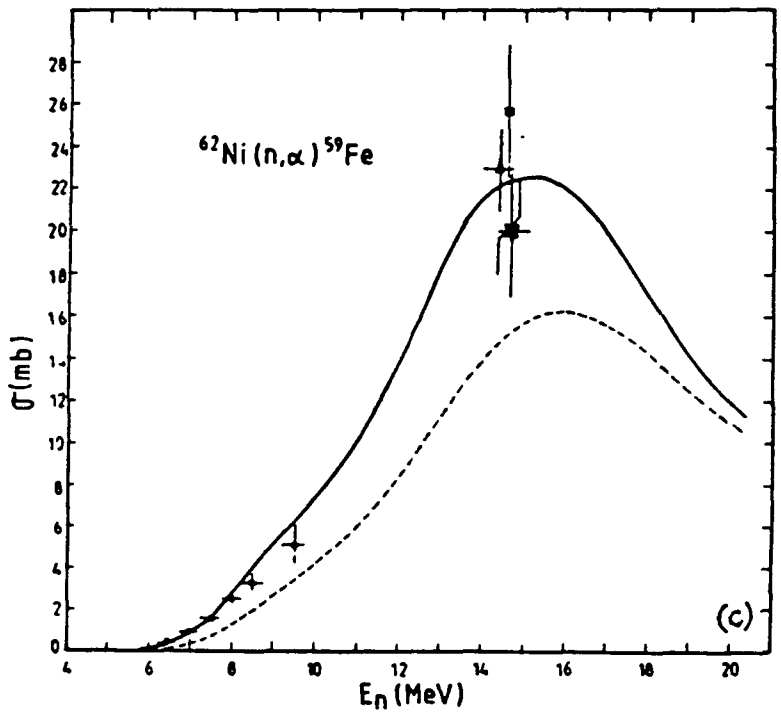

Fig. 27

Calculations of Long-Lived Isomer Production in Neutron Reactions

M.B. Chadwick and P.G. Young
Theoretical Division, Los Alamos National Laboratory, Los Alamos, New Mexico 87545

We present theoretical calculations for the production of the long-lived isomers ^{93m}Nb (1/2-,16yr), ^{121m}Sn (11/2-, 55 yr), ^{166m}Ho (7-, 1200 yr), ^{184m}Re (8+, 165 d), ^{186m}Re (8+, 2×10^5 yr), ^{178m}Hf (16+, 31 yr), ^{179m}Hf (25/2-, 25 d), and ^{192m}Ir (9+, 241 yr), all of which pose potential radiation activation problems in nuclear fusion reactors if produced in 14-MeV neutron-induced reactions. We consider $(n, 2n)$, (n, n'), and (n, γ) production modes and compare our results both with experimental data (where available) and systematics. We also investigate the dependence of the isomeric cross section ratio on incident neutron energy for the isomers under consideration. The statistical Hauser-Feshbach plus preequilibrium code GNASH was used for the calculations. Where discrete state experimental information was lacking, rotational band members above the isomeric state, which can be justified theoretically but have not been experimentally resolved, were reconstructed.

I. INTRODUCTION

Fusion systems operating on the deuterium-tritium reaction give rise to intense neutron fluxes that cause structural components to be activated. The first wall, in particular, is subjected to neutron damage that could require its replacement every few years. Disposal or reuse of the material would be facilitated if the activation could be kept to low limits, and therefore there is a search for materials that will give rise to the minimum activation. The neutron fluxes in fusion systems are expected to be so high that multiple reactions will be possible in which a given nucleus interacts with a succession of neutrons. As a result, it is often important to have activation cross sections for unstable as well as stable nuclides. As there is often a lack of experimental data on activation cross sections of interest, it is important to be able to assess these cross sections theoretically. In this paper we shall present calculations of activation cross sections for a number of long-lived isomeric states which are considered important for fusion reactor design.

The isomeric state production cross sections that we have considered were calculated at the request of the United Kingdom and United States fusion programs, which are in the process of establishing nuclear data libraries and inventory code packages to enable activation in virtually any material to be estimated. In a recent paper [1] we presented theoretical calculations of the production cross sections of hafnium isomers in 14 MeV reactions, using the GNASH [2] code. These calculations were performed prior to the release of experimental measurements [3] of the cross sections for hafnium isomer production, and agreement to within a factor of 2-3 was found. Because the cross sections under consideration were rather small and the isomer spins very large, the agreement obtained was encouraging, and suggested that our theoretical approach can be extended for use in other isomer-production calculations. We

have, therefore, now determined production cross sections for long-lived isomers in Nb, Sn, Ho, Re and Ir at 14 MeV. In addition, we have determined the variation of the production cross section with incident neutron energy, since neutron energies below 14 MeV are produced in fusion reactors in inelastic collisions. As the energy variation of the hafnium isomer production was not shown in Ref.1 we summarize our previous results for hafnium and give this variation.

The systematics of neutron-induced isomeric cross section ratios at 14.5 MeV have been been studied by Kopecky and Gruppelaar [4]. They used a simplified version of the GNASH code to determine the ratio of the cross section to the isomeric state and ground state in (n,n'), (n,p), (n,t), (n,α), and $(n,2n)$ reactions, replacing the realistic nuclear level structure by two discrete states (the ground state and the isomeric state) plus a continuum of statistically described states. Their approach is, therefore, considerably simpler than our calculations and so we have compared our results with the Kopecky systematics. We shall show that while such systematics are very useful, in many cases a full calculation (with a realistic description of the nuclear structure) is important in accurately determining isomer ratios. Also, Kopecky and Gruppelaar point out that their calculation is particularly sensitive to the simple model parameters that they adopt for the $(n,2n)$ reaction. Our investigations into an analogous simple model confirm this, and indicate that for certain reactions one should be wary about using simple systematic predictions. Finally, our calculations also include isomeric ratios for states formed in (n,γ) reactions, which are particularly resistant to simple systematics-based descriptions.

In Section II we give a brief description of the theoretical models that we use to describe the nuclear reactions, and in section III we show our results, and compare them with the Kopecky systematics and experimental data where available. We shall use the hafnium isomer calculations as a detailed example of our approach, and then indicate the isomer ratios, and their energy dependences, that we obtain for other nuclei. We give some conclusions concerning our general approach in Section IV.

II. DESCRIPTION OF THE CALCULATIONS

A. General Description

The GNASH nuclear theory code [2] is based on the Hauser-Feshbach statistical theory with full angular momentum conservation, and with width fluctuation corrections obtained from the COMNUC code [5] using the Moldauer approach. Preequilibrium emission processes, which are important for incident energies above about 10 MeV, are calculated using the exciton model of Kalbach [6]. Transmission coefficients for neutrons and charged particles are calculated using an optical model, and gamma-ray transmission coefficiens are obtained from giant dipole resonance approximations [7,8],making use of detailed balance. The level structure for each residual nucleus in a calculation is divided into discrete and continuum regions, with the former obtained from experimental complilations and the latter from phenomenological level density representations.

B. Optical Model

Both the Hauser-Feshbach theory and the exciton model require optical potentials to calculate transmission coefficients and inverse reaction cross sections. The coupled

channels code ECIS [9] was used for deformed nuclei, and the code SCAT2 [10] for spherical nuclei. Before using an optical potential to generate transmission coefficients and reaction cross sections, the potentials were checked by comparing their predictions of elastic and total cross sections with experimental data, where available.

C. Gamma-Ray Transmission Coefficients

Transmission coefficients for gamma-ray emission coefficients were obtained using detailed balance, exploiting the inverse photoabsorption process. The Brink-Axel hypothesis is used, permitting the cross section for photoabsorption by an excited state to be equated with that of the ground state. The gamma-ray transmission coefficients were obtained from the expression

$$T^{X\ell}(\epsilon_\gamma) = 2\pi f_{X\ell}(\epsilon_\gamma)\epsilon_\gamma^{2\ell+1} , \tag{1}$$

where ϵ_γ denotes gamma-ray energy, $X\ell$ indicates the multipolarity of the gamma-ray, and $f_{X\ell}$ is the energy-dependent gamma-ray strength function. The strength functions for E1 decay were calculated either from standard Lorentzian expressions [7], given by

$$f_{E1}(\epsilon_\gamma) = K_{E1}\frac{\sigma_0\epsilon_\gamma\Gamma^2}{(\epsilon_\gamma^2 - E^2)^2 + \epsilon_\gamma^2\Gamma^2} \tag{2}$$

or from the generalized Lorentzian of Kopecky and Uhl [8] (which actually represents a partial breakdown of the Brink-Axel hypothesis),

$$f_{E1}(\epsilon_\gamma, T) = K_{E1}\left[\frac{\epsilon_\gamma\Gamma(\epsilon_\gamma)}{(\epsilon_\gamma^2 - E^2)^2 + \epsilon_\gamma^2\Gamma(\epsilon_\gamma)^2} + \frac{0.7\,\Gamma\,4\pi^2T^2}{E^5}\right]\sigma_0\Gamma , \tag{3}$$

where

$$\Gamma(\epsilon_\gamma) = \Gamma\frac{\epsilon_\gamma^2 + 4\pi^2T^2}{E^2} \tag{4}$$

$$T = \sqrt{\frac{B_n - \epsilon_\gamma}{a}} , \tag{5}$$

and $K_{E1} = 8.68 \times 10^{-8}\text{mb}^{-1}\ \text{MeV}^{-2}$ (nominally) but was usually determined empirically by matching the theoretical gamma-ray strength function for s-wave neutrons to experimental values compiled by Mughabghab [11]. The quantities B_n and a are the neutron binding energy and Fermi gas level density parameter, respectively. The Lorentzian parameters of the giant-dipole resonance, E and Γ, are taken from the tables of Dietrich and Berman [12].

In addition to E1 radiation, M1 and E2 components are also included. For M1, a standard Lorentzian expression was used for the gamma-ray strength function. When the Kopecky-Uhl formulation was employed, a giant resonance formulation was also used to calculate the E2 strength function [8]; otherwise, a Weisskopf expression (f_{E2} = constant) was incorporated.

The level density model of Gilbert and Cameron [13] was used in the Hauser–Feshbach calculations. At high energies the Fermi gas model is used along with a constant temperature form for lower energies. A gaussian distribution of spin states is taken to describe the angular momenta of levels at a certain excitation energy

$$\rho(E,J,\pi) = \frac{(2J+1)}{2\sqrt{2\pi}\sigma^2}\exp\frac{-(J+\frac{1}{2})^2}{2\sigma^2}\rho(U) \tag{6}$$

where $U = E-\Delta$ (Δ is the pairing energy) and σ^2 is the spin cut–off parameter which is determined via $\sigma^2 = 0.146\sqrt{aU}A^{\frac{2}{3}}$ for the Fermi gas region. The spin cut-off factor is also determined from the spin distribution of observed low lying discrete levels and in the constant temperature region σ^2 is linearly interpolated between this value and the value of σ^2 where the Fermi gas region begins. In the high energy region the Fermi gas expression for $\rho(U)$ is

$$\rho(U) = \frac{\sqrt{\pi}}{12}\frac{1}{2\sqrt{\pi}\sigma}\frac{\exp 2\sqrt{aU}}{a^{\frac{1}{4}}U^{\frac{5}{4}}} \tag{7}$$

and at lower energies the constant temperature form is given by

$$\rho(E) = \frac{1}{T}\exp\frac{(E-E_o)}{T} \tag{8}$$

The pairing energy used to determine U is obtained from the Cook parameter set [14] and the level density parameters were calculated from the slow neutron resonance parameters of Mughabghab. The constant temperature $\rho(E)$ is chosen to match (both in value and in first derivative) the Fermi gas $\rho(U)$ at an energy E_{match} and to fit the known discrete levels at the lowest excitation energies. The parameters E_o, T and E_{match} are varied to achieve this.

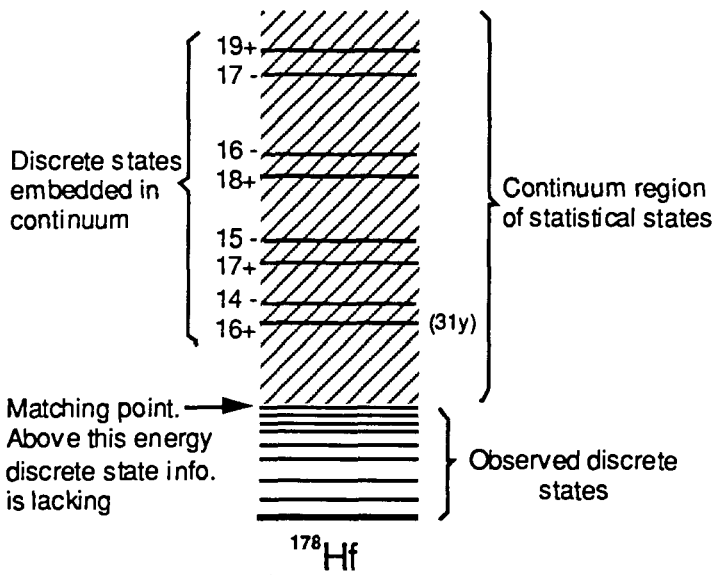

Fig. 1. A schematic representation of the combination of discrete, statistical and discrete levels embedded in the statistical continuum region used to describe the nuclear structure of ^{178}Hf.

The production cross section of a certain isomeric state is often particularly sensitive to the discrete nuclear level structure, since the gamma cascade of discrete states into the isomeric state will enhance its production. In many cases, the isomeric state of interest is a band-head, with a rotational band built upon it, though often the rotational band members have not been experimentally resolved and lie in a high-excitation energy region. Accordingly, the energies of the rotational levels were assessed theoretically (obtaining the moment of inertia from observed rotational bands at lower excitation energies) and GNASH was modified to allow these discrete levels to be embedded within the continuum of statistically described levels. In the case of our calculation of Hf isomers [1], this procedure was particularly important; we found that over 40% of the production of the ^{178}Hf(16+) in an $(n, 2n)$ reaction came from the decay of the 14- level and the inferred discrete rotational band states above the 14- and 16+ levels. In Fig. 1 we show schematically the combination of discrete and statistical levels for the case of the ^{178}Hf nucleus.

III. RESULTS

A. The Hafnium Isomers: A Detailed Example

By way of example, in this subsection we shall give details of the calculations for the production of hafnium isomers. Full details can be found in Ref. [1] .

The possibility of including small amounts of tungsten and tantalum in the first-wall material has been suggested, and after a few reactions on these nuclei hafnium could be produced. The presence of hafnium in a fusion reactor could pose serious activation problems due to the possible build-up of the isomeric state ^{178}Hf (J^π = 16+) with a 31-yr half life. This state, if produced in sufficient quantity, could lead to the first wall being active for a very long time after its removal from the reactor, and the high excitation energy of the state (2.447 MeV) results in harmful gamma radiation on its decay.

The ^{179}Hf$(n, 2n)$ and ^{178}Hf(n, n') reactions both give the ^{178}Hf(16+) isomer, with the (n,2n) reaction expected to be the dominant production mode. There is, however, also an isomeric state in ^{179}Hf($J^\pi = \frac{25}{2}-$) with a 25-day half life that is sufficiently long-lived for subsequent neutron-induced reactions to occur. Once this ^{179m}Hf($\frac{25}{2}-$) isomer is produced, it would be expected that subsequent $(n, 2n)$ reactions could take place with a relatively large cross section leading to ^{178m}Hf(16+) as the spin difference between these isomers is small. Thus we calculate the ^{179m}Hf($\frac{25}{2}-$) $(n, 2n)^{178m}$Hf(16+) reaction as well as those for the production of the ^{179m}Hf($\frac{25}{2}-$) state. Fig. 2 indicates the pathways that have been investigated.

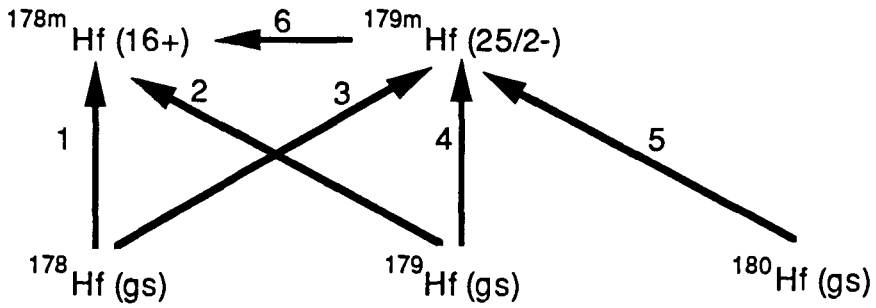

Fig. 2. Reaction pathways investigated for the hafnium isomers. Pathways 2, 5 and 6 are $(n, 2n)$ reactions; pathways 1 and 4 are (n, n') reactions, and pathway 3 is a (n, γ) reaction.

Both the 16+ state and the $\frac{25}{2}-$ state are rotational band heads, though none of the other members of the rotational bands have been detected. In addition, there is a 14- band head state above the 16+ state that decays into the latter. Since a sizable fraction of the production cross section of these high-spin states comes from the gamma decay of higher-energy states, the rotational states were included explicitly into the calculation, their energies being estimated by determining the moment of inertia from low-lying rotational bands. These rotational levels were then embedded into the continuum of statistically described states (see Fig. 1 for a schematic illustration). Because the hafnium isotopes are highly deformed, the coupled channels code ECIS [9] was used to evaluate the transmission coefficients and the direct scattering cross sections to low-lying states. The optical potential that we used [15] described the total elastic and total cross sections fairly well.

In Table I below we show our theoretical results, along with experimental measurements where available. The experimental numbers of Patrick *et al.* [3] have been extracted from data assuming that the ratios of our theoretical results for production of the same isomeric state though different reactions are correct. In the experimental numbers that are quoted, the natural abundances of Hf have been taken into account. Reactions 1 through 6 are of importance for the determination of the production of the ^{178m}Hf(16+) state in fusion reactors, and are numbered according to the pathways in Fig. 2. Reactions 7,8 and 9 are also shown to allow further comparisons of our calculations with data.

TABLE I

Theoretical Cross Sections for the Production of Isomeric States in Hafnium Compared with Data Where Available*

Isomer Production Reaction	Theoretical Cross Section (mb)	Experimental Cross Section[a] (mb)
1. ^{178}Hf$(n,n')^{178m}$Hf(16+, 31 yr)	4.8×10^{-2}	
2. ^{179}Hf$(n,2n)^{178m}$Hf(16+, 31 yr)	2.9	5.91 ± 0.64
3. ^{178}Hf$(n,\gamma)^{179m}$Hf(25/2-, 25 days)	1.9×10^{-5}	
4. ^{179}Hf$(n,n')^{179m}$Hf(25/2-, 25 days)	5.7	12.8 ± 1.5
5. ^{180}Hf$(n,2n)^{179m}$Hf(25/2-, 25 days)	7.4	16.7 ± 1.9
6. ^{179m}Hf$(n,2n)^{178m}$Hf(16+, 31 yr)	158	
7. ^{180}Hf$(n,2n)^{179n}$Hf(1/2-, 18.7 s)	220	598 (Sothras) 690 (Rurarz) 570 (Prasad)
8. ^{180}Hf$(n,n')^{180n}$Hf(8-, 5.5 h)	19	12.4 (Hillman)
9. ^{179}Hf$(n,2n)^{178n}$Hf(8-, 4 s) + ^{178}Hf$(n,n')^{178n}$Hf(8-, 4 s)	1200	1452 ± 116 (Salaita) 749 ± 75 (Sothras)

*The reactions are numbered according to the pathways shown in Fig. 2.

[a]All Experimental Data are taken from the Brookhaven National Laboratory SCISRS file, except those of Patrick *et al.* [3].

B. The (n,2n) Isomeric Cross Section Ratios

We have concentrated on the $(n, 2n)$ reaction mechanism for isomer production since, at 14 MeV, this is the dominant process through which most of the reaction flux goes. The following isomeric states, in addition to the hafnium states, have been considered in detail: ^{121m}Sn (11/2-, 55 yr) , ^{166m}Ho (7-, 1200 yr), ^{184m}Re (8+, 165 d), ^{186m}Re (8+, 2×10^5 yr), and ^{192m}Ir (9+, 241 yr). In all cases the experimentally measured discrete states have been examined and a matching point above which experimental data is missing has been determined. Rotational bands above the isomers were determined theoretically and included in the calculation, as discussed above. Optical potentials were found and checked against elastic and total scattering data, where available. In Table II below we show our results for the isomeric cross section ratio (the ratio of cross section to the isomeric state to the sum of the cross sections to ground state and isomeric state), for neutron energies between 8 and 14 MeV.

TABLE IIa
Isomeric Cross Section Ratios in (n,2n) Reactions

Neutron Energy (MeV)	^{122}Sn (n,2n) ^{121m}Sn (11/2-)	^{167}Ho (n,2n) ^{166m}Ho (7-)	^{179}Hf (n,2n) ^{178m}Hf (16+)	^{180}Hf (n,2n) ^{179m}Hf (25/2-)
8	0.	0.52	0.	0.
9	0.61	0.42	3.8×10^{-6}	5.1×10^{-6}
10	0.61	0.41	1.2×10^{-4}	1.6×10^{-4}
11	0.67	0.43	3.0×10^{-4}	5.3×10^{-4}
12	0.68	0.45	5.7×10^{-4}	1.1×10^{-3}
13	0.70	0.47	8.9×10^{-4}	2.4×10^{-3}
14	0.72	0.49	1.4×10^{-3}	3.6×10^{-3}

TABLE IIb
Isomeric Cross Section Ratios in (n,2n) Reactions

Neutron Energy (MeV)	^{185}Re (n,2n) ^{184m}Re (8+)	^{187}Re (n,2n) ^{186m}Re (8+)	^{192}Ir (n,2n) ^{192m}Ir (9+)
8	0.06	0.13	0.016
9	0.15	0.19	0.11
10	0.20	0.22	0.19
11	0.24	0.25	0.24
12	0.28	0.28	0.28
13	0.31	0.31	0.31
14	0.33	0.33	0.31

The isomer ratios above can be compared with the Kopecky systematics for $(n, 2n)$ reactions. Kopecky and Gruppelaar [4] showed that a simplified version of GNASH predicted 14-MeV isomer cross-section ratios that have a 'parabolic' dependence on the isomer spin, with a peak at isomer spins between 3 and 5. Their calculated isomeric ratio described the library of experimental ratios reasonably well, though they commented that for the case of the $(n, 2n)$ calculation their results were particularly sensitive to the model parameters describing the simplified nuclear structure. In Fig. 3 we show the 14 MeV isomer ratios from Tables IIa and IIb, compared with the Kopecky systematics. The differences between the line (the Kopecky prediction) and our theoretical results (triangles) can be understood as a measure of the need to

perform full GNASH calculations with realistic nuclear structure and optical models. In the case of the hafnium isomers (25/2- and 16+) we have shown the experimental isomer ratio, from Patrick *et al.* In most cases the Kopecky systematics yield isomer ratios that are close to our detailed GNASH calculations. Our GNASH calculations for the isomer production cross section ratios of the 25/2- and 16+ levels in hafnium are seen to lie below the experimental numbers by about a factor of 2. The Kopecky systematics overestimate the isomeric ratio for the 25/2- by about a factor of 4-5, and interpolating their curve to an isomer spin of 16 suggests that their systematics agree with the experimental measurement reasonably well.

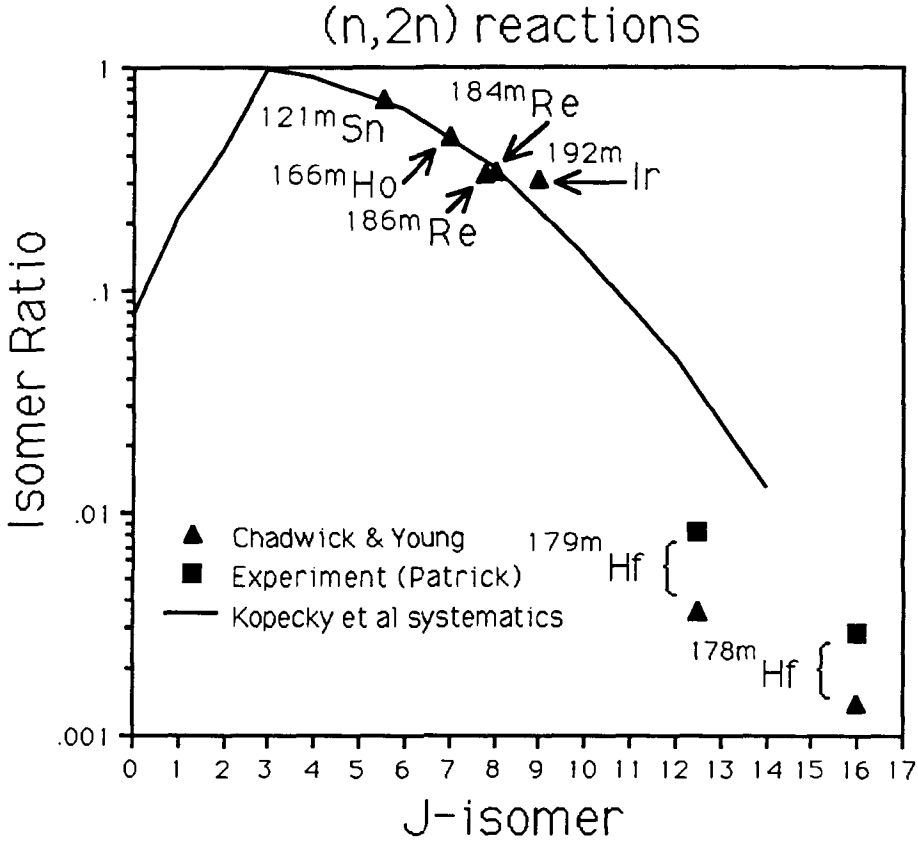

Fig. 3. The $(n, 2n)$ isomeric cross section ratio as a function of isomer spin, for 14 MeV incident neutrons. The Kopecky systematics are compared with our GNASH calculations, and a comparison with data is made for the 25/2- and 16+ Hf isomers.

As well as $(n, 2n)$isomeric cross section ratios for 14 MeV incident neutron energies, Table II contains the ratios for lower neutron energies, down to the threshold of about 8 MeV for $(n, 2n)$ reactions. The energy dependence of the isomeric ratio is of importance when assessing activation in a reactor induced by neutrons with degraded energies, after inelastic scattering processes have occurred. In Fig. 4 we show the variation of the isomer ratio with isomer spin for three different incident neutron energies: 14, 11 and 9 MeV.

It is seen that, for a given incident neutron energy, the $(n, 2n)$ isomer ratio decreases with increasing isomer spin (at least for isomer spins above 4). This feature, which is also seen in experimental data and in the Kopecky calculations [4], can be simply understood in the following way. In $(n, 2n)$ reactions both outgoing neutrons generally have low energies and are dominated by s-wave transitions. However, in order to produce a high-spin isomer, the intermediate nuclear states also have to be

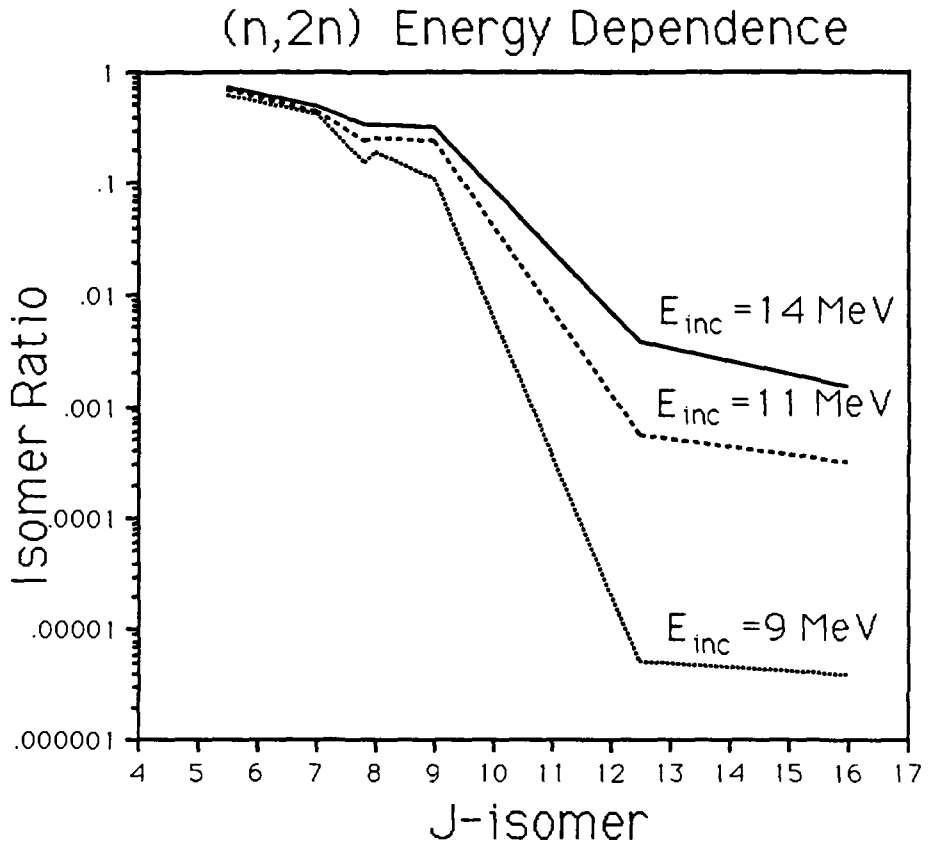

Fig. 4. The $(n, 2n)$ isomeric cross section ratio as a function of isomer spin, for three different incident neutron energies. The lines connect GNASH calculations for the same isomers that are shown in Fig. 3.

of high spin, and since the transmission coefficients at 14 MeV decrease with increasing l for large l, it would be expected that the isomer ratio would decrease strongly with increasing isomer spin. This same explanation accounts for another feature of our results. It is clear from our GNASH calculations that the variation of the isomer ratio with isomer spin is much stronger for lower incident neutron energies. At lower energies the decrease of the transmission coefficients with increasing l is even greater, resulting in a drastically reduced population of high-spin isomers in $(n, 2n)$ reactions.

C. The (n, n') Isomeric Cross Section Ratios

The ground states of ^{178}Hf and ^{179}Hf are stable and are naturally occuring in hafnium, and natural niobium is monoisotopic in ^{93}Nb. Therefore we have considered the (n, n') reactions to the isomeric states for these nuclei. In addition we have also calculated the (n, n') reaction on ^{166}Ho to the isomeric state, the ground state of ^{166}Ho having a 1.1 day lifetime. We have determined the isomeric cross section ratio as a function of incident neutron energies between 1 and 14 MeV, and our results are shown in Table III.

For the high-spin isomers [all except ^{93m}Nb (1/2-)], the isomer ratio is seen to be a strongly-decreasing function of incident energy, and the higher isomer spins have stronger energy dependences. This is because the angular momentum brought in by the projectile neutron decreases with decreasing energy, and therefore results in a reduction in the high-spin isomer population. It is interesting to note that the energy

TABLE III
Isomeric Cross Section Ratios in (n, n') Reactions

Neutron Energy (MeV)	^{93}Nb (n,n') ^{93m}Nb (1/2-)	^{166}Ho (n,n') ^{166m}Ho (7-)	^{178}Hf (n,n') ^{178m}Hf (16+)	^{179}Hf (n,n') ^{179m}Hf (25/2-)
1	9.7×10^{-2}	8.3×10^{-3}	0.0	0.0
2	8.9×10^{-2}	2.8×10^{-2}	0.0	4.5×10^{-5}
3	8.5×10^{-2}	5.5×10^{-2}	2.2×10^{-15}	3.8×10^{-4}
4	8.8×10^{-2}	8.7×10^{-2}	4.4×10^{-11}	1.1×10^{-3}
5	8.9×10^{-2}	0.12	1.5×10^{-9}	2.8×10^{-3}
6	8.8×10^{-2}	0.15	1.5×10^{-8}	4.3×10^{-3}
7	8.7×10^{-2}	0.19	8.6×10^{-8}	7.1×10^{-3}
8	8.6×10^{-2}	0.24	3.9×10^{-7}	1.7×10^{-2}
9	8.6×10^{-2}	0.28	2.3×10^{-6}	3.2×10^{-2}
10	8.6×10^{-2}	0.30	1.2×10^{-4}	3.5×10^{-2}
11	8.6×10^{-2}	0.32	3.3×10^{-5}	3.4×10^{-2}
12	8.6×10^{-2}	0.34	7.2×10^{-5}	3.9×10^{-2}
13	8.7×10^{-2}	0.34	1.4×10^{-4}	3.7×10^{-2}
14	8.8×10^{-2}	0.36	2.8×10^{-4}	4.3×10^{-2}

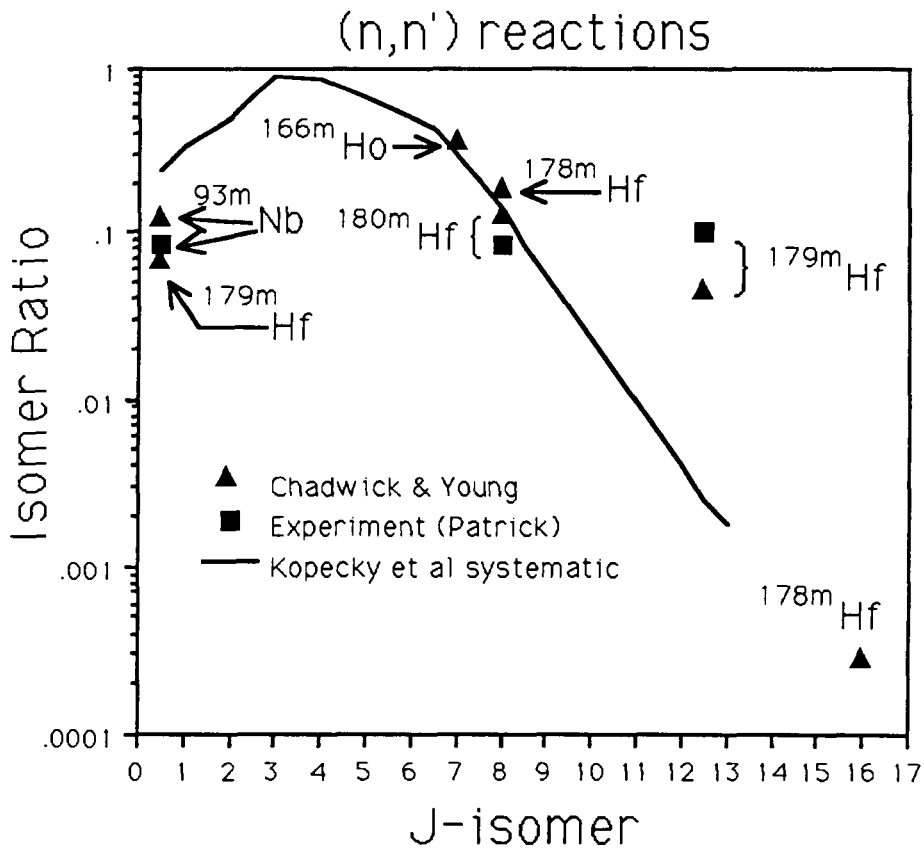

Fig. 5. The (n, n') isomeric cross-section ratio as a function of isomer spin for 14-MeV incident neutrons. The Kopecky systematics for one-step reactions are compared with GNASH calculations and with experimental data.

dependence of the (n,n') isomer cross-section ratio is weaker than that of the $(n,2n)$ reaction for the very-high spin isomers (i.e. those in hafnium). In the case of the (n,n') reaction on ^{93}Nb, the fact that the long-lived isomer is of low spin results in an isomeric cross section ratio which is approximately energy-independent.

The Kopecky-Gruppelaar systematic calculations for the (n,n') isomeric cross section ratio again show a peak at an isomer spin J^m = 3-5, and are compared in Fig. 5 with our calculations at 14 MeV. As well as showing our results from Table III in this figure, we include isomeric ratios at 14 MeV for the production of the ^{178m}Hf(8-), ^{179m}Hf(1/2-) and ^{180m}Hf(8-) states which we have also determined. In general the Kopecky-Gruppelaar systematics agree fairly well with our detailed GNASH calculations (to within a factor of 2-3). One notable exception is the isomer cross section ratio for the production of the ^{179m}Hf(25/2-), for which our calculation exceeds the systematics by more than an order of magnitude (and the experimental result of Patrick *et al* exceeds the systematics by an even greater factor). This is probably due to the fact that Kopecky *et al* adopt a ground-state spin of 0.5 in their model calculation, whereas in this case the ground-state spin is 4.5. Hence they overestimate the spin change in the reaction and consequently underestimate the isomeric cross section ratio.

In Fig. 6. we show our theoretical calculations for the ^{93}Nb$(n,n')^{93m}$Nb isomer production compared with experimental data, for incident energies between 0 and 20 MeV. We stress that this calculation was performed with a standard set of input parameters, and no parameter adjustment has been done to improve the agreement. The experimental value for the isomer production cross section at 14 MeV was combined with a value of 0.44 b for the total ^{93}Nb(n,n') cross section (taken from ENDF/B-VI), to obtain the experimental isomer ratio plotted in Fig. 5. It is evident that our theoretical calculation for the ^{93m}Nb isomer ratio in Fig. 5 agrees well with this experimental number, though the Kopecky-Gruppelaar systematics overestimate the ratio by a factor of about 3. This is an interesting comparison to make because the

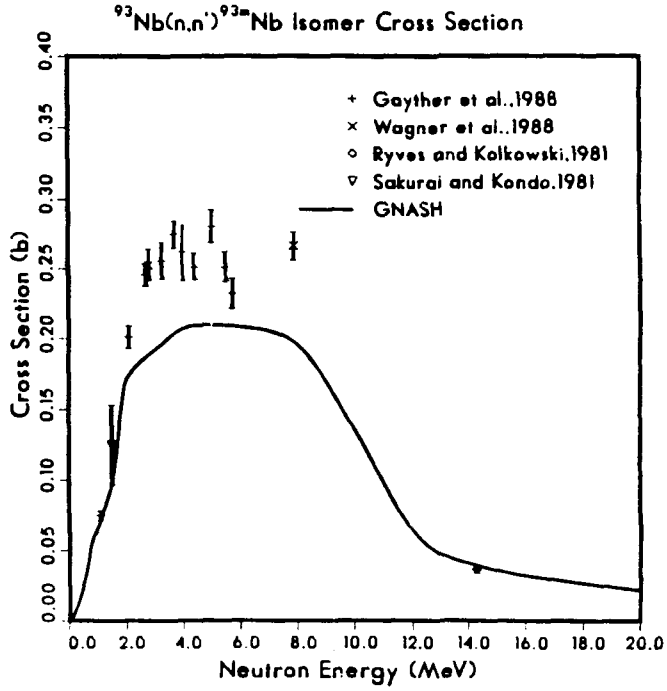

Fig. 6. Our theoretical calculations for the production of ^{93m}Nb (1/2-,16yr) via (n,n') reactions as a function of incident neutron energy, compared with experimental data.

systematics of Kopecky and Gruppelaar, for low spin isomers, were based on a model in which: (a) the nucleus ^{93}Nb was chosen; (b) a ground state spin of [4 + the isomeric spin] (i.e. 4.5 here) was adopted; (c) no nuclear structure other than the ground and isomeric state was included. Therefore, apart from the neglect of nuclear structure, their model corresponds to the ^{93}Nb physical situation. Since their systematics overestimate the experimental value, whilst our calculation describes the data well, this comparison demonstrates the need to perform detailed calculations with a realistic description of the nuclear structure.

D. Isomeric Cross Section Ratios for (n, γ) Reactions

A limited amount of cross-section data for total (n, γ) radiative capture reactions is available at neutron energies in the MeV region, and simple systematic behavior with atomic number A has been noted for 14-MeV neutrons [16]. In the case of (n, γ) reaction to isomeric states, however, experimental data are much more limited and consist mostly of data for thermal incident neutrons. Thermal (n, γ) isomer ratios for an assortment of heavy nuclei are plotted versus the spins of the isomeric states in Fig. 7. Clearly, simple systematic behavior is much less evident for thermal neutron capture data than for 14-MeV particle-production cross sections, especially for isomeric states with spins greater than 5. This situation, coupled with the almost complete lack of experimental data at higher energies, results in a pressing need for reliable theoretical estimates of (n, γ) isomer ratios.

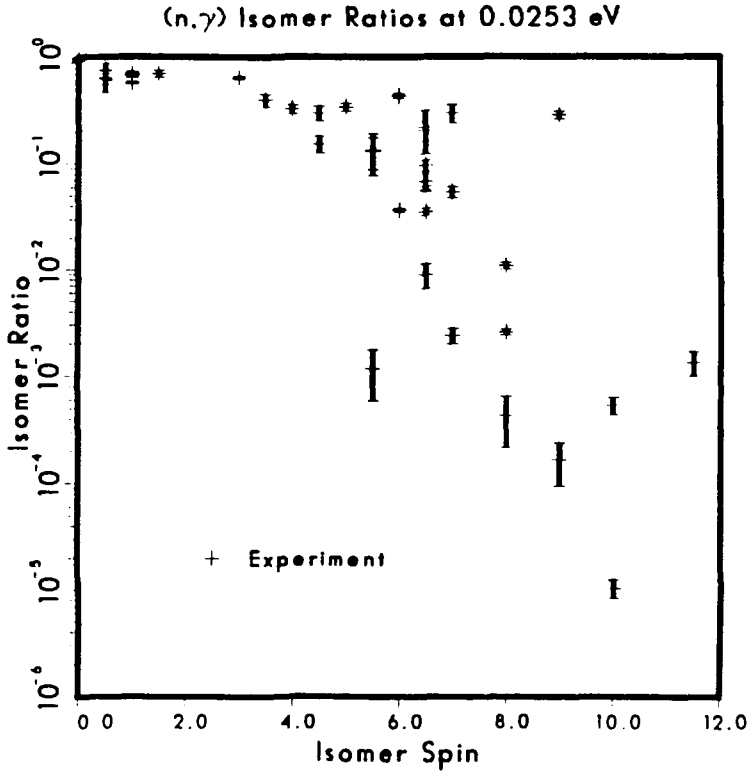

Fig. 7. Experimental isomer ratios for (n, γ) reactions with thermal neutrons, plotted as a function of spin of the isomeric states.

The GNASH code was used to calculate (n, γ) cross sections leading to isomeric states in ^{166}Ho(7^-, 1200 y), ^{178}Hf(16^+, 31 y; 8^-, 4 s), ^{179}Hf ($25/2^-$, 25.1 d; $1/2^-$, 18.7 s), ^{186}Re (8^+, 2 x 10^5 y), and ^{188}Re (6^-, 18.6 m). Except as noted below, the generalized Lorentzian [8] form was utilized for the gamma-ray strength functions.

The calculations were performed down to an incident energy of at least 1 keV in each case, at which energy the neutron transmission coefficients are completely dominated by s-waves, and it is possible to make a crude comparison with the thermal neutron experimental data. A selection of the isomeric ratios [relative to the total (n,γ) cross section] that results from the calculations for ^{165}Ho$(n,\gamma)^{166m}$Ho, ^{177}Hf$(n,\gamma)^{178m}$Hf, and ^{187}Re$(n,\gamma)^{188m}$Re reactions are shown in Fig. 8. The calculated isomer ratios are given explicitly in Table IV.

A feature of isomer ratios of Fig. 8 is a general trend of increasing ratio with increasing neutron energy. This behavior reflects the fact that more angular momentum is brought into the reactions as the neutron energy is increased thus increasing the population of higher spin states. For both the ^{165}Ho$(n,\gamma)^{166m}$Ho, and ^{187}Re$(n,\gamma)^{188m}$Re reactions, an anomaly is seen in the calculated isomer ratios near 300 keV that interrupts this general trend of increasing isomer ratios with neutron energy. This effect is thought to result from the fact that thresholds for one or more high spin states in the target nuclei open in this energy region. The presence of these open channels to higher spin states permits neutron decays to occur more readily from higher spin states in the compound nucleus, thus reducing the high-spin population available for cascading to the isomeric state. As the incident neutron energy is further increased, more and more channels of all spins are opened, and the anomalous effect is overwhelmed by the increasing angular momentum brought into the reaction.

The agreement (or lack of agreement) between our calculated isomer ratios at lower energies and the thermal neutron measurements depends upon the extent to which the average properties (widths) embodied in our statistical model coincide with the very few channels involved in the thermal neutron measurements. Clearly, large differences between the calculations at $\sim$ 1 keV and the thermal measurements are possible, and such are seen in the case of the ^{177}Hf$((n,\gamma)^{178m}$Hf isomer ratios ($\sim$ factor of 20 differences). In the cases of the ^{165}Ho$(n,\gamma)^{166m}$Ho and ^{187}Re$(n,\gamma)^{188m}$Re reactions, however, the differences between the calculated ratios near 1 keV and the thermal experimental values are much smaller, of the order of 30%.

To investigate the behavior of isomer ratios with neutron energy and with isomer spin, a simple parametric study was performed using the ^{187}Re$(n,\gamma)^{188m}$Re reaction as a base case. In this study various values of spin between 0 and 16 were assumed for the isomeric state in ^{188}Re at $E_x = 172$ keV, and the isomer ratio was calculated as a function of incident neutron energy for each isomer spin. The ^{187}Re$(n,\gamma)^{188m}$Re reaction was chosen because the real isomer ($J^\pi = 6^-, E_x = 172$ keV) is not fed by any of the known discrete states, so all the isomer's excitation comes from decays from the continuum. Additionally, the calculated isomeric state branching ratio for the real isomer is consistent (within 30%) at the lowest energy of the calculation (0.1 keV) with the measured ratio for thermal neutrons. The results of these calculations, performed using a standard Lorentzian [7], are shown in Fig. 9 for incident neutron energies of 0.001, 1, and 14 MeV. The calculated isomer ratios show strong dependence on both incident neutron energy and on isomer spin. The calculations for the higher spin states are thought to depend strongly on details of the gamma-ray strength functions as well as on the level density in the compound nucleus, since populating the isomeric states occurs almost exclusively through multiple γ-ray cascades in the compound nucleus.

While it is attractive to consider using calculations such as those illustrated in Fig. 9 to search for systematic relationships that might be useful in making simple predictions of isomer ratios, we found that the calculated results for the various

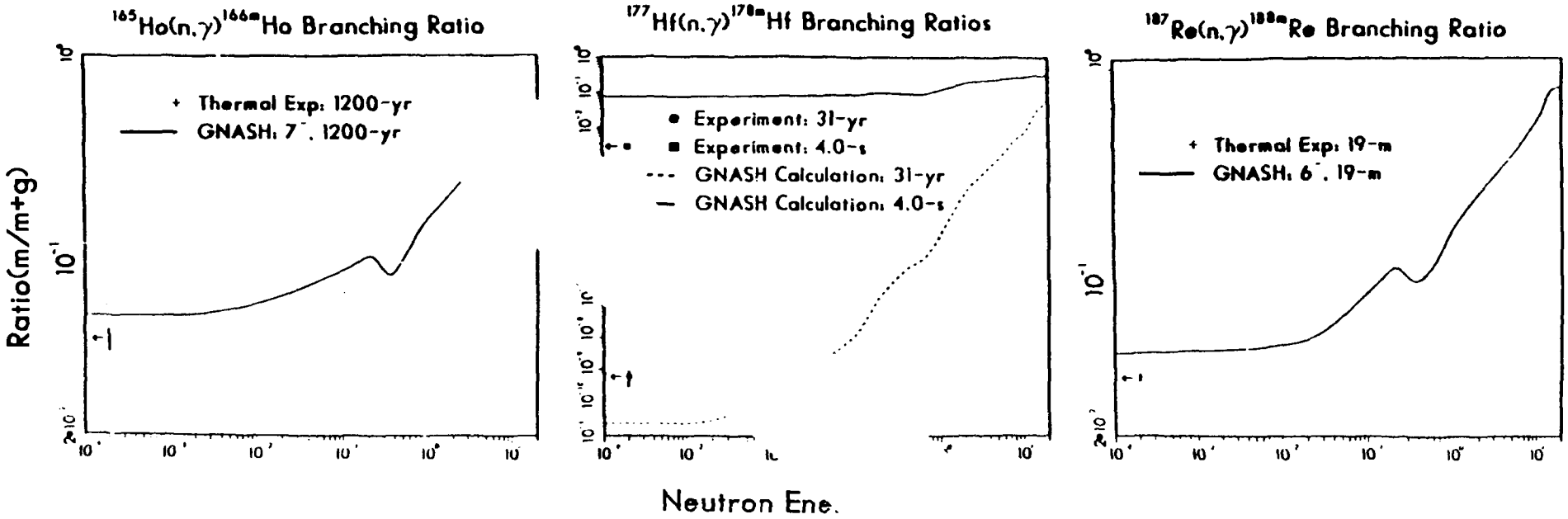

$^{n,\gamma)^{178m}}$Hf, and
from thermal

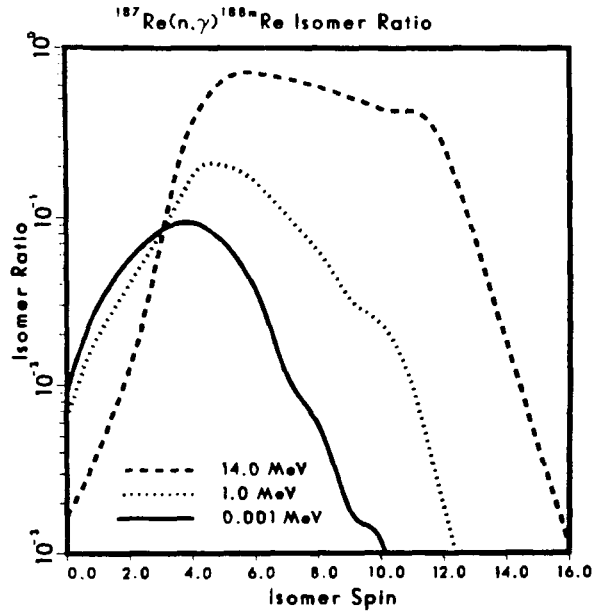

Fig. 9. Calculated isomer ratios as functions of incident neutron energy and isomer spin for the $^{187}\mathrm{Re}(n,\gamma)^{188m}\mathrm{Re}$ reaction. The calculations were performed by replacing the spin of the actual isomer in $^{188}\mathrm{Re}(j^{\pi}=6^{-},E_x=172$ keV) by values from 0 to 20.

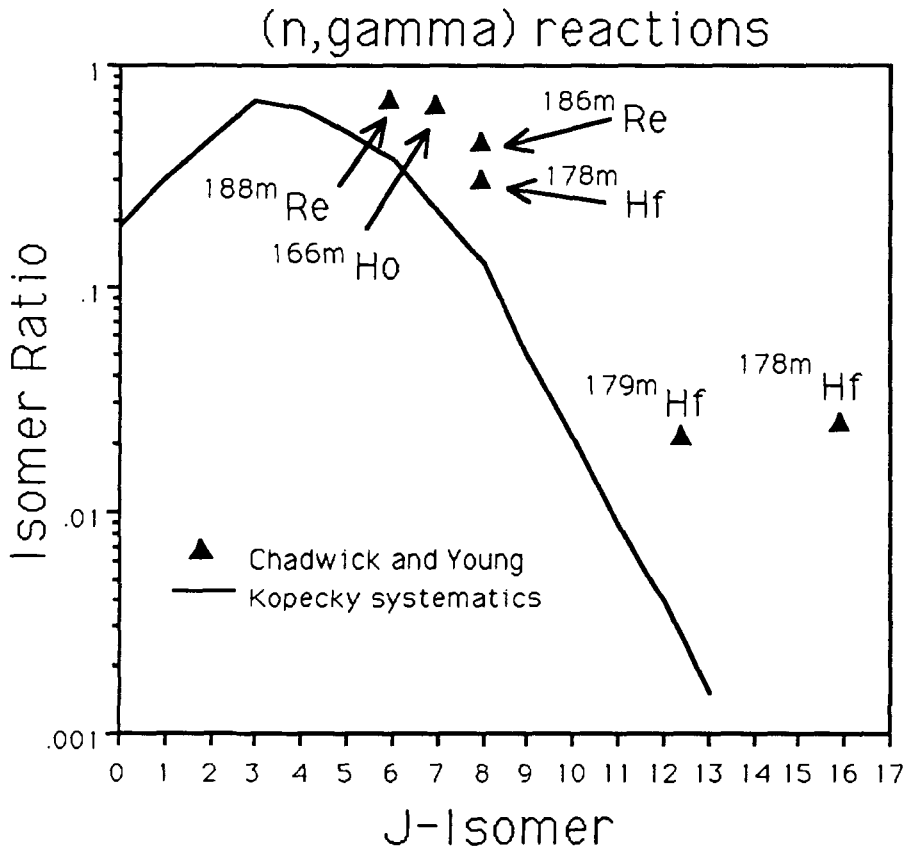

Fig. 10. The (n,γ) isomeric cross-section ratio as a function of isomer spin for 14-MeV incident neutrons. The Kopecky systematics for one-step reactions are compared with GNASH calculations.

cases were strongly dependent on the properties of the nuclei in question. The (n,γ) reaction is specifically excluded from the "one-step reaction" systematics identified by Gruppelaar *et al.* [16], because the validity of those systematics was primarily

TABLE IVa
Isomeric Cross Section Ratios in (n,γ) Reactions

Neutron Energy (MeV)	^{165}Ho (n,γ) ^{166m}Ho (7-)	^{178}Hf (n,γ) ^{178m}Hf (8-)	^{178}Hf (n,γ) ^{178m}Hf (16+)
0.001	0.069	0.069	2.3×10^{-11}
0.01	0.078	0.071	2.0×10^{-10}
0.1	0.11	0.081	8.2×10^{-9}
0.2	0.13	0.092	1.1×10^{-7}
0.4	0.11	0.086	6.9×10^{-7}
0.6	0.14	0.087	1.3×10^{-6}
0.8	0.17	0.10	4.5×10^{-6}
1.0	0.19	0.11	7.1×10^{-6}
2.0	0.25	0.17	1.1×10^{-4}
4.0	0.32	0.21	6.3×10^{-4}
6.0	0.38	0.23	1.7×10^{-3}
8.0	0.43	0.25	3.9×10^{-3}
10.0	0.48	0.26	5.9×10^{-3}
12.0	0.57	0.28	1.1×10^{-2}
14.0	0.66	0.30	2.5×10^{-2}

TABLE IVb
Isomeric Cross Section Ratios in (n,γ) Reactions

Neutron Energy (MeV)	^{178}Hf (n,γ) ^{179}Hf (25/2-)	^{185}Re (n,γ) ^{186m}Hf (8+)	^{187}Re (n,γ) ^{188m}Re (6-)
0.001	1.9×10^{-13}	2.1×10^{-3}	0.048
0.01	2.7×10^{-12}	2.5×10^{-3}	0.051
0.1	1.4×10^{-10}	8.1×10^{-3}	0.088
0.2	1.5×10^{-9}	0.014	0.114
0.4	5.4×10^{-9}	0.016	0.099
0.6	2.8×10^{-8}	0.018	0.12
0.8	7.6×10^{-6}	0.022	0.14
1.0	1.6×10^{-7}	0.027	0.17
2.0	5.3×10^{-6}	0.061	0.24
4.0	9.8×10^{-5}	0.13	0.33
6.0	5.2×10^{-4}	0.18	0.40
8.0	1.8×10^{-3}	0.24	0.47
10.0	4.0×10^{-3}	0.29	0.52
12.0	9.3×10^{-3}	0.35	0.59
14.0	2.2×10^{-2}	0.45	0.69

established for (n,n'), (n,p), and (n,α) reactions and was doubtful for (n,γ). However, it was necessary for those authors to use the one-step reaction systematics for (n,γ) reactions in the REAC-ECN-3 library, due to the lack of other alternatives. A comparison between the one-step reaction systematics of Gruppelaar *et al.* and our calculated (n,γ) isomer ratios at $E_n = 14$ MeV is given in Fig. 10. The calculated ratios are seen to differ significantly from the systematics, thus confirming the

conclusion of Gruppelaar *et al.* that the one-step reaction systematics might not be valid for (n,γ) reactions. This further highlights the need for careful nuclear theory calculations for important reactions.

IV. CONCLUDING REMARKS

We present calculations of the energy dependence of isomer ratios for long-lived metastable states in ^{93}Nb, ^{121}Sn, ^{166}Ho, ^{184}Re, ^{186}Re, ^{178}Hf, ^{179}Hf, and ^{192}Ir, populated by means of (n,n'), $(n,2n)$, and (n,γ) reactions. The calculated ratios for $(n,2n)$ reactions generally support predictions from systematics at 14 MeV except for isomer spins above $\sim$ 12. The agreement with systematics is not as good for (n,n') reactions as is the case for $(n,2n)$, but the systematics obviously are good enough to still be useful in developing large activation libraries. In the case of (n,γ) reactions, the theoretical values cannot be compared directly with the thermal neutron measurements but are roughly consistent at the lower energy range of the calculations.

Because of the limited amount of experimental data available on isomer ratios, nuclear theory codes such as GNASH provide a useful complement to the data base. The calculations are particularly important for (n,γ) reactions, as experimental data are extremely limited and systematics provide little guidance, as well as for determining the energy dependence of (n,n') and $(n,2n)$ isomer ratios, for which there is little experimental information. In general, we recommend that evaluations of important long-lived isomers be based on detailed theoretical analyses matched to the available experimental data. The use of systematics should be limited to providing data for less important reactions. In cases where systematics are used, particular care should be exercised with (n,γ) isomeric ratios, and the procedure, which is sometimes used, of setting the isomer ratio to 1/2 of the total (n,γ) cross sections should *never* be used at low energies, as it can lead to errors of many orders of magnitude.

We would like to thank Robin Forrest and Ed Cheng for guidance concerning data needs, and Doug Muir for some helpful suggestions.

V. REFERENCES

[1] M.B. Chadwick and P.G. Young, 'Calculations of the Production Cross Sections of High-Spin Isomeric States in Hafnium', Nucl. Sci. and Eng. **108**, 117 (1991).

[2] E.D. Arthur, 'The GNASH Preequilibrium-Statistical Model Code', Los Alamos National Laboratory report LA-UR-88-382 (1988); P.G. Young and E.D. Arthur, 'GNASH: A Preequilibrium, Statistical Nuclear-Model Code for Calculation of Cross Sections and Emission Spectra', Los Alamos Scientific Laboratory report LA-11753-MS (1990).

[3] B.H. Patrick, M.G. Sowerby, C.G. Wilkins and L.C. Russen, 'Measurements of 14-MeV Neutron Cross Sections for the Production of Isomeric States in Hafnium Isotopes,' presented at the Specialists' Mtg. Neutron Activation Cross Sections for Fission and Fusion energy Applications, Argonne, Illinois, September 13-15 1989.

[4] J. Kopecky and H.Gruppelaar, 'Systematics of Neutron-Induced Isomeric Cross Section Ratios at 14.5 MeV', ECN report ECN-200 (1987).

[5] C.L. Dunford, 'Compound Nucleus Reaction Programs COMNUC and CASCADE', AI-AEC-12931, Atomics Int. (1970).

[6] C. Kalbach,'The Griffin Model, Complex Particles and Direct Nuclear Reactions', Z. Phys. **A283**, 401 (1977).

[7] D.M. Brink, 'Some Aspects of the Interaction of Fields with Matter', D.Phil. Thesis, Oxford (1955); P. Axel, 'Electric Dipole Ground State Transition Width Strength Function', Phys. Rev. **126**, 671 (1962).

[8] J. Kopecky and M. Uhl, 'Test of Gamma-Ray Strength Functions in Nuclear Reaction Model Calculations,' Phys. Rev. C **42**, 1941 (1990).

[9] J. Raynal, 'Optical Model and Coupled-Channel Calculations in Nuclear Physics', SMR-9/8, International Atomic Energy Agency (1972).

[10] O. Bersillon, 'SCAT2 - A Spherical Optical Model Code',in Progress Report of the Nuclear Physics Division, Bruyeres-le-Chatel (1977), CEA-N-2037, p. 111 (1978).

[11] S.F. Mughabghab, 'Neutron Resonance Parameters and Thermal Cross Sections', Parts A and B, in Neutron Cross Sections, V. 1, Academic Press Inc., New York, (1981) (part A) and (1984) (part B).

[12] S.S. Dietrich and B.L. Berman, 'Atlas of Photoabsorption Cross Sections Obtained with Monoenergetic Photons', Atomic and Nuclear Data Tables, 199 (1988).

[13] A. Gilbert and A.G.W. Cameron, 'A composite Nuclear-Level density formula with Shell Corrections', Can. J. Phys. **43**, 1446 (1965).

[14] J. L. Cook, H. Ferguson, and A. R. Musgrove, Aus. J. Phys. **20**, 477 (1967).

[15] E. D. Arthur, P. G. Young, A. B. Smith, and C. A. Philis, Trans. Am. Nucl. Soc. **39**, 793 (1981).

[16] H. Gruppelaar, H. A. J. van der Kamp, J. Kopecky, and D. Nierop, 'The REAC-ECN-3 Data Library with Neutron Activation and Transmutation Cross Sections for Use in Fusion Reactor Technology,' ECN report ECN-207 (1988).

EVALUATION OF ISOMERIC EXCITATION FUNCTIONS IN NEUTRON INDUCED REACTIONS.

O. Grudzevich, A. Ignatyuk, K. Zolotarev

The possibilities of isomer levels experimental excitation functions description with theoretical models are discussed. It is shown, that the experimental data in many cases can be described by theoretical models quite well without parameter fitting. However, large discrepancies are observed for some reactions. By our opinion, these discrepancies are due to uncertainties of discrete level schemes, schemes of gamma-transitions between levels and spin dependence of level density. Small values of isomeric ratios (< 0.1) have been described with the largest errors. The simple formulae for energy dependence of isomeric ratio for (n,g) reaction has been proposed.

INTRODUCTION.

An interest to isomeric levels population cross-sections (ILPCS) from the viewpoint of theory is connected with the unique possibility to investigate mechanism of the transmission of angular momenta in different reactions. A good enough description of isomeric ratios in thermal neutrons radioactive capture was achieved in [1]. Thorough analyses of isomeric levels excitation functions (ILEF) for neutron inelastic scattering has been done in [2]. Successful descriptions of experimental data for (n,n') and (n,2n) reactions were obtained in [3,4,15].

Apart from fundamental aspects of the reaction theory, attention to the problem are derived from practical needs. It is necessary to know a lot of ILEF's in (n,g), (n,n'), (n,p), (n,d), (n,t), (n,a) and (n,2n) reactions for wide region of target mass and energy to predict long-lived activities in fission and fusion nuclear reactors [5]. Experimental data on ILPCS are too rare. It seems quite logical to use theoretical model calculations to evaluate data we need.

Despite of obvious achievements in describing of some isomeric cross sections, situation in general is questionable. The systematics of experimental data even at 14 MeV or at thermal neutron energies has not been proposed yet. The cross-sections of levels with the same spins, in the same reactions and for near isotopes are differed by factor of 3-5.

Theoretical models application to calculate ILPCS in different reactions and in the wide region of target mass and energy is devoted to this paper. An influence of model parameters on calculation results is tested.

1. THEORETICAL MODEL.

The isomer excitation functions have been calculated in the framework of statistical theory of nuclear reactions in Hauser-Feshbach formalism by STAPRE code [6]. Level densities were calculated with phenomenological superfluid model of excited nuclei [7]. The level densities parameters were taken from systematics [8]. The experimental discrete level schemes (energy, spin, parity) (DLS) and experimental gamma-transitions schemes (GTS) were used at low excitation energy. Transmission coefficients of particles have been computed by SCAT2 code. The energy dependence of gamma strength functions was calculated as proposed in [11]. Calculated strength functions were renormalized to experimental data on averaged gamma widths of neutron resonances [12].

The descriptions of experimental isomeric levels excitation functions of 93Nb(n,n'), 93Nb(n,2n) and 85Rb(n,g) reactions by theoretical calculations are shown in fig.1. The optical model parameter (OMP) set for neutrons[13] and experimental gamma-transition and discrete levels schemes [9] were used. A good enough description has been obtained without parameter fitting. The reason is that optical parameter set [13] is specially fitted for nuclei with A=90, and that experimental gamma-transitions schemes are well known.

In the most cases, there are no input data to compute isomeric cross-sections with good accuracy. So it is interesting to investigate the sensitivities of theoretical results to input data:

- optical model parameter set;
- spin dependence of level densities;
- low-laying discrete levels schemes;
- gamma-transition schemes.

Five variants of calculation's results for 103mRh isomer's level with J=7/2+, E=39.8 keV in 103Rh(n,n') reaction are shown in

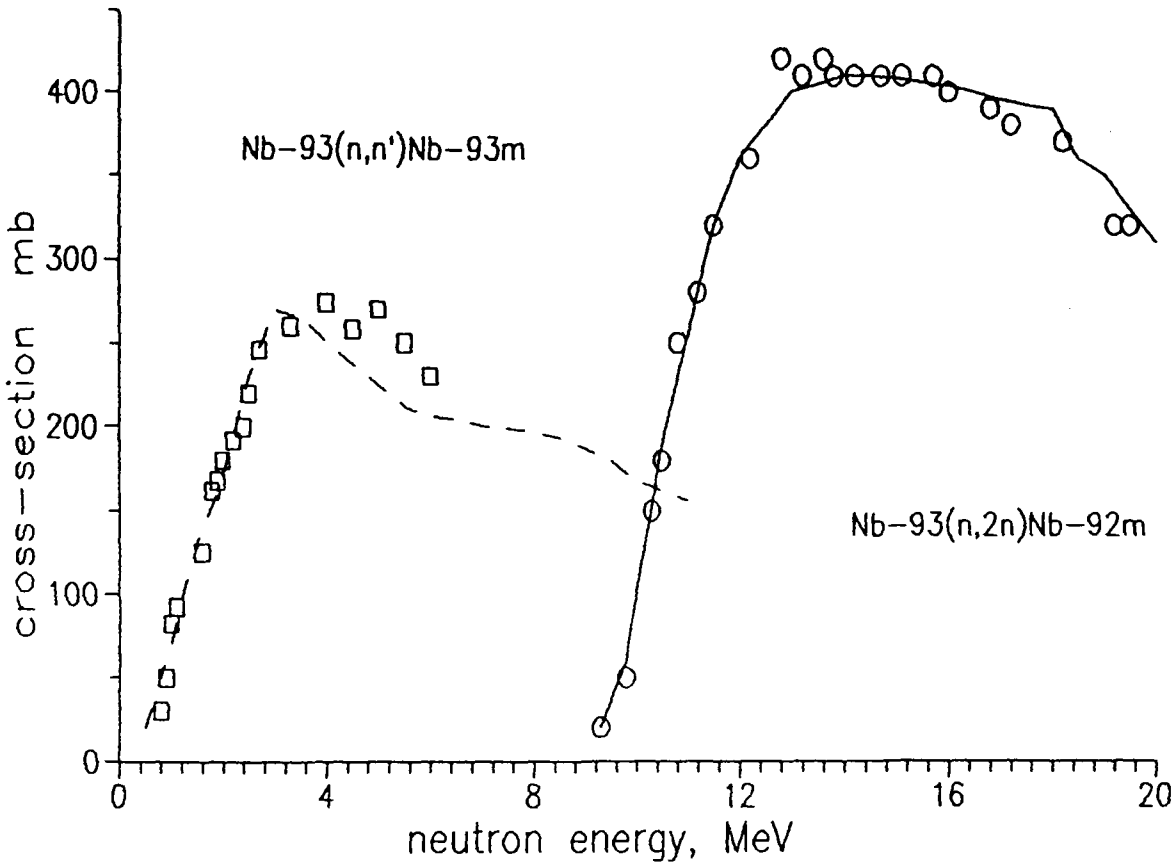

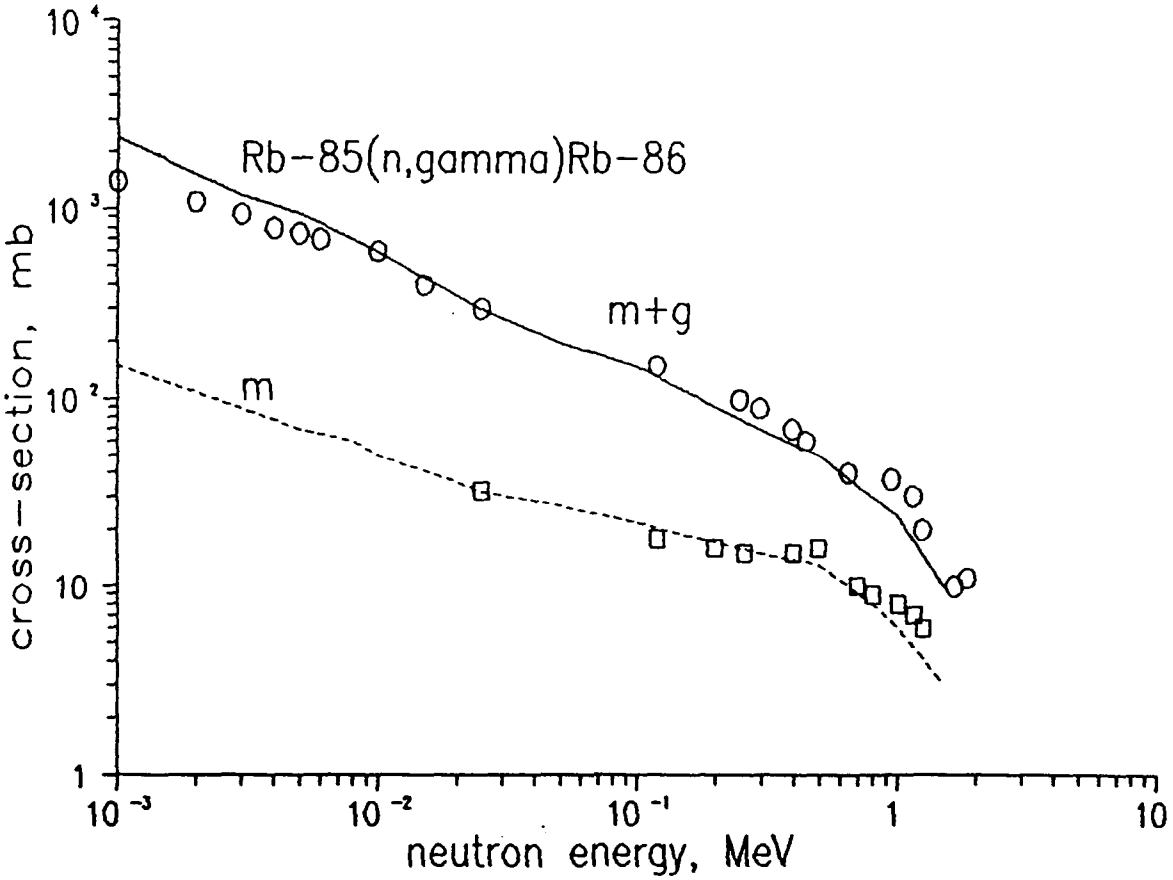

Fig.1 Data on the isomeric levels excitations functions in 93Nb(n,n') and 93(n,2n) - a); 85Rb(n,g) - b). Experimental data are shown by points, curves - results of STAPRE calculations.

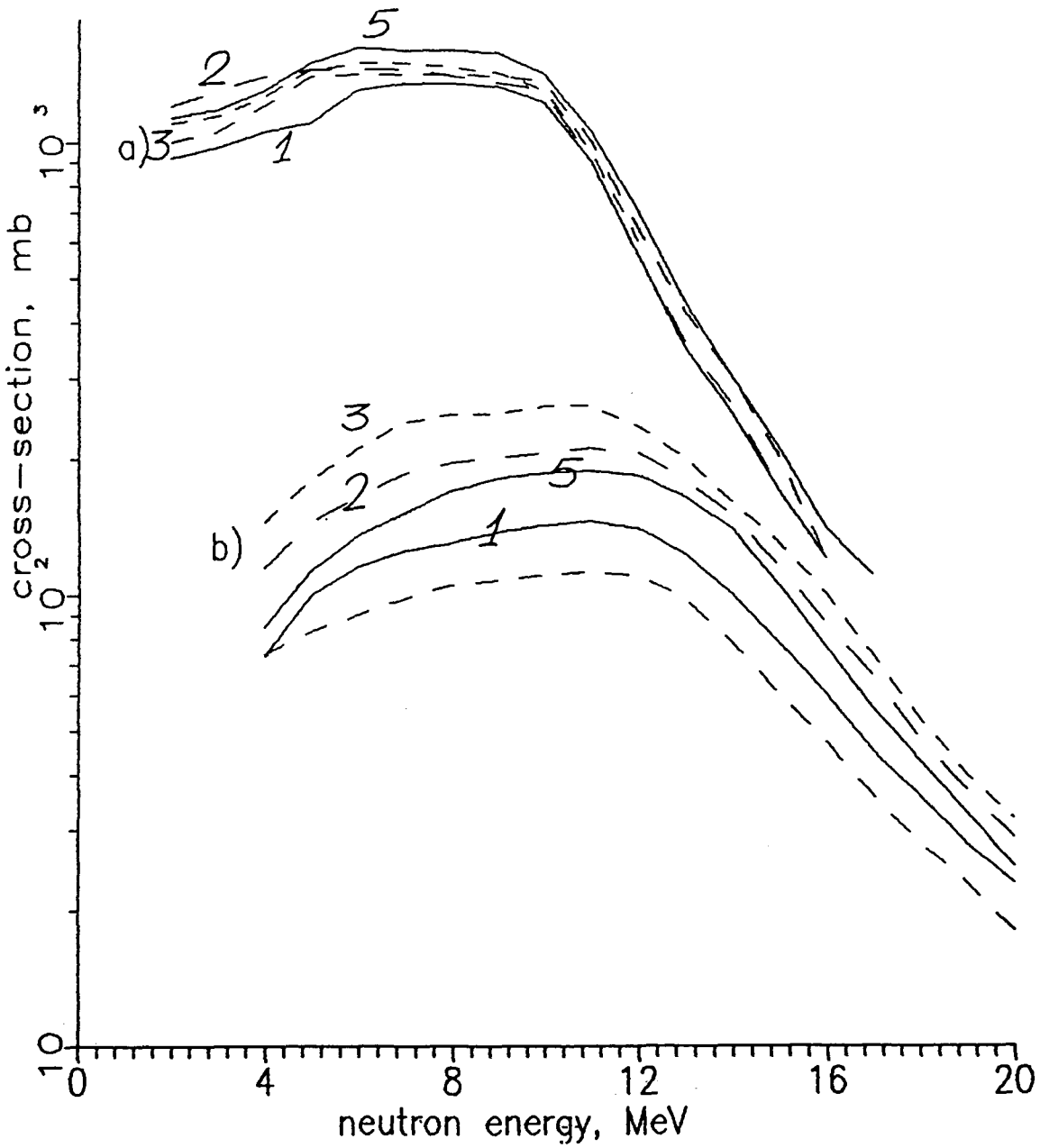

Fig.2 The influence of model parameters and residual nuclear characteristics on reaction cross section:

a) 103Rh(n,n')103mRh, Jm=7/2+, E=39.8 keV.

Curve 1 corresponds to the calculations with input data set: 16 discrete levels of residual nucleus and experimental GTS's between them, neutron OMP set by Becchetti- Greenlees. Curve 2 - neutron OMP set by Wilmore-Hodgson, the rest as in 1. Curve 3 - calculated gamma-transition scheme, the rest as in 1. Curve 4 - level density formalism is used after isomer's level, the rest as in 1. Curve 5 - spin cut off parameter was increased by 1.25 factor, the rest as in 4.

b) The same for 58Ni(n,p)58mCo. Jm=5+, E=24.9 keV.

fig. 2a. The same results for 58mCo isomer with J=5+, E=24.9 keV in 58Ni(n,p) reaction are presented in fig.2b.

Curve 1 corresponds to the calculations with input data set: 16 discrete levels of residual nucleus and experimental GTS's between them, neutron OMP set by Becchetti- Greenlees. Curve 2 - neutron OMP set by Wilmore-Hodgson, the rest as in 1. Curve 3 - calculated gamma-transition scheme, the rest as in 1. Curve 4 - level density formalism is used after isomer's level, the rest as in 1. Curve 5 - spin cut off parameter was increased by 1.25 factor, the rest as in 4.

As one can see from fig.2, all above mentioned characteristics influence on the value and on the energy dependence of ILPCS.

The influence of optical model parameter set on the cross-section changes can be explained by changing of neutron absorption cross-section. The OMP set also changes angular momenta distribution. The influence of residual nuclei characteristics on ILPCS leads, as a rule, to redistribution of the reaction cross section between isomer and ground states. Thus, increasing of spin cut off parameter leads to increasing of density of levels with high spins and, hence, to increasing of population of level with higher spin. As neutron energy increases an influence of s2 parameter increases (curve 4 and 5). One should remember that s2 changing and different numbers of discrete levels lead to re-normalization of reaction cross section.

It is no matter of our talk to discuss description of excitations functions near reaction threshold. It is necessary to fit level density to cumulative number of discrete levels and to fit optical parameter set to experimental strength functions at this energy. We suppose that all these operations have been done quite correctly.

Let us consider the influence of the main characteristics on the value of isomeric ratio R=Sm/(Sm+Sg), where Sm and Sg are isomer and ground state cross-sections, consequently. The results of isomeric ratio calculations are shown in fig.3. The variants are as in fig.2. It can be seen that there are great influences of GTS's and S2 values, but the influence of OMP is smaller than in fig.2.

It is obvious the evaluation of isomeric excitation functions may be more simple done when using of isomeric ratio and known

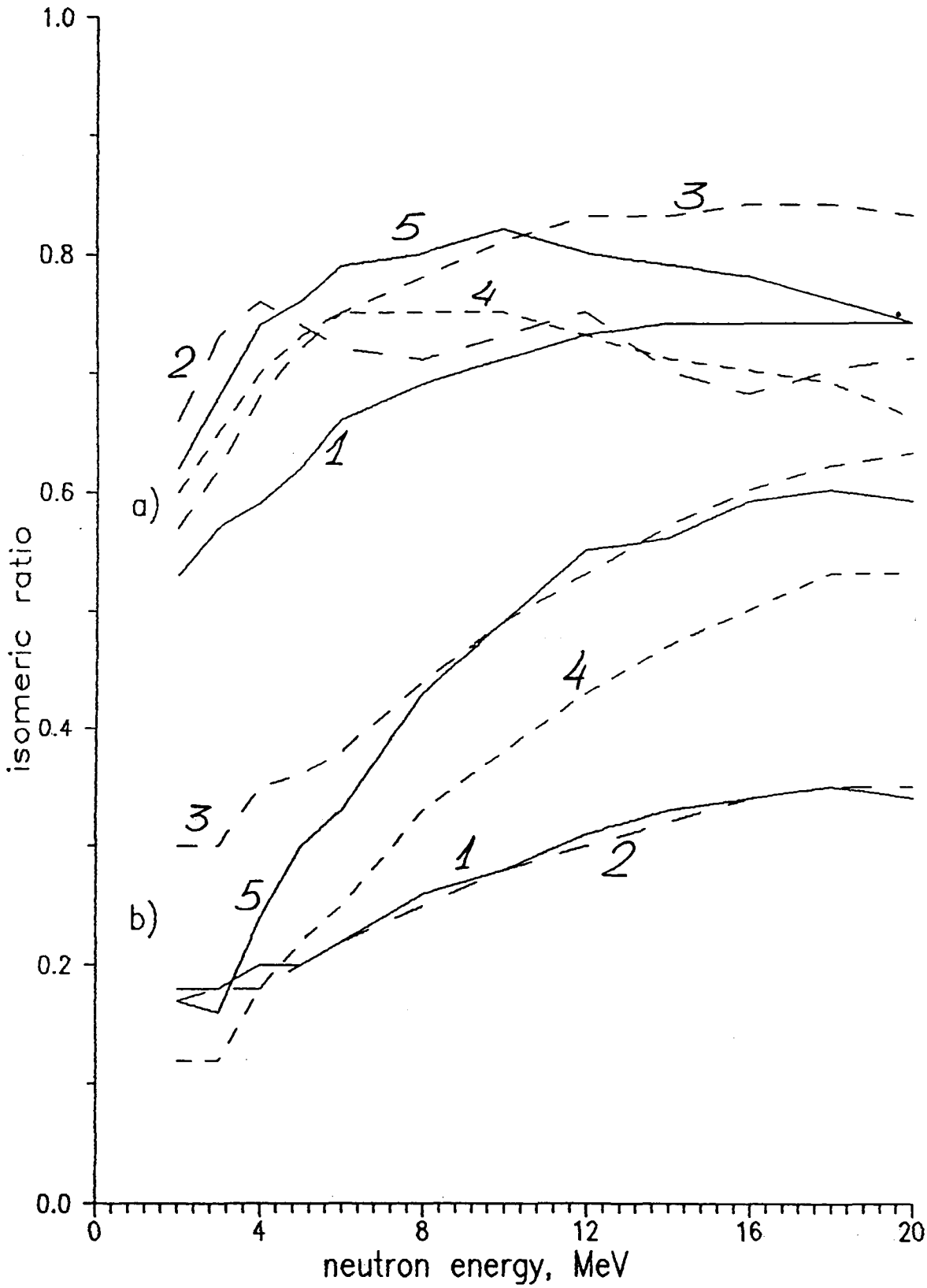

Fig.3 The same as in fig.2, but for isomeric ratios.

reaction cross-section. Thus our goal is to investigate and to evaluate isomeric ratios. It can be seen that the isomeric ratio for threshold reactions (fig.3) are smooth function. In case of neutron capture reaction isomeric ratio changes in large extent

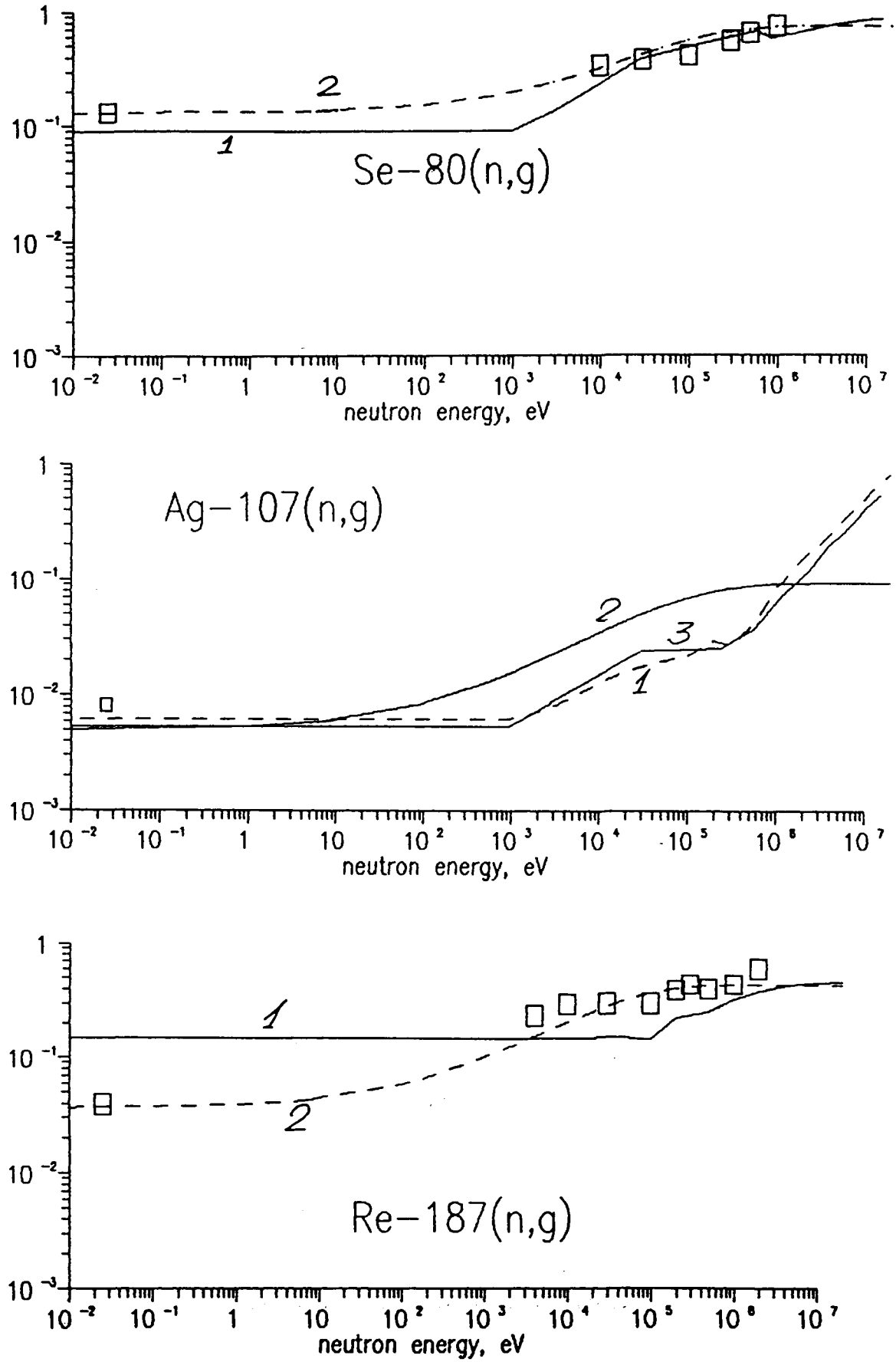

Fig.4 Data on isomeric ratios of 80Sr(n,g), 107Ag(n,g) and 187Re(n,g) reactions. Experimental data are shown by points, curves - calculation results: 1- STAPRE code, 2- by formula (1), 3- SINCROSACT.

(fig.4) when neutron energy increases from thermal to fast. The fact connects with increasing of total spin of compound nuclear due to influence of p- and higher waves in entrance channel.

Let us analyse the capacities of above theoretical methods to predict the isomeric ratio in wide target mass region both at 14.5 MeV and at thermal neutron energies in more details.

2. POSSIBILITIES OF ISOMERIC RATIOS PREDICTIONS.

The results of STAPRE calculations of isomeric ratios for nuclei with $50 < A < 150$ and at 14.5 MeV neutron energy are shown in table 1. The values of R1 were obtained using theoretical spin dependence of the level density and S2 parameter (superfluid model and rigid body moment of inertia), R2 values - using S2/2. The R values in tables 1-3 and figures denotes ratio of S>/(Sm+Sg), where symbol 'S>' is used for cross-sections of isomeric pair member with higher spin.

It is hard to see any correlations between Rexp and R1 (fig. 6a, 7a). Reasonable agreement is observed for (n,2n) reaction, but in can be seen that R1 values are as a rule higher then Rexp. The contributions of the states with higher spins are overestimated. Situation is better when using S2/2 value in calculations (fig. 5b, 6b, 7b). The values of k2=Rexp/R2 are shown in fig.8b and in table 2.

The data comparison for (n,g) reaction at thermal neutron energy are shown in table 3 and in fig.9. The situation is quite different then for threshold reactions. There are large discrepancies of data. Reasonable agreement between Rexp and R1 are only for isomeric ratios greater then 0.1. There are no special features connected with high values of spins. It is hard to understand the fact of great discrepancies for small R values. It may be connected with more sensitivity to gamma- transitions schemes than in case of large R values or with computing methods. But answer for this question is very interesting because there are a large amount isomers with small R.

3. SPIN DEPENDENCE OF LEVEL DENSITY.

As above mentioned the overestimation of high momenta contributions for threshold reactions cross-sections may be connected with both uncertainties of high spin transmission

Table 1. The comparison of experimental isomeric ratios (Rexp) with calculated ones. R1 values were calculated by STAPRE code with spin cut off parameters corresponded to rigid body moment of inertia, R2 - with S2/2.

isomers	Jm	E,keV	reactions	Rexp	R1	R2
58mCo	5+	24.88	(n,2n)	0.60	0.67	0.67
			(n,p)	0.53	0.56	0.48
62mCo	5+	22.0	(n,p)	0.53	0.55	0.47
			(n,a)	0.58	0.59	0.50
69mZn	9/2+	140	(n,2n)	0.56	0.55	0.48
			(n,p)	0.41	0.62	0.45
			(n,a)	0.53	0.60	0.45
75mGe	7/2+	139.7	(n,2n)	0.60	0.81	0.79
			(n,p)	0.50	0.81	0.70
86mRb	6-	556.1	(n,2n)	0.38	0.36	0.32
			(n,p)	0.15	0.32	0.18
95mNb	1/2-	235.7	(n,p)	0.85	0.84	0.79
			(n,a)	0.73	0.82	0.80
106mAg	6+	90.0	(n,2n)	0.41	0.53	0.46
			(n,p)	0.42	0.55	0.45
115mCd	11/2-	180	(n,2n)	0.49	0.56	0.35
			(n,p)	0.45	0.69	0.43
			(n,a)	0.21	0.73	0.26
112mIn	4+	155.5	(n,2n)	0.80	0.86	0.85
			(n,p)	0.36	0.79	0.60
123mSn	3/2+	24.0	(n,2n)	0.62	0.81	0.75
			(n,p)	0.39	0.83	0.45
127mTe	11/2-	88.26	(n,2n)	0.55	0.66	0.63
			(n,p)	0.50	0.69	0.60
133mXe	11/2-	233.2	(n,2n)	0.45	0.65	0.57
			(n,p)	0.46	0.69	0.60
148mPm	6-	137	(n,p)	0.60	0.54	0.46
			(n,a)	0.52	0.72	0.53

Table 2. Mean values of k1 and k2.

reaction	<k1> k1	<k2> k2	<k1>/<k2>
(n,2n)	0.86+- 0.21	0.98+-0.26	1.13
(n,p)	0.73+- 0.21	0.93+-0.19	1.27
(n,a)	0.78+- 0.20	0.96+-0.19	1.23

Table 3. Isomeric ratios of (n,g) reaction at thermal neutron energy.

isomers	Jm	Jg	Rexp	R1
60mCo	2	5	0.451	0.440
69mZn	9/2	1/2	0.0672	0.089
81mSe	7/2	1/2	0.131	0.250
86mRb	6	2	0.11	0.018
85mSr	1/2	9/2	0.31	0.37
90mY	7	2	0.78-3	0.14-4
95mNb	1/2	9/2	0.971	0.964
105mRh	6	1	0.313	0.260
111mCd	11/2	1/2	0.0127	0.0085
115mCd	11/2	1/2	0.107	0.0073
121mSn	11/2	3/2	0.0071	0.088
123mSn	3/2	11/2	0.006	0.02
125mSn	3/2	11/2	0.03	0.05
127mTe	11/2	3/2	0.13	0.011
129mTe	11/2	3/2	0.0698	0.022
125mXe	9/2	1/2	0.17	0.085
133mXe	11/2	3/2	0.111	0.15-3
135mXe	11/2	3/2	0.0113	0.84-4
148mPm	6	1	0.43	0.36
151mEu	0	3	0.641	0.78
151mEu	8	3	0.44-3	0.39-2

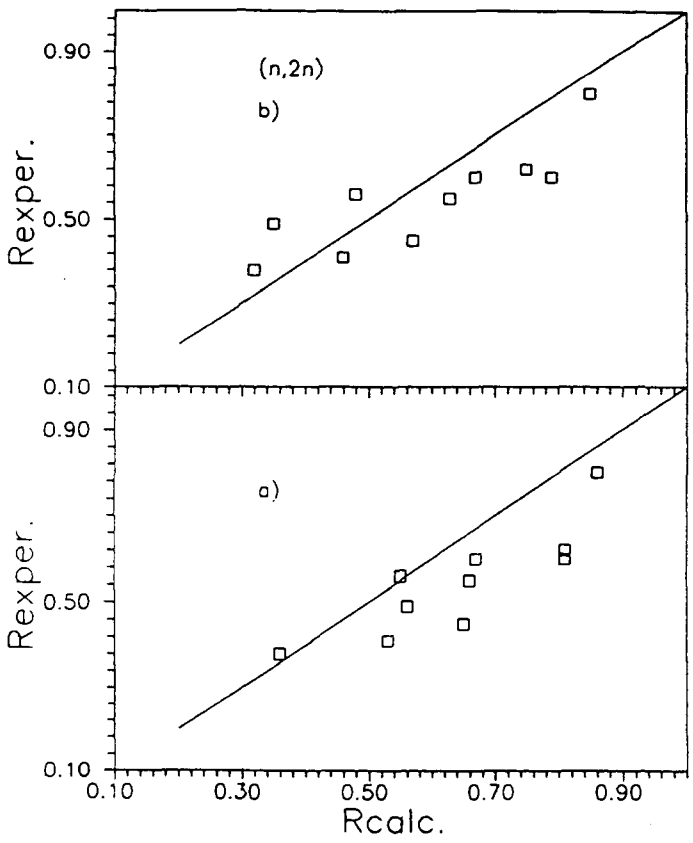

Fig.5 Correlations between experimental and calculated isomeric ratios for (n,2n) reaction, a)- Rcalc=R1, b)-Rcalc=R2.

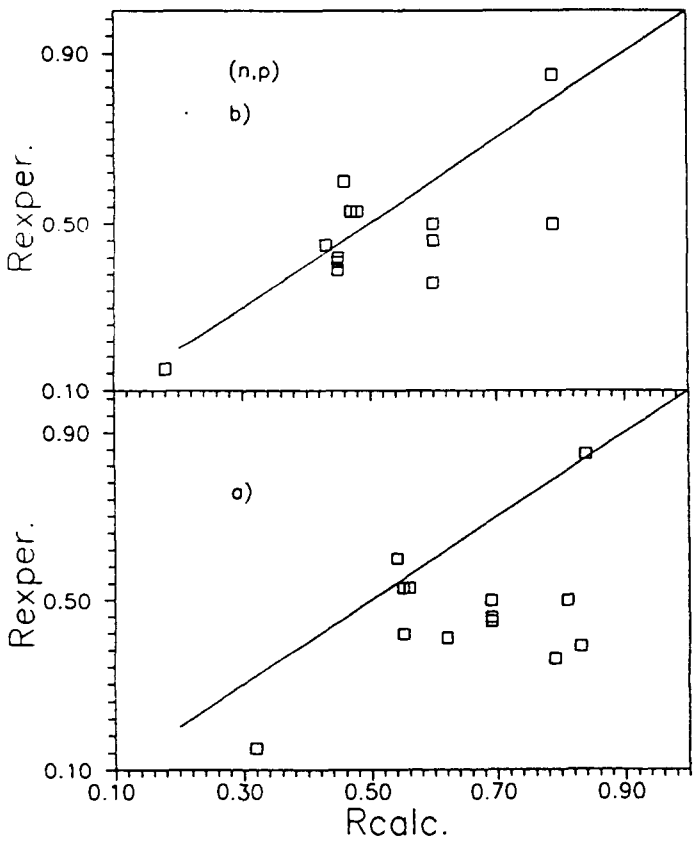

Fig.6 The same as in fig.5 but for (n,p) reaction.

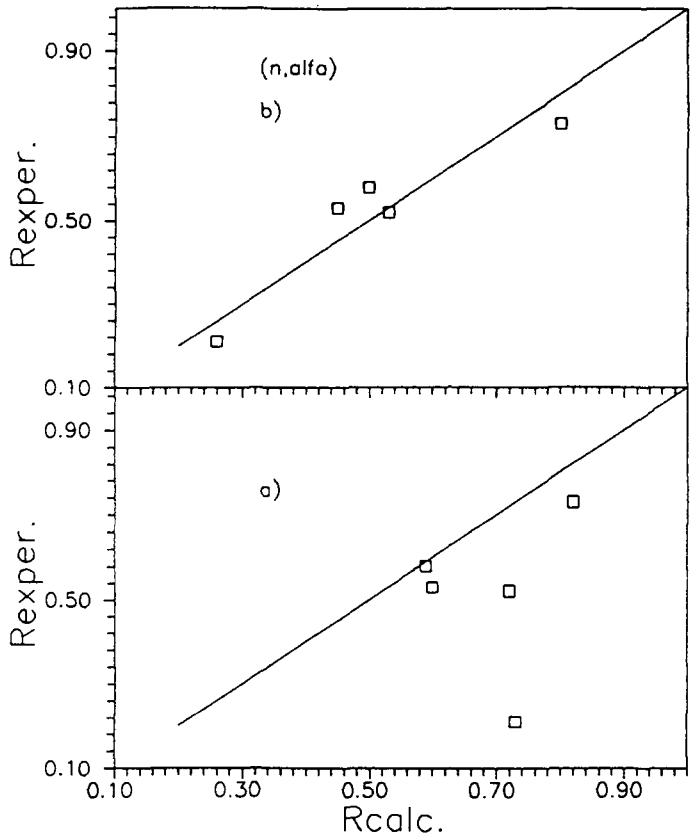

Fig.7 The same as in fig.5 but for (n,alpha) reaction.

coefficients [3] and spin dependence of level density. The S2 values has been extracted from neutron angular distributions in (p,n) reaction in [16]. Spin cut off parameters from that analyses corresponds to rigid body moment of inertia for nuclei with A < 100, but for A > 100 it was obvious tendency of decreasing S2 by factor 2-10.

The S2 values has been extracted for transactinides in [23], from analysis of spin distribution of low laying discrete levels. Extracted values were smaller than calculated ones considerably.

The same tendency can be seen from our analyses too. However, there are no necessity to decrease spin cut off parameter in analysing isomeric ratios in (n,g) reaction, in spite of the fact that population of isomer does not depends on spin distribution in entrance channel.

We have no the base to change dependences of S2 parameter from energy and from mass number, but we believe that self-consistent analyses of all experimental data connected with spin dependence of level density is very actual today.

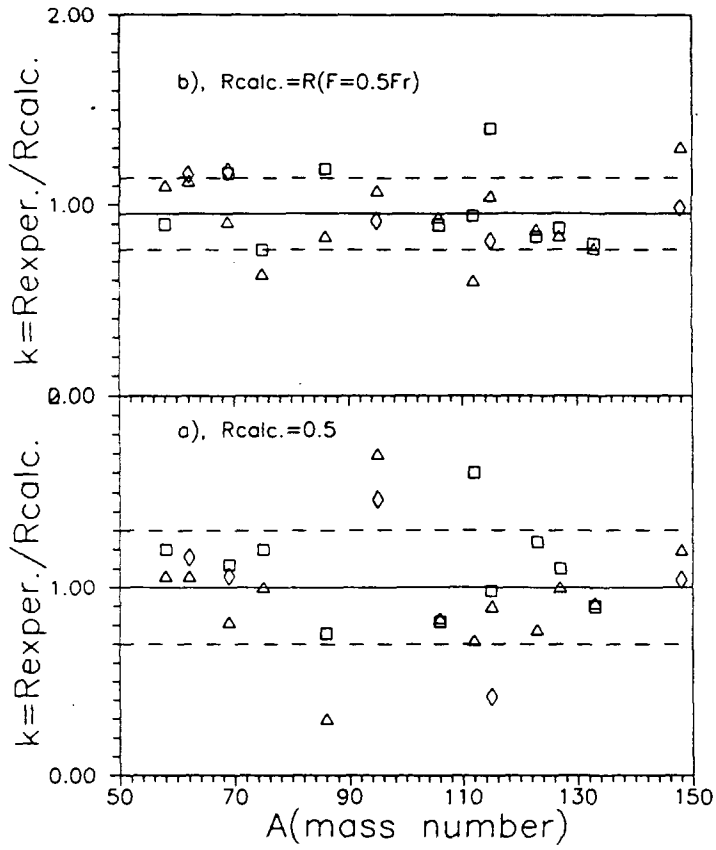

Fig.8 Dependence of isomeric ratios on mass number. (n.2n)- ; (n,p)- ; (n,alpha)- .

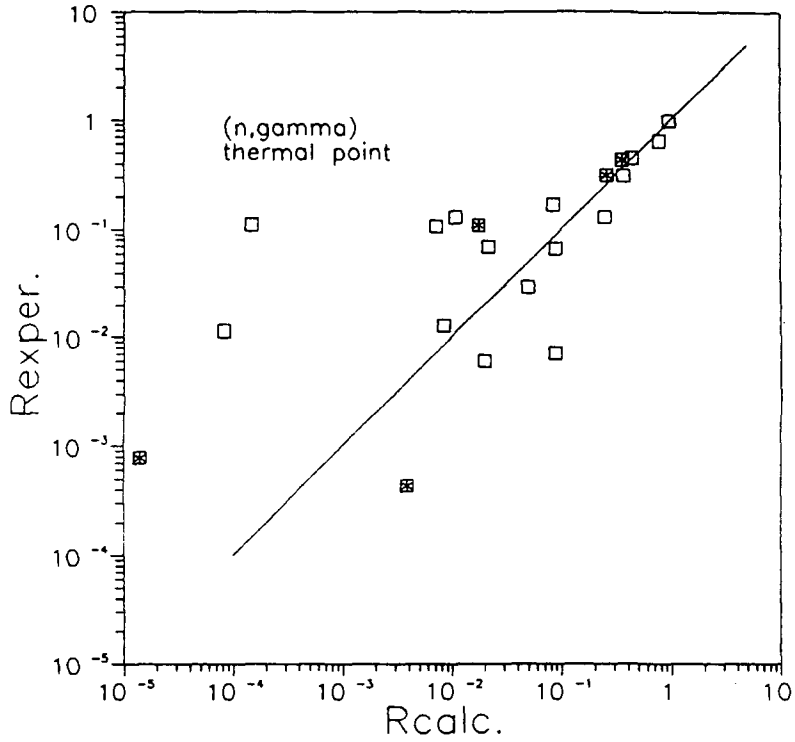

Fig.9 The same as in fig.5, but for (n,g) reaction. Rcalc=R1. Stars represent data on J > 6.

Table 4. Data on 109Ag(n.2n) reaction cross-sections.

reaction	En,MeV	cross section, mb	
		measured	calculated
109Ag(n,2n)108mAg	14.1	200(39) [24]	
	14.19	224(6) [23]	
	14.28	215(11) [23]	
	14.44	223(10) [23]	
	14.5	204(37) [24]	
	14.77	230(7) [23]	
	14.80	212(11) [22]	
	14.83	233(7) [23]	
	14.90	208(37) [24]	
	14.90	191(7) [25]	
	14-15		665(73) [19]
	14-15		577(50) pr.work
109Ag(n,2n)108gAg	14.1	604(66) [29]	
	14.1	1000(100) [31]	
	14.30	848(31) [26]	
	14.40	1186(42) [27]	
	14.5	311(156) [30]	
	14.67	842(30) [26]	
	14.80	710(107) [41]	
	14.73	1136(101) [27]	
	14-15		900 pr.work

4. ISOMERIC RATIOS SYSTEMATICS.

It is well known that according to the Hauser-Feshbach theory of particle and gamma cascade the isomeric levels are populated via three ways: a) through the particle emission, b) by gamma cascades from highly excited levels in continuum and finally c) by gamma-transitions between low-laying discrete levels. In general the contribution of each of these depends on the reaction type, the nucleus structure, the position and characteristics of the

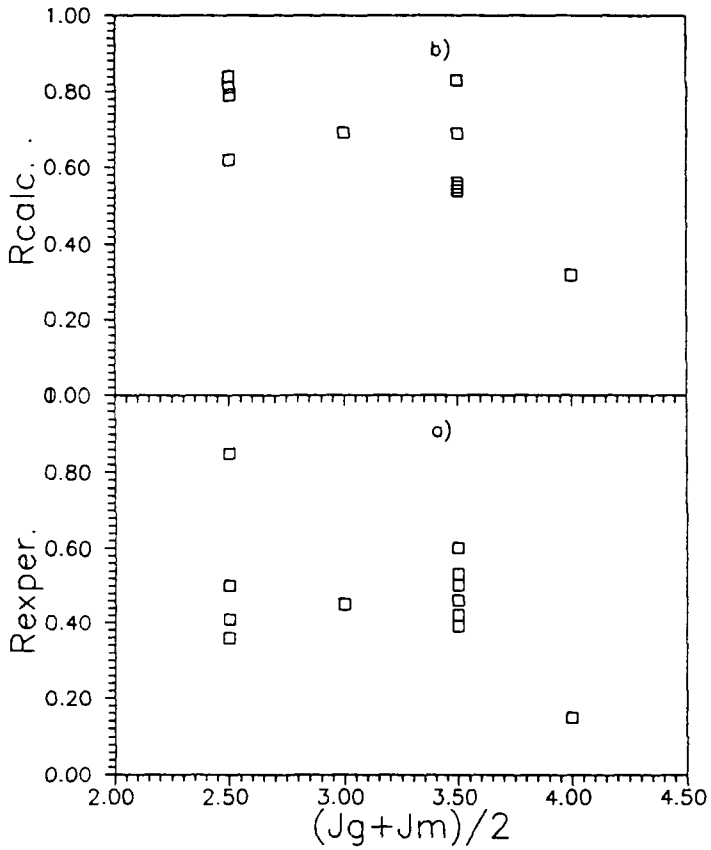

Fig.10 Dependence of experimental a) and calculated b) isomeric ratios for (n,p) reaction.

isomer levels. But it would be quite natural to suppose that the last steps of gamma-cascades plays the dominant role. So, the population of isomeric levels would be determined mainly by the scheme of discrete levels and the spin distribution of nuclear levels for the excitation energy U=(2-3) E, where E is the average energy of gamma-rays.

The smooth dependences exists for processes a) and b), but c) processes has individual features depended on specific character of nuclei. This is the main reason as we think, unsuccessful attempts to create good enough systematics of isomeric ratios as the function of same nucleus characteristics. This conclusion is confirmed by our results also.

A strong energy dependence of isomeric ratio in neutron capture reaction may be connected with increasing of of p-neutrons wave contribution to absorption cross-section. An evaluation of isomeric ratio in (n,g) reaction has special features: partial isomeric ratios for l-wave neutron should be used in reproducing of cross-section curves from parameters of resolved resonances. However, this approach is time consuming and

Table 5. Data on 151Eu(n.2n) reaction cross-sections.

reaction	En,MeV	cross section, mb	
		measured	calculated
151Eu(n,2n)150mEu	14.1	1215(53) [22]	
	14.1	1162(93) [24]	
	14.19	1190(27) [23]	
	14.41	1215(36) [23]	
	14.50	1147(83) [24]	
	14.77	1219(28) [23]	
	14.8	1127(55) [25]	
	14.8	1276(64) [22]	
	14-15		1325(94) [37]
	14.2		1150 pr. work
151Eu(n,2n)150gEu	14.7	467(43) [48]	
	14.8	497(45) [52]	
	14.8	480(96) [50]	
	14.8	550(55) [51]	
	14.8	500(200) [49]	
	14.2		640 pr. work
151Eu(n,2n)150Eu	14.28	1702(138) [53]	
	14.7	1737(192) [48]	
	14.76	1752(145) [53]	
	14.2		1790 pr. work

un-effective because experimental data on R1 are absent. An averaged value with energy dependence tested on experimental data may be used :

$$R(E)=Ro+(R(E1)-Ro)*V1(E)/V1(E1),$$

where V1 - penetrability of centrifugal barrier for p-neutrons, Ro and R1 experimental isomeric ratios at thermal and E1 neutron energy, consequently.

Figure 4 represents i) results of calculations: by formula (1) - curve 1, by STAPRE code - curve 2, SINCROSACT [5] - curve 3; ii) experimental data on isomeric ratio in (n,g) reaction - points. It could be seen that the results of calculations by simple formula

Table 6. Data on 179Hf(n.2n) reaction cross-sections.

reaction	En,MeV	cross section, mb		
		measured	calculated	
179Hf(n,2n)178m2Hf	14.8	5.91(64) [32]		
	14.8	6.3(6) [22]		
	14.9	6.0(3) [25]		
	14		2.9	[14]
	14-15		4.5	pr.work
179Hf(n,2n)178m1Hf	14.8	749(75) [33]		
	14.8	754(80) [35]		
	14.8	1452(116) [34]		
	14-15		600	pr.work

Table 7. Data on 187Re(n.2n) reaction cross-sections.

reaction	En,MeV	cross section, mb		
		measured	calculated	
187Re(n,2n)186mRe	14.1		693	[36]
	14.5		606(258)	[38]
	14.8	135(65) [22]		
	14-15		591(122)	[19]
	14-15		630	pr. work
187Re(n,2n)186gRe	14.1	1766(161) [40]		
	14.8	1426(93) [39]		
	14.8	1436(72) [41]		
	14-15		1300	pr. work
187Re(n,2n)186Re	14.16		2091(71)	[37]
	14.66		2048(86)	[37]
	14-15		1930	pr. work

Table 8. Data on 193Ir(n.2n) reaction cross-sections.

reaction	En,MeV	cross section, mb	
		measured	calculated
193Ir(n,2n)192m2Ir	14.1		160 pr. work
193Ir(n,2n)192(g+m1)	14.1	2005(100) [42]	
	14.1	2058(100) [43]	
	14.5	1885(116) [44]	
	14.7	2179(148) [45]	
	14.8	1630(160) [46]	
	14.1		1900 pr. work

(1) are in well agreement with the results of rigorous calculations and experimental data.

5. CROSS-SECTIONS EVALUATIONS FOR PRESENT C R P.

We have evaluated the isomer excitation functions of 109Ag(n,2n)108mAg, 151Eu(n,2n)150mEu, 179Hf(n,2n)178m2Hf, 187Re(n,2n)186mRe and 193Ir(n,2n)193m2Ir reactions for present CRP Meeting. Three stages of data preprocessing have been included in evaluations: 1) experimental data compilation and analysis; 2) theoretical calculations of excitation functions; and 3) re-normalization (fitting) (if it was necessary) of calculated curves to reproduce available experimental data. Results of our work are presented in tables 4-8.

109Ag(n,2n)

All available experimental data were obtained during last 2 years. The measurements have been performed by Blinov M. e.a. [24], Lu Hanlin e.a. [23], J.Meadows e.a. [25], and Y. Ikeda e.a. [22]. Data [23] were obtained for 5 neutron energies in 14.19-14.83 MeV region. The measurements [24] provide data on excitation function for neutron energy region from 13.7 to 14.9 MeV (4 points). Data [22] and [25] were done only for one neutron energy 14.8 and 14.9 MeV, consequently. All measurements [22-24] have been performed by activation techniques.

Reaction 93Nb(n,2n)92mNb was used as monitor in [22-24]. 8 dosimetry reactions were used simultaneously in [25] for neutron fluence determination. It should be stressed that all data [22-25] are in good agreement. However, results of our calculations by STAPRE code disagree with experimental data by factor 2. We can not explain this disagreement by input data uncertainties.

151Eu(n,2n).

All data available have been measured by activation method. Experimental data on 150mEu excitation cross section in (n,2n) reaction have been measured in [47,48] for 14.8 and 14.7 MeV. 27Al(n,a)24Na reaction cross section was used for neutron fluence monitoring. S.Qaim e.a. [48] have used also 75As(n,2n)74As reaction for this purposes. Data [22,23,24,25] have been measured recently, but these data correspond to 14 MeV only. 93Nb(n,2n)92mNbreaction was used as monitor in [22,23,24]. J.W.Meadows e.a. [25]have used eight dosimetry reactions simultaneously for neutron fluencemonitoring.

Data on excitation of ground state of 150Eu in (n,2n) reaction have been measured in [48,49,50,51,52] for 14.7 and 14.8 MeV.

Experimental data on 151Eu(n,2n) reaction have been measured in [48,53]. J.Frehaut e.a. [53] have measured cross section for neutron energy region from 8.44 to 14.76 MeV.

179Hf(n,2n).

Data by Lu Hanlin [23] on excitation function of 178m2Hf isomer in energy region from 4.2 to 14.8 MeV were reported at previous Meeting (11-12 September 1989). Unfortunately, these data are not available for us. There are data [22,25,32] on 179Hf(n,2n)178m2Hf reaction cross section. These data have been measured by activation method for two energy points: 14.8 MeV [22,32] and 14.9 MeV [25]. Neutron fluence monitoring in [25] has been done by dosimetry reactions as for 109Ag. Y.Ikeda e.a.[22] used 93Nb(n,2n)92mNb reaction cross section for this purposes. The results [22,25,32] are in good agreement.

Available data on excitation of 178m1Hf in (n,2n) reaction [33,34,35] are sums of two cross sections: 179Hf(n,2n)178m1Hf and 178Hf(n,n')178m1Hf.

Input data set for excitation function calculation is unreliable because there are no information on GTS's. We have used methods proposed in [15] to compute cross sections. We are agreed with M.B.Chadwick e.a. that the results are good surprisingly.

187Re(n,2n)

Now we know only one work [22] with experimental data on isomer cross section. Cross section value at 14.8 MeV has been measured in [22] by activation method. 93Nb(n,2n)92mNb reaction cross section was used for neutron fluence monitoring.

There are data [39,40,41] on 186Re ground state excitation for 14.1 MeV [40] and for 14.8 MeV [39,41]. All data have been measured by activation method. We have renormalized these data to new values of standards. The results of our calculations are in reasonable agreement with experimental data [22,39,40,30].

193Ir(n,2n).

There are no experimental data on 192m2Ir excitation cross section. There are data on 193Ir(n,2n)192(g+m1)Ir reaction cross section [42-46]. All data have been measured by activation method.

M.Herman e.a. [44] have measured cross section for five energy points form 13.0 to 17.9 MeV. 56Fe(n,p)56Mn reaction cross section was used as monitor.

B.Bayhurst e.a.[42] have measured cross section values for nine energy points from 8.61 to 21.24 MeV. 27Al(n,a)24Na and 90Zr(n2n)89Zr reactions were used for neutron fluence monitoring.

Cross section values have been measured for single energy: 14.1 MeV [43], 14.7 MeV [45], 14.8 MeV [46]. J.Temperley e.a. [43] have used 56Fe(n,p)56Mn to determine neutron fluence. S.M.Qaim e.a. have used 75As(n,2n) reaction as monitor. Data by A.A.Druzhinin e.a. are the results of absolute measurements.

All experimental data on 193Ir(n,2n) reaction cross section apart from data [46] are in good agreement at 14.5 MeV.

We have renormalized data [43,44,45] to the new standard cross sections values.

The results of our calculations are in reasonable agreement with experimental data available. We hope the calculated value of m2 isomer cross section are good enough.

CONCLUSION.

The comparison of calculations with experimental data shows: 1) A good agreement (20%) between experimental values and the theoretical calculations can be achieved in many cases without

parameters fitting. However, there are a great discrepancies for small isomeric ratios (R < 0.1) in (n,g) reaction. The reason of these discrepancies should be investigated.

2) Experimental data errors put a contribution in spread of k2=Rexp/Rcalc values. Successful investigation of spin dependence of level density on the base of isomeric ratios is impossible, because the prescission of experimental data are too low.

3) Considerable influence of gamma-transition schemes on calculated isomeric ratio decreases both the capacities of rigorous theoretical models calculations and the validities of systematics based on smooth dependences to predict unknown values.

REFERENCES.

1. Huizenga J.R., Vandenbosh R. Phys. Rev., 120, 4, 1960, p.1305.
2. Vonach H. Excitation of Isomeric States in (n,n') Reactions.
3. Grudzevich O.T., Kagalenko A.B., Kornilov N.V., Pashchenko A.B. TSNIIATOMINFORM, Moscow, 1988, v.3, p.349 (in Russian).
4. Ignatyuk A.V., Kornilov N.V., Maslov V.M., Pashchenko A.B. Atomic Energy, v.63, 1987, p.110 (in Russian).
5. Summary Report of a Consultants' Meeting on First Results of FENDL-1 testing and start FENDL-2 (prepared by A.B. Pashchenko and D.W. Muir) IAEA, Vienna, Austria,25-28 June, 1990, INDC/NDS-241,1990
6. M.Uhl, B.Stromaier, IRK 76/01, Vienna, 1976
7. Ignatyuk A.V. Statistical properties of excited nuclei, Moscow, ENERGOATOMIZDAT, 1985 (in Russian).
8. Grudzevich O.T., Ignatyuk A.V., Playskin V.I. TSNIIATOMINFORM, Moscow, 1988, v.2, p.96 (in Russian).
9. Lederer C.M. and Shirley V.S. TABLE OF ISOTOPES, 7th edition, New York, 1978.
10. G.A. Bartholomew et al. Advances in Nuclear Physics, v.7, Plenum Press, N.Y.(1973).
11. P.Axel Physical Review, 126(1962) 671.
12. Belanova T.S., Ignatyuk A.V., Pashchenko A.B., Playskin V.I. Radioactive capture of neutrons, Moscow, 1986, ENERGOATOMIZDAT.
13. Arthur E.D. Nucl. Sci. Eng. 1980, v.76, p.137.
14. Chadwick M.B., Young P.G., Oxford University Nuclear Physics Laboratory report, OUNP-89-21.

15. Grudzevich O.T., Zelenetsky A.V., Pashchenko A.B.
Preprint FEI-2058, Obninsk, 1989
16. Biruykov N.S., et. al. Nuclear Physics,
v.30, 1(7), 1979, p.26 (in Russian)
17. J. Kopecky and V. Gruppelaar, Report ECN-200, 1987.
18. Report NEANDC-259'U'. Proc. of a Specialists' Meeting on Neutron Activation Cross-Section for Fission and Fusion Energy Applications, Argonne National Laboratory, USA, 13-15 th September 1989. Edited by M.Wapuer and H. Vonach, Institute fur Radium forschnung und Kernphysik, Vienna, Austria, 1990.
19. Report INDCCNDS-232/L. Activation Cross-Sections for the Generation of Long-Lived Radionuclides Importance in Fusion Reactor Technology. Proc. of an IAEA Consultants' Meeting held by Argonne National Laboratory, Argonne, USA, 11-12 September 1989, Edited by Wang DaHai, 1990.
20. Badikov S.A., Grudzevich O.T., Ignatyuk A.V., Pashchenko A.B. et. al. Proc. of Intern. Conf., Julich, 1991.
21. Antsipov G.V., Konshin V.A., Maslov V.M. et. al. Evaluated nuclear data of U-235, Minsk, Nauka i Tehnika, 1985.
22. Y. Ikeda, A.Kummar, C.Konno Proc. of Intern. Conf. Nuclear Data for Science and Technology, 13-17 may, 1991, Julich, FRG.
23. Lu Hanlin e.a. Proc. of an IAEA Consultant's Meeting, ANL, 11-12 September, 1989, p.33.
24. M.V.Blinov e. a. Proc. of an IAEA Consultant's Meeting, ANL, 11-12 September, 1989, p.87.
25. J.W.Meadowes e.a. Proc. of an IAEA Consultant's Meeting, ANL, 11-12 September, 1989, p.79.
26. T.B.Ryves e.a. Silver cross-sections for 14 MeV neutrons, J. JP/g, v.14, p.77, 1985.
27. W.Augustyniak e.a. J. Nucl. Phys. v. A247, p.231, 1975.
28. S.K. Mukherjce e.a. J. PPS, v.77, p.508, 1961.
29. S.Yasumi J. JPJ, v.12, p.443, 1957.
30. E.B.Paul, R.L.Clarke J. CJP, v.31, p.267, 1953.
31. S.G.Forbes J. Phys. Rev., v.88, p.1309, 1952.
32. B.H.Patrick e.a.Proc. of an IAEA Consultant's Meeting, ANL, 11-12 September, 1989, p.69-77.
33. S.Sothras J. DA/B, v.38, p.280, 1978.
34. G.N.Salaita, D.K.Eapen J. ANS, v.16, p.59, 1973.
35. R.Prasad e.a. J. Nucl. Phys., v.88, p.349, 1966.

36. K.Shibata e.a. Rep. JAERI-1319,1990.
37. H.Vonach e.a. Rep. INDC/P(89)-16, 1989.
38. H.Gruppelaar e.a. Rep. ECN-207, 1988.
39. A.A.Druzhinin e.a. J. YF, v.5(1), p.18, 1967.
40. R.A.Karam e.a. Rep. AD-402668, March, 1963.
41. C.S.Khurana, H.S.Hans J. Nucl. Phys., v.28, p.560, 1961.
42. B.P.Bayhurst e.a. J. Phys. Rev. C, v.12, p.451, 1975.
43. J.K.Temperley, D.E.Barnes Rep. BRL-1491, Aug. 1970.
44. M.Herman, A.Marcinkowski, K.Stankiewich J. Nucl. Phys. A, v.430, p.69, 1984.
45. S.M.Qaim J. Nucl. Phys. A, v.185, p.614, 1972.
46. A.A.Druzhinin e.a. J. YF, v.14, n.4, p.682, 1971.
47. D.R.Nethaway e.a. J. Nucl. Phys., v. A190, p.635, 1972.
48. S.M.Qaim e.a. J. Nucl. Phys., v. A224, p.319, 1974.
49. R.G.Wille, R.W.Fink J. Phys. Rev., v. 118, p.242, 1960.
50. H.Spenke J. Nucl. Phys., v.51, p.329, 1964.
51. C.S.Khurana, H.S.Hains J. Nucl. Phys., v.28, p.560, 1961.
52. A.Bary J. DA/B, v.32, p.5091, 1972
53. J.Frehaut e.a. Proc. Intern. Conf. Gaussig, nov. 1975.

Implications of the IAEA CRP on Long-lived Activation Cross Sections on Waste Disposal and Materials Recycling for Fusion Reactor Materials

E.T. Cheng
TSI Research, Inc.
225 Stevens Avenue, #110
Solana Beach, CA USA 92075

Abstract

Waste disposal and materials recycling are important issues for the development of fusion power reactors. The recent criteria were summarized and discussed. The allowable concentrations of natural elements in the first wall and blanket components of a lithium self-cooled fusion blanket with vanadium structure, were assessed for the "Class C" shallow-land waste disposal consideration. The activation cross reactions recently developed under the IAEA Coordinated Research Program on Activation Cross Sections for the Generations of Long-Lived Radionuclides were incorporated to improve the REAC-2 library. Recommendations were given on measurements of some estimated cross sections: $^{158}Dy(n,p)^{158}Tb$, $^{191}Ir(n,g)^{192m2}Ir$, $^{180}Ta(n,t)^{178m2}Hf$, $^{187}Re(n,2n)^{186m}Re$ and $^{185}Re(n,g)^{186m}Re$. Another independent measurement on $^{179}Hf(n,2n)^{178m2}Hf$ was suggested. Measurements or estimates of transaction cross sections for the long-lived radionuclides, namely ^{26}Al, ^{94}Nb, ^{108m}Ag, ^{158}Tb, ^{166m}Ho, $^{178m2}Hf$, ^{186m}Re, and $^{192m2}Ir$, were recommended for the investigation of long-term materials recycling issue.

1. Introduction

Fusion power reactors constructed with low activation fusion materials are attractive because of the reduced risks associated with the prompt and latent radiation dose to the population due to the released radioactive inventory during a reactor accident, and

waste disposal related environmental issues [1,2]. The general considerations for low activation materials are: (1) Low inventory of long-lived radioactive materials to minimize the environmental impacts due to the disposal of decommissioned nuclear components. Reuse of component materials is an option to reduce the quantity of nuclear waste to be disposed of; (2) Reduced shutdown gamma-ray dose rate within and outside the reactor components to allow for both remote and hands-on maintenance; (3) Reduced radioactive inventory to minimize the prompt and latent radiation dose released during a reactor accident; and (4) Reduced afterheat to minimize the material temperature rise that will cause the rupture of structural component for the release of radioactive inventory. An initial investigation was done of accident safety, waste management, materials recycling, effluent, and maintenance considerations for all natural materials [3]. Criteria for low activation materials have recently been discussed [4]. In this paper the recent development on criteria for waste disposal and materials recycling was summarized and applied to a candidate fusion reactor. An assessment on the concentration limits for all natural elements is presented, incorporating the results of the IAEA Coordinated Research Program on Measurements of Activation Cross Sections leading to the production of long-lived radionuclides [5].

2. Waste Disposal and Materials Recycling: Criteria and Issues

The criteria for low activation materials in a fusion power reactor were previously discussed [1] and recently reassessed [4]. In Ref. 1, the definition of a low activation material is primarily determined by the ability to qualify after service in the reactor as a shallow-land burial radioactive waste. However, the shallow-

land burial waste disposal, although being emphasized in the United States, is in general not acceptable in Europe and other countries. Recycling of irradiated materials is an attractive alternative being investigated for fusion reactor development.

2.1 Waste Disposal

The shallow-land burial waste disposal is regulated by a set of specific activity limits (SAL) for long-lived (half-life longer than 5 years) radionuclides. In the U.S., this set of SALs is specified in the federal regulations 10 CFR 61 [6], which is primarily determined for and limited by the fission and industrial low-level radioactive wastes. Recently Fetter et al. have evaluated the SALs for all radioactive nuclides based on the 10 CFR 61 methodology [7]. For the purpose of our assessment for low activation materials, we have adopted Fetter et al. evaluations on SALs because of its completeness and self-consistency. In principle, Fetter et al. and 10 CFR 61 evaluations should provide similar SALs since both were evaluated based on the same methodology and criteria. However, by comparing Fetter et al. and 10 CFR 61 evaluations, we noted a few discrepancies. These discrepancies occur primarily for the long-lived radionuclides which are beta emitters. Table 1 shows some of the major discrepancies in SALs: ^{14}C , ^{63}Ni, and ^{99}Tc. The corresponding elemental concentration limits using the 10 CFR 61 and Fetter et al. evaluations to qualify as shallow-land burial waste will differ accordingly. Table 1 also shows the allowable N, Cu, Ni, and Mo concentrations using these two evaluations for comparison. The reason for the difference between 10 CFR 61 and Fetter et al. evaluations on the SALs is mainly due to the account for reduced intruder dose due to added stability of metal waste in Fetter et

Table 1

Comparison of Specific Activity Limits and relevant Allowable Elemental Concentrations for Shallow-land Burial Waste Disposal from 10 CFR 61 and Fetter et al. Evaluations

Radionuclide	Specific Activity Limits (Ci/m^3) 10 CFR 61	Fetter et al.
^{14}C	80	6,000
^{63}Ni	7,000	7,000,000
^{99}Tc	30	0.6

Element (*)	Allowable Elemental Concentration 10 CFR 61	Fetter al al.
N (^{14}C)	987 ppm	7.4 %
Cu (^{63}Ni)	0.14 %	no limit
Ni (^{63}Ni)	0.48 %	34 %
Mo (^{99}Tc)	100 ppm	2 ppm

* Contributing long-lived radionuclide.

al. evaluations [7], while 10 CFR 61 evaluations gave only a factor of 10 reduction for metal waste.

2.2. Materials Recycling

Recycle of used materials will help to reduce the quantity of nuclear waste to be disposed of. The European Community countries are particularly interested in this approach [2,8]. Otherwise a deep geologic disposal of nuclear waste is the only option. The criteria for materials recycling is determined primarily by the gamma dose rate for remelt and subsequent re-fabrication of the material to be reused. For hands-on recycling, the limit for the gamma dose rate is 2.5 mR per hour (0.025 mSv/h) [4]. The cooling time after decommissioning is assumed to be 100 years or less. However, if the recycling is to be handled remotely, the limit will be 1 R/h (10 mSv/h) at 50 years after decommissioning [4]. In the studies performed in Europe, it was revealed that impurity elements, rather than the main alloying elements, are very often the important factors to determine the shutdown gamma dose rate [4,8].

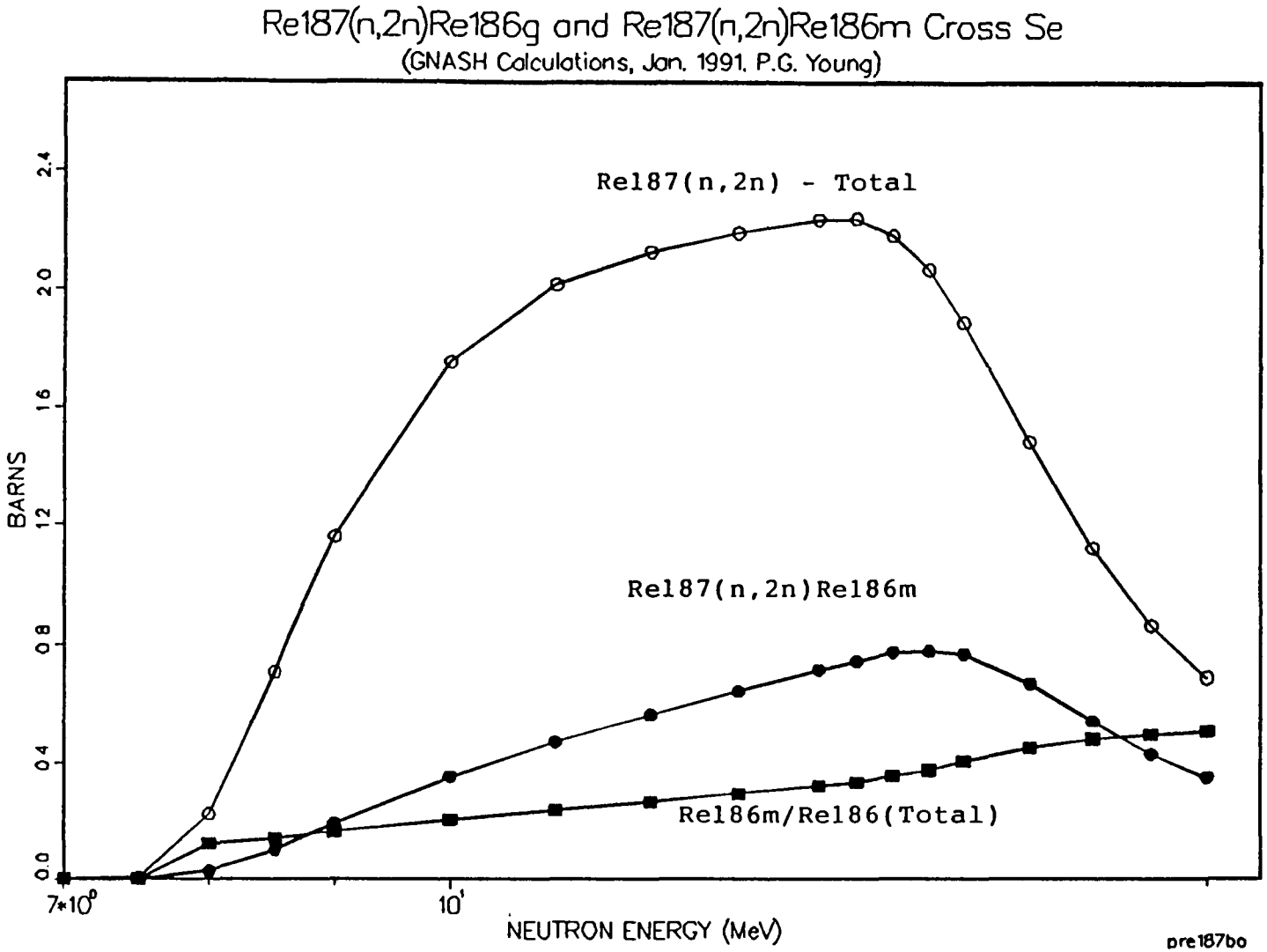

Fig. 1 Calculated total 187Re(n,2n) and 187Re(n,2n)186mRe Cross Sections and the ratio of these two cross sections [Source: P.G. Young, LANL, 1991].

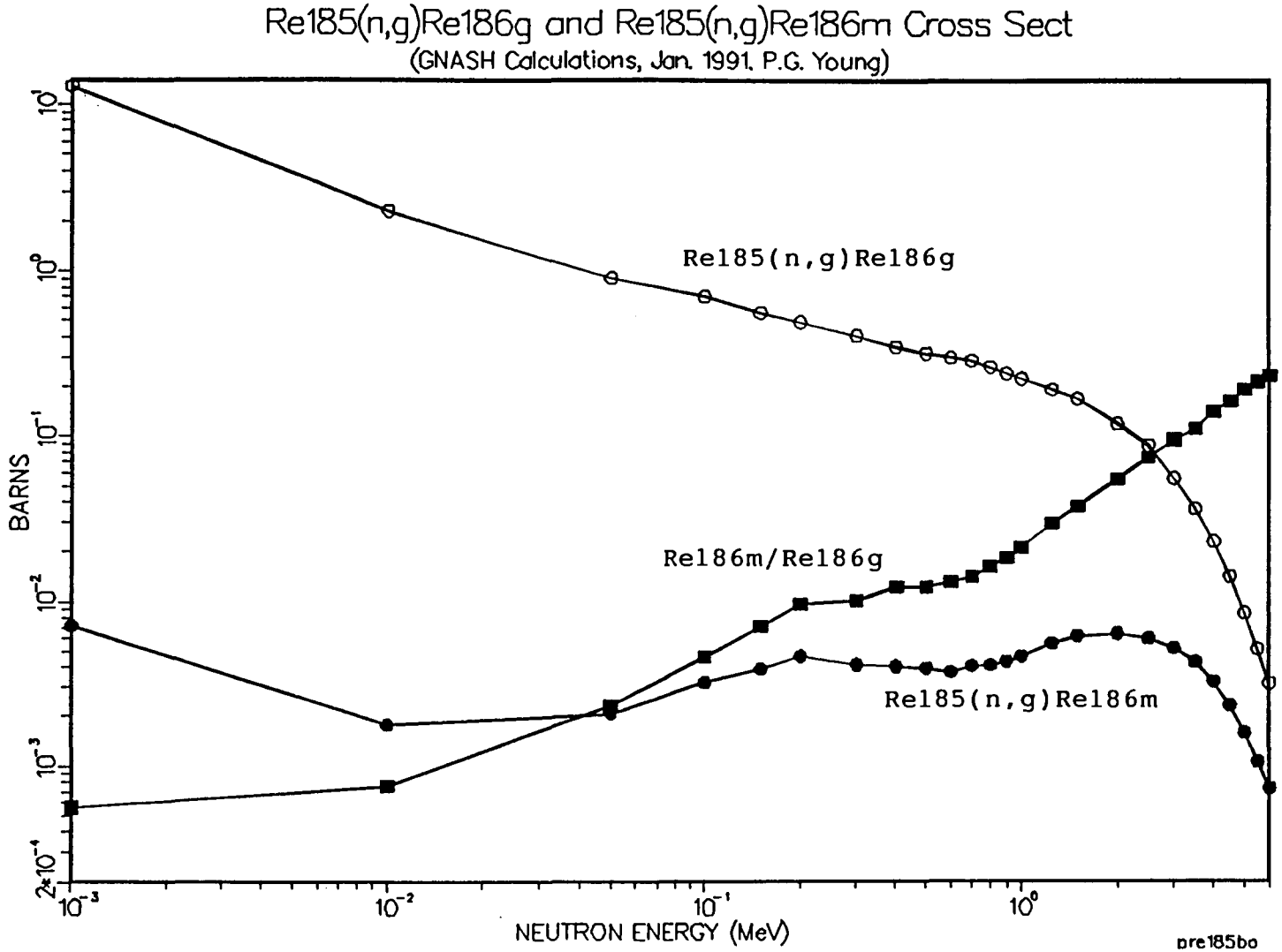

Fig. 2 Calculated 185Re(n,g)186gRe and 185Re(n,g)186mRe cross sections, and the ratio of these two cross sections [Source: P.G. Young, LANL, 1991].

3. Methods of Analysis

Neutron spectra were calculated using the methods described in Ref. 3, i.e., ENDF/B-V based nuclear data library and REAC activation calculation code and library (REAC-2) system [9]. Note that newly measured and evaluated cross sections leading to the production of long-lived radionuclides under the IAEA CRP activity [5] were also included in the analysis to either supplement or update the REAC2 activation cross section library [10]. The blanket model used for producing the neutron spectra needed for the analysis is similar to the liquid lithium self-cooled vanadium alloy structured blanket evaluated in the Blanket Comparison and Selection Study (BCSS) [10]. The blanket model consists of a 3 mm first wall (100% vanadium alloy), a 0.5 m breeding zone (7.1% vanadium alloy + 73.7% liquid lithium), and a 0.5 m reflector (10% vanadium alloy + 10% liquid lithium + 80% vanadium). A neutron wall loading of 5 MW/m^2 was assumed for all activation calculations. The operating time was taken to be 4 years continuously resulting in a toil exposure of 20 $MW\text{-}y/m^2$ at the first wall component.

4. Assessment and Discussion

In the following, assessments and discussions were given for the natural elements considering waste disposal and materials recycling criteria described in Sec. 2.

4.1. Waste Disposal

Assessment was made for shallow-land burial (10 CFR 61 Class C) waste disposal of the natural elements in the first wall and blanket locations of a fusion power reactor. Table 2 gives the allowable concentrations for all natural elements in the first wall and blanket components of the V/Li fusion blanket to qualify for shallow-land burial waste disposal. The criteria assumed are the

Table 2

Concentration Limits and Major Contributing Radionuclides in the First Wall and Blanket Components of a Lithium Self-cooled Vanadium Alloy Fusion Blanket for Shallow-land Burial Waste Disposal[+] after 20 MW-y/m^2 Exposure (Based on REAC2 Calculations and Revisions)

ELEMENT	CONCENTRATION LIMIT FIST WALL	BLANKET	MAJOR CONTRIBUTORS
N	3.4%	7.4%	^{14}C(100%)
Al*	0.19%	1%	^{26}Al(100%)
Si*	50%	no limit	^{26}Al(100%)
S	48%	no limit	^{32}Si(100%)
Cl	11%	15%	^{36}Cl(99%);^{32}Si(1%)
Ar	2.4%	9.8%	^{39}Ar(99%);^{36}Cl(1%)
K	1.9%	5.9%	^{39}Ar(60%);^{36}Cl(40%)
Ca	21%	no limit	^{39}Ar(96%);^{36}Cl(4%)
Ni	11%	34%	^{59}Ni(61%);^{60}Fe(32%);^{63}Ni(7%)
Cu*	33%	no limit	^{63}Ni(89%);^{60}Fe(11%)
Se	0.25%	0.93%	^{79}Se(100%)
Br	4.0%	14%	^{79}Se(57%);^{81}Kr(43%)
Kr	6.8%	no limit	^{81}Kr(94%);^{79}Se(6%)
Sr	39%	no limit	^{79}Se(67%);^{81}Kr(33%)
Zr	3.1%	43%	^{94}Nb(99%);^{99}Tc(1%)
Nb	1.2ppm	1.3ppm	^{94}Nb(100%)
Mo	0.14ppm	2.0ppm	^{99}Tc(95%);^{98}Tc(4%);^{94}Nb(1%)
Ru	96ppm	410ppm	^{99}Tc(92%);^{97}Tc(4%);^{98}Tc(4%)
Rh	142ppm	617ppm	^{99}Tc(100%)
Pd	22ppm	204ppm	^{108m}Ag(100%)
Ag*	0.8ppm	1.7ppm	^{108m}Ag(100%)
Cd	17ppm	690ppm	^{108m}Ag(100%)
In	0.97%	78%	^{108m}Ag(100%)
Sn	13%	32%	^{121m}Sn(97%);^{108m}Ag(3%)
Ba	61%	no limit	^{137}Cs(100%)
La	18%	no limit	^{137}La(100%)
Sm	7.4%	53%	^{152}Eu(61%);154Eu(29%);^{150m}Eu(10%)
Eu*	300ppm	870ppm	^{150m}Eu(74%);^{152}Eu(24%);^{154}Eu(2%)
Gd	10ppm	65ppm	^{158}Tb(100%)
Tb*	0.2ppm	0.6ppm	^{158}Tb(100%)
Dy*	0.58%	no limit	^{158}Tb(100%)
Ho	1.2ppm	1.3ppm	^{166m}Ho(100%)
Er	34ppm	138ppm	^{166m}Ho(100%)
Tm	186ppm	820ppm	^{166m}Ho(100%)
Lu	2.9%	3.0%	$^{178m2}Hf$(100%)
Hf*	12%	20%	$^{178m2}Hf$(100%)
Ta*	no limit	no limit	$^{178m2}Hf$(100%)
W*	no limit	no limit	^{186m}Re(96%);$^{178m2}Hf$(4%)

Re*	8.3%	13%	^{186m}Re(95%);^{192m2}Ir(5%)
Os*	64ppm	150ppm	^{186m}Re(100%)
Ir*	5.6ppm	9.0ppm	^{192m2}Ir(100%)
Pt	33ppm	170ppm	^{192m2}Ir(100%)
Au	0.25%	4.1%	^{192m2}Ir(100%)
Hg	31%	no limit	^{192m2}Ir(100%)
Pb	7.7%	33%	^{208}Bi(96%);^{210m}Bi(4%)
Bi	1.7ppm	56ppm	^{208}Bi(96%);^{210m}Bi(4%)

+Specific activity limits for shallow-land burial waste disposal evaluated by S. Fetter et al. [see Fusion Eng. Design 13 (1990) 239] were adopted.
*New measurements and educated estimates are considered.

NOTES:

ELEMENTS HAVING NO CONCENTRATION LIMITS IN FIRST WALL AND BLANKET MATERIALS ARE THOSE NOT LISTED ABOVE (Z < 84). THESE INCLUDE THE FOLLOWING 36 ELEMENTS: H, He, Li, Be, B, C, O, F, Ne, Na, Mg, P, Sc, Ti, V, Cr, Mn, Fe, Co, Zn, Ga, Ge, As, Rb, Y, Sb, Te, I, Xe, Cs, Ce, Pr, Nd, Ta, W, AND Tl.

- TANTALUM AND TUNGSTEN ARE NO LONGER LIMITED DUE TO RECENT CROSS SECTION MEASUREMENTS AND BRANCHING RATIO ESTIMATES.

- HAFNIUM IS ALLOWED FOR MORE THAN 10% (PER 20 MW-Y/$m^{2)}$ IN THE FIRST WALL, ALSO DUE TO RECENT MEASURED DATA.

specific activity limits for long-lived radionuclides evaluated by Fetter et al as described in Sec. 2. Table 2 also identifies the major long-lived radionuclides which are contributing to the limitation of the relevant natural elements for "Class C" waste disposal. As specified in Table 2, there are 13 elements whose allowable concentrations for "Class C" waste disposal are affected by the results of the IAEA CRP activities. These elements are: Al, Si, Cu, Ag, Eu, Tb, Dy, Hf, Ta, W, Re, Os, and Ir. Table 3 compares the calculated (REAC-2) and revised (using IAEA CRP results) concentration limits for these elements in the first wall and blanket components. Compared to REAC-2, the newly measured and estimated cross sections are summarized below. Note that the natural elements and their allowable concentrations for "Class C" waste disposal that are affected by the cross section status are also commented when appropriate.

Table 3

CALCULATED (REAC-2) AND REVISED CONCENTRATION LIMITS FOR SEVERAL ELEMENTS IN THE FIRST WALL AND BLANKET COMPONENT OF A V/LI FUSION REACTOR FOR SHALLOW-LAND BURIAL+ WASTE DISPOSAL AFTER 20 MW-Y/M2 EXPOSURE

+Specific activity limits evaluated by S. Fetter et al. [see Fusion Eng. Design, 13 (1990) 239] were adopted.

ELEMENT	CONCENTRATION LIMIT			
	FIRST WALL		BLANKET	
	REAC-2	REVISED	REAC-2	REVISED
Al	770ppm	0.2%	0.41%	1%
Si	19%	50%	no limit	no limit
Cu	33%	30%	no limit	no limit
Ag	0.8ppm	1ppm	1.7ppm	2ppm
Eu	210ppm	300ppm	610ppm	870ppm
Tb	0.2ppm	0.2ppm	0.6ppm	0.6ppm
Dy	151ppm	0.6%	0.21%	no limit
Hf	169ppm	5.9%	276ppm	9.7%

Comment: Measured $^{27}Al(n,2n)^{26g}Al$ (Iwasaki, et al.) cross section at 14 MeV is 20 mb, a factor of 2.5 reduction.

Comment: Same as Al.

Comment: Estimated (Qaim) $^{65}Cu(n,t)^{63}Ni$ cross section is 450 micro-b, a factor of 45 reduction; measured $^{63}Cu(n,p)^{63}Ni$ (Greenwood) cross section is 54 mb, a factor of 1.8 increase. However, the total ^{63}Ni production rate changes very little due to the cancellation of the two cross section effects.

Comment: Measured (IAEA) $^{109}Ag(n,2n)^{108m}Ag$ cross sections confirmed REAC-2 results. The ^{108m}Ag half-life is recently measured (PTB) to be about 300 years instead of 127 years as generally known.

Comment: Measured (IAEA) cross sections are within 30% of REAC-2 values.

Comment: Measured (IAEA) cross sections confirmed REAC-2 values.

Comment: Estimated (Vonach) $^{158}Dy(n,p)^{158}Tb$ cross section at 14 MeV is 50 mb, a factor of 40 reduction. This has to be confirmed by measurement.

Comment: Recent measurement (Harwell) of $^{179}Hf(n,2n)^{178m2}Hf$ cross section is 5.9 mb, a factor of 350 reduction.

Ta	5.3%	no limit	61%	no limit

Comment: Estimated (Qaim) $^{180}Ta(n,t)^{178m2}Hf$ cross section at 14 MeV is 0.05 micro-barns, more than 5 orders of magnitude reduction. This cross section value has to be confirmed by experiment.

W	1.5%	15% - no limit	3.6%	36% - nolimit

Comment: Estimated (Vonach) $^{182}W(n,n'Alpha)^{178m2}Hf$ cross section at 14 MeV is 0.02 mb, a factor of 130 reduction. This has to be confirmed by measurements. Branching ratios for the production of ^{186m}Re from ^{185}Re and ^{187}Re have been calculated by P. Young (LANL). Factors of 10 to 100 reduction are assumed from REAC calculations. Measurements are needed to confirm the branching ratio estimate.

Re	833ppm	0.83 - 8.3%	0.13%	1.3 - 13%

Comment: Branching ratios for the production of ^{186m}Re have been calculated by P. Young. Factors of 10 to 100 reduction are assumed. Confirmation is needed by measurements.

Os	0.64ppm	6.4 - 64ppm	1.5ppm	15 - 150ppm

Comment: Same as Re.

Ir	56ppb	5.6ppm	90ppb	9.0ppm

Comment: Estimated (Vonach) $^{191}Ir(n,g)^{192m2}Ir$ cross section at 1 keV is about 94 mb, a factor of 100 lower. This has to be confirmed by measurements.

a. $^{27}Al(n,2n)^{26g}Al$. Measured [11-14] cross sections at 14 MeV are less than 20 mb which is more than a factor of 2.5 reduction compared to REAC-2 values. This change will cause the allowable Al and Si concentrations to increase accordingly, since ^{26g}Al is the dominating long-lived radionuclides produced in both Al and Si.

b. $^{65}Cu(n,t)^{63}Ni$. The cross section estimated by Qaim for this reaction [15] is about 450 micro-barns, which is a factor of 45 reduction compared to REAC-2 values.

c. $^{63}Cu(n,p)^{63}Ni$. The measured cross section by Greenwood [5] is 54 mb at 14.9 MeV. This measured cross section data is a factor of 1.8 more than assumed in REAC-2. The concentration limit for "Class C" disposal of the natural copper element is influenced by both $^{65}Cu(n,t)^{63}Ni$ and $^{63}Cu(n,p)^{63}Ni$ cross sections. Due to the

Table 4

Concentration Limits of Natural Elements in First Wall/Reflector/Shield of a Li/V ARIES Fusion Reactor for Meeting 1 mR per Hour Contact Dose Rate Requirement After 100 Years of Cooling

Neutron Wall Loading: 5 MW/m2
First Wall/Reflector Exposure Time: 4 Years
Shield Exposure Time: 32 Years (Lifetime)

	First Wall	Reflector	Shield
< 1 ppb	-	-	-
1 - 10 ppb	Ag, Tb	Ag	-
0.01 - 0.1 ppm	Cd, Eu, Ho, Nb	Eu, Ho, Nb, Tb	-
0.1 - 1 ppm	Hf	Hf	Ag
1 - 10 ppm	Mo	Co	Eu, Ho, Nb, Tb
10 - 100 ppm	Al, Co, Cu, Dy, Ni, W	Cd, Mo,	Hf
0.01 - 0.1%	Zr	Cu, Ni	Co
0.1 - 1%	Ca, Ti	Al, Dy, W	Mo
1 - 10%	Ta	Ca	Cd
10 - 100%	-	Fe, Ti, Zr	Al, Cu, Ni, W
> 100%	Ar, Fe, K, Mn, N, Na, Cr, V, Zn	Ar, K, Mn, N, Na, Cr, Ta, V, Zn	Ar, Dy, Fe, K, Mn, N, Na, Cr, Ta, V, Zn

*Newly measured or estimated cross sections were accounted for Al, Dy, Hf, Ta, and W.

cancellation of these two cross section changes, the change in the concentration limit is very small, about 10%, as seen in Table 3.

d. $^{109}Ag(n,2n)^{108m}Ag$. Measured [5] cross sections confirmed REAC-2 values (within 20%). The ^{108m}Ag half-life was recently measured at

PTB. The new half-life (about 300 years) should be adopted for future analysis.

e. $^{151}Eu(n,2n)^{150m}Eu$ and $^{153}Eu(n,2n)^{152}Eu$. Measured cross sections [5] agree within 30% to REAC-2 values.

f. $^{150}Tb(n,2n)^{158}Tb$. Measured cross sections [5] agree very well to REAC-2 values.

g. $^{158}Dy(n,p)^{158}Tb$. Estimated cross section by Vonach [16] is 50 mb, which is a factor 40 lower than given in the REAC-2 library. The allowable concentration for Dy as an impurity element in the fusion materials increases by a factor of 40 accordingly.

h. $^{179}Hf(n,2n)^{178m2}Hf$. Measured cross section [5], 5.9 mb at 14.8 MeV, is a factor of 350 reduction compared to REAC-2 values. The concentration limit for "Class C" waste disposal of the Hf element increases accordingly because $^{178m2}Hf$ is the main long-lived radionuclide restricting the use of Hf for the waste disposal concern.

i. $^{180}Ta(n,t)^{178m2}Hf$. Estimated (Qaim [15]) cross section at 14 MeV is 0.05 micro-barns, which is more than 5 orders of magnitude lower than given in the REAC-2 library. If the estimate is valid, Ta would be used with no restriction as far as "Class C" waste disposal is cencerned, as shown in Table 3.

j. $^{182}W(n,n'Alpha)^{178m2}Hf$. Estimated (Vonach [16]) cross section at 14 MeV is 0.02 mb, which is a factor of 130 lower than REAC-2 values.

k. $^{187}Re(n,2n)^{186m}Re$ and $^{185}Re(n,g)^{186m}Re$. Branching ratios for the production of ^{186m}Re from ^{187}Re and ^{185}Re have been calculated by P. Young [17] using the THRESH code. These cross sections and the ratios of $^{186m}Re/^{186g}Re$ and $^{186m}Re/^{186total}Re$ are shown in Fig. 5.1 and 2 [17]. Factors of 10 to 100 reduction can be assumed depending on the neutron spectrum for the W, Re, and Os elements compared to

REAC-2 values for the production of ^{186m}Re. The concentration limit of W, Re, and Os for "Class C" waste disposal would vary accordingly.

1. ^{191}Ir(n,g)^{192m2}Ir. Estimated (Vonach [16]) cross section is about 94 mb at 1 keV, which is a factor of 100 lower than predicted by the REAC-2 library. The allowable concentration limit for the Ir element as an impurity in the fusion materials for "Class C" waste disposal increases accordingly.

Based on the above discussions, confirmation of the estimated cross sections seems warranted for the following cross sections:

a. ^{158}Dy(n,p)^{158}Tb and ^{191}Ir(n,g)^{192m2}Ir for verifying the allowable impurities, Dy and Ir, in the first wall and blanket materials.

b. ^{179}Hf(n,2n)^{178m2}Hf for the diverter material Hf. A model calculation [5] shows that the cross section is a factor of 2 lower than measured. Another independent measurement is needed to check it.

c. ^{180}Ta(n,t)^{178m2}Hf for the verification of using Ta without restriction as a diverter material, and or minor alloying element for the candidate structural material, ferritic steel.

d. ^{187}Re(n,2n)^{186m}Re and ^{185}Re(n,g)^{186m}Re for verifying the use of W and Re as diverter materials and alloying elements.

4.2. Materials Recycling

As far as the materials recycling issue is concerned, more extensive investigations have been performed in Europe [8] than in the U.S.. In this paper, only a brief comparison on some of the natural elements is given. Table 4 shows the concentration limits of some natural elements for hands-on recycling of irradiated first wall, blanket and shield components.

Note that, as shown in Table 4, these concentration limits, mainly due to gamma-ray emitting long-lived radionuclides, are

factors of 10 to 100 of magnitude more stringent than that allowed for "Class C" waste disposal.

For the long-term application of the materials recycling concept to fusion, reuse of reactor materials for hundreds to thousands of years has to be investigated. In this case, not only the activation cross sections leading to the generation of long-lived radionuclides, but also the half-lives and reaction cross sections which lead to the decay and transmutation of the induced long-lived radionuclides, will need to be adequately known.

These long-lived rationuclides include ^{26}Al, ^{94}Nb, ^{108m}Ag, ^{158}Tb, ^{166m}Ho, $^{178m2}Hf$, ^{186m}Re, and $^{192m2}Ir$. It is probably very difficult to measure the transmutation cross sections for these radionuclides due to the concern of samples availability. However, model calculations could, perhaps, provide some educated guess about these cross sections to help the initial-stage investigation in this area.

References

[1] R. Conn et al., "Lower Activation Materials and Magnetic Fusion Reactors," Nucl. Technol./Fusion, 5, 291 (1984).

[2] N.O. Jarvis, Low-activity Materials: Reuse and Disposal, AERE-R 10860, UKAEA Harwell Report, July 1983.

[3] S. Piet et al., "Initial Integration of Accident Safety, Waste Management, Recycling, Effluent, and Maintenance Considerations for Low-Activation Materials," Fusion Technol., 19, 146 (1991).

[4] Proc. Workshop on Low Activation Materials, Executive Version, Vol. I, Culham, GB, 8-12 April 1991.

[5] Wang DaHai, ed., Proc. IAEA Consultants' Meeting held at ANL, September 1989, INDC(NDS)-232/L, IAEA Nuclear Data Section.

[6] Code of Federal Regulations, Licensing Requirements for Land Disposal of Radioactive Waste, Title 10, Part 61, Washington, DC, Nuclear Regulatory Commission, December 30, 1982.

[7] S. Fetter, E.T. Cheng, F.M. Mann, "Long-term Radioactive Waste from Fusion Reactors: Part II," Fusion Eng. Des., 13 (1990) 239.

[8] M.J. Plews, A.R. Davis, G.J. Butterworth, "The Cost-benefit of Recycling Low Activity Stees from Fusion Reactors," CLM-R296, UKAEA Culham Laboratory Report, August 1989.

[9] F.M. Mann, "REAC2: Status of Codes and Libraries," Fusion Technol., 15 (1989)449.

[10] D.L. Smith et al., Blanket Comparison and Selection Study, Final Report, ANL/FPP-84-1, Argonne National Laboratory (1984); see also D.L. Smith et al., Fusion Technol. 8 (1985) 10.

[11] R.K. Smither and L.R. Greenwood, J. Nucl. Mater. 122 & 123 (1984)1071.

[12] M. Sasao, et al., Phys. Rev. C35 (1987) 2327.

[13] S. Iwasaki, J.R. Dumais, and K. Sugiyama, Proceedings of the International Conference on Nuclear Data for Science and Technology, Mito, 1988, ed. S. Igarasi, JAERI, Japan, p. 295.

[14] T. Nakamura et al., Phys. Rev. C43 (1991) 1831.

[15] S. Qaim, private communication, 1990.

[16] H. Vonach, private communication, 1990.

[17] P.G. Young, private communication, 1991.

MEASUREMENTS OF ACTIVATION CROSS SECTIONS FOR SOME LONG-LIVED NUCLIDES IMPORTANT IN FUSION REACTOR TECHNOLOGY*

M.V.Blinov, A.A.Filatenkov, S.V.Chuvaev
V.G.Khlopin Radium Institute, St.Petersburg, 194021, Russia

Abstract

The Ag-109(n, 2n)Ag-108m, Eu-151(n, 2n)Eu-150 and Eu-153(n, 2n)Eu-152 cross sections have been measured in the neutron energy interval of 13.7 - 14.9 MeV. The measurements were performed at the neutron generator NG-400 of the Radium Institute using (D-T) neutrons. At the same facility the upper limit has been obtained for the W-182(n, n'a)Hf-178m2 cross section. Neutron capture of the Mo-98 that lead ultimately to the production of the long-lived Tc-99 has been studied at neutron energies 0.7 - 2.0 MeV. For these purposes, the Van de Graaf accelerator (EG-5) was employed that produced monochromatic neutrons in the (p-T) reaction. Both at EG-5 and NG-400 measurements, special efforts were made to minimize neutron spectrum impurities which unavoidably arise in irradiation environments.

1. Introduction

A growing social thrill for ecological problems demands an especial attention to the disposal of radioactive waste, among which long-lived radionuclides are of great importance [1]. Recently, an IAEA CRP was established that is devoted to calculations and measurements of long-lived radioactivity produced in the fusion reactor. In view of the high complexity of similar investigations, the needed data were extremally poor up to the last time [2].

One of the main experimental difficulties is the necessity to work with rather weak "useful" activities hidden usually in a much more intensive background. For measurements of corresponding cross sections, high power neutron sources seem to have an obvious advantage because they spare the time of sample irradiation and activity measurement, and besides, allow to diminish to some extent uncertainties caused by finite sizes of samples and detectors.

However, high power neutron sources, as a rule, generate neutrons of spectra which are studied far not so well as, for example, spectra of

* This work was carried out under IAEA scientific agreement No. 5677

neutrons produced by conventional neutron generators. So in the cases when the cross sections to be measured change rapidly in the covered neutron energy interval, this may lead to somewhat ambiguous results (e.g. in region near the reaction threshold). An additional uncertainty emerges when the measured or interfering cross sections have a much higher value at the lower neutron energies (e.g. the (n, g)-reaction), where scattered neutrons can produce considerable effects which are difficult to correct for. In the similar situation, the low current accelerators should be prefered where rather pure neutron fields can be generated.

Among the cross sections measured by us in the frame of this agreement, two were expected to have high sensitivity to contaminations of neutron spectra, namely, the Eu-153(n, 2n)Eu-152 and Mo-98(n, g)Mo-99 cross sections. Three other reactions appeared to be less sensitive to peculiarities of the real neutron facilities. Unfortunately, disturbance of neutron spectra is not the only error source, and in order to increase the relaibility of the final results, it is highly desirable to conduct measurements under conditions that differ as strongly as possible. From this point of view, it is very interesting to compare the data obtained at irradiation in pure but weak neutron fields with those obtained at irradiation by moderate and power neutron fluxes.

2.Experimental proceedures

2.1. Sample preparation

In our measurements we used various forms of samples assembled in packages of several types. In the Mo-98(n, g) reaction study, metallic disks of the natural molybdenum 0.3 mm thick and 14.1 mm in diameter were used. Each of them was installed in the middle of an assembly which also contained pairs of the Au- and In-foils used as neutron flux monitors. The total thickness of the assembly was 1.5 mm.

The Ag-109(n, 2n)Ag-108m cross section were measured with two types of sample packages. The first used the enriched Ag-109 (99.4%). This was a metallic powder encapsulated in a lavsan packet and arranged in a thin-wall plastic tube together with two similar packets containing the enriched europium isotopes (see below). In front and in the back of the packets, the niobium foils were mounted to determine the neutron flux. Typically, such a sample package was 14.5 mm in diameter and 7 mm in hight.

The other type of samples used in the Ag-109(n, 2n) experiment was a metallic foil of natural silver sandwiched between the niobium foils. This sandwich was 0.7 mm thick and 14.1 mm in diameter.

For the Eu-151(n, 2n)Eu-150 and Eu-153(n, 2n)Eu-152 cross section measurement, also two variants of samples were prepared. The first contained oxides of the enriched Eu-151 (97,5%) and Eu-153 (99.2%) as well

as the enriched metalic Ag-109 (see above). Three packets with distinct isotopes were placed in a plastic tube parallel to each other. The common neutron flux was determined by the niobium foils framing the packages.

In the second variant, the oxide of the natural europium was thoroughly mixed with the niobium oxide. The use of a homogeneous mixture of the studied and reference nuclei reduced considerably the uncertainties connected with the geometrical factor in irradiation and activity measurement. Each sample weighed about 1 g. The ratios of the Eu-153-, Eu-151- and Nb-93-nuclei were 4.63 : 4.24 : 1.

Since the W-182(n, n'a)Hf-178m2 cross section was expected to be very small, the close geometries of irradiation and measurement are highly desirable. Therefore, a homogenious mixture of tungsten acid and niobium oxide was used initially. The total weight of this sample was 12.9 g, and it contained 14.4 nuclei of W-182 per a Nb-93 nucleus.

As before, another type of sample package was used for this cross section measurement too. Ten metallic foils of the natural tungsten were placed close to the neutron target. The eleventh foil was sandwiched between two niobium foils and distanced from the target at 42 mm. This was used to obtain in the same experiment the W-182(n, 2n)W-181 cross section, relative to which the W-182(n, n'a) cross section could be determined most convenient. The size of each W-foil was 11 mm * 0.1 mm.

2.2. Irradiation conditions

The Mo-98(n, g)Mo-99 reaction was studied in the 0.7 - 2.0 MeV neutron energy range. Irradiations were conducted using monochromatic neutrons of the 3H(p, n)3He reaction. The proton beam diameter of the Van de Graaf accelerator was about 2 mm. During irradiation the beam was rotated drawing a circle with the diameter up to 8 mm on the titanium-tritium target. Since the target was cooled by an air jet, the beam current was restricted by the magnitude of 8 microA.

The sample package contained the Mo-, Au- and In-fcils was located at 0 deg with respect to the incident beam direction and 23 mm from the target. The irradiations were performed at proton energy of 1.6, 2.1, 2.3, 2.6 and 2.8 MeV that corresponded to the mean neutron energy of 0.74, 1.26, 1.46, 1.76 and 1.97 MeV. The neutron energy spread (FWHM) resulted from proton slowing-down in the target and angular dependence of neutron energy was 0.12, 0.11, 0.10, 0.10 and 0.09 MeV, respectivelly. These quantities were calculated using the recommended c.m.s. data on the (p-T)-reaction kinematics [1] and the sheets of charged particle energy losses in materials [2].

The samples were irradiated usually 12 hours, accumulating neutron fluence (3 - 5)*10^{12} n/cm^2. Small neutron flux variations were registered by means of a long counter.

The Ag-109(n, 2n)Ag-108m, Eu-151(n, 2n)Eu-150, Eu-153(n, 2n)Eu-152 and W-182(n, n´a)Hf-178m2 cross sections were measured at the neutron generator NG-400 using the H-3(d, n)He-4 reaction neutrons. Irradiations were carried out at the accelerating voltage varied from 240 to 280 kV. The mean neutron energy determined mainly by the angle relative to the deuteron beam line was ranged from 13.6 to 14.9 MeV.

At the study of the Ag-109(n, 2n), Eu-151(n, 2n) and Eu-153(n, 2n) reactions, sample packages were placed at different angles at the distance of 3 - 4 cm from the target. The total neutron fluence collected by a sample was (2 - 5)*10^{12} n/cm^2.

In the case of the W-182(n, n´a) cross section measurement, the samples occupied a position close to the target at 0 degrees relative to the beam. The water cooling of the target was used. The mean value of the neutron fluence recieved by the sample was ~ 10^{14} n/cm^2.

Space-energy neutron distribution was calculated for real experimental conditions using the recommended data on kinematic characteristics of the (D-T) reaction [1] and the specific ionization losses of deutrons in various substances [2] (Fig. 1).

2.3 Neutron field study

In order to reveal the role of scattered neutrons, some special measurements were performed. So, measuring Mo-98(n, g)Mo-99 cross section at the EG-5, we carried out two runs of irradiations, with the water cooling of the target and with the air one. In all cases both the Au- and the In-foils were used for neutron fluence determination. Consequently, in each irradiation the two fluence magnitudes could be obtained, which had quite different sensitivities to the scattered neutron contamination, because one of the reference reactions had the threshold about of 0.4 MeV (the In-115(n, n´)In-115m reaction) and the other had the cross section raising as 1/v in the low energy region (the Au-197(n, g)Au-198 reaction). The ratio of these two neutron fluence magnitudes differs in the considered cases. The use of the water cooling increases the relative Au-activities by 1.2 - 1.6 times. It is worth noticing that the thickness of the water layer was approximately 3 mm in that case.

To illustrate the effect of neutrons scattered by light materials of the target chamber we carried out another experiment at the NG-400 in which the water cooling of the target was used, and besides, the polyethylene "head" with the walls of 10 mm was put on the target chamber. In such a manner, the Au-197(n, g)Au-198 and In-115 (n, n´)In-115m cross sections were determined, which have a high sensitivity to the small contamination of neutrons with En < 1 MeV and En = (1-6) MeV, respectively. In Fig. 2 they are compared with the corresponding cross sections measured under the normal conditions, where the production of scattered neutrons was reduced: we used the thin wall chamber (2.2 mm) and the thin target backing

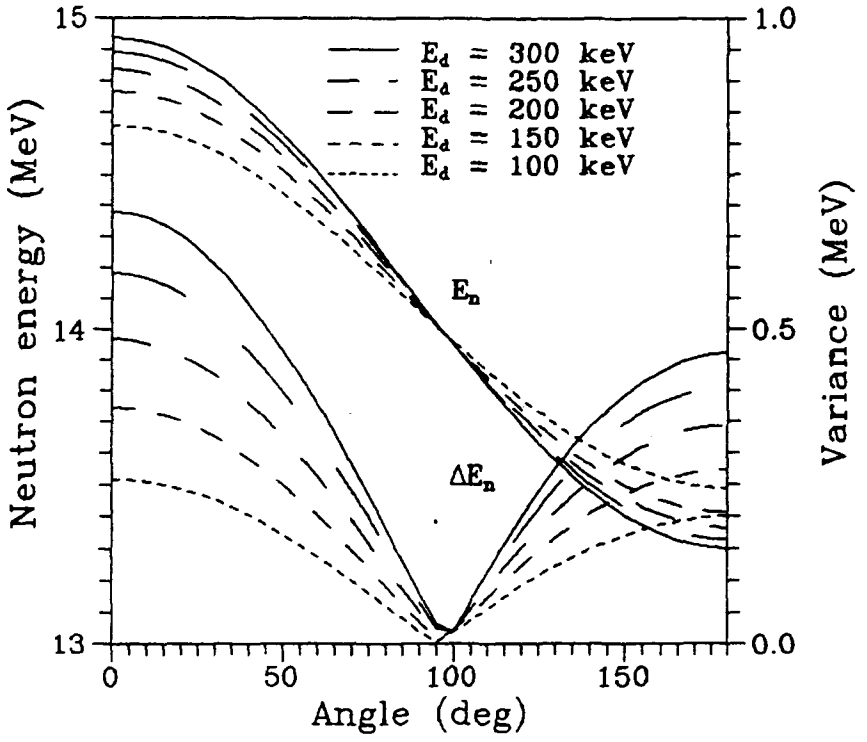

Fig. 1. Space-energy distribution of neutrons generated in T(d, n)-reaction. The target thickness - 1 mg/cm2.

(0.3 mm), cooled by the air jet. The experimental hall has the dimensions 10 m * 10 m * 6 m.

For the determination of the slow scattered neutron contribution it is very convenient to use natural europium (47.8% Eu-151 and 52.2% Eu-153). Eu-152 isotope is formed simultaneously in the flux of fast neutrons due to both Eu-153(n, 2n) reaction and Eu-151(n, g) one. The latter reaction was proceeded mainly by capture of scattered slow neutrons. The contribution of the Eu-151(n, g) reaction in our case was ~ 1%. The same type of measurement we carried out using another neutron generator NG-200. This generator had the rotating target and water cooling (neutron yield ~10^{12} n/s). The experimental room was comparatively small. In this case the Eu-151(n, g) reaction contribution was 15 - 20%. We can compare our results with the data of the JAERI (great rotating target, neutron yield > 10^{12} n/s, small experimental room). For the accelerator the contribution of this (n, g) reaction was about 40%. We consider there is a correlation between experimental conditions and scattered slow neutron contribution. This is a sum effect of neutrons scattered by target chamber, surrounding materials and by the walls. So using natural europium gives a good possibility of the neutron field analysis.

We carried out the measurements of the neutron reactions Al-27(n, a) and In-115(n, n') based on the Nb-93(n, 2n) reference reaction cross section. It was assumed Nb(n, 2n) cross section at the 14.5 MeV neutron energy was equal 460 ± 5 mb and was constant in the 13.5 - 15.0 Mev interval in the limits of ± 2%. These

measurements were performed to compare the results of the determination of the reference reaction cross section under various experimental conditions. From the comparison of our results with another data [5 - 7] it was found that there is a rather good agreement between them.

2.4. Activity measurement

The induced gamma-activities were measured with a Ge(Li)-detector having the energy resolution 2.7 keV and peak efficiency 7.9% at 1332.5 keV gamma-ray energy. A computer DVK-3M fitted for on line data acquisition was provided with a program set adapted for gamma-activation analysis.

The gamma-spectrometer efficiency was determined by means of standard gamma-sources, activities of which were attestated with error of 1.5 - 2.0% at the confidence probability of 0.99.

The calibrations were periodically repeatet showing constancy of the efficiency value in bounds of 0.5% for the gamma-ray energy range 200-3000 keV.

Corrections for gamma-ray self-absorbtion and the change of the effective distance between the sample center and the detector center were measured experimentally. Besides, we have a possibillity to deduce these corrections using the code SPEDAC aimed to the volume gamma-activity measurement that yielded fairly close results. Typically, those were of order of several percent, though in individual cases they could exceed 40% (the large homogenious tungsten sample).

2.5. Cross section computation

Experimental data were processed by an IBM PC AT (286) using GAMANAL, SPEDAC and ACTICS codes. The last was specially written to treat the neutron activation information. It included various libraries, such as energies and yields of the induced gamma-activity, geometries and histories of the conducted irradiations, masses and sizes of the available samples, etc. The cross sections were calculated by the formulas taking into account two generations of the induced radioactivity.

In order to decrease the errors due to poor statistics of the treated gamma-spectra, the mean weighted values of the cross sections were obtained using data on all the observable gamma-peaks.

The main errors of the experimental results were the following: the uncertainties of the fluence measurement - (2 - 5)% and the uncertainties of the induced activity determination (2 - 4)%. The uncertainties of the half life determination were included in the total errors (except Ag-108m).

3. Results

Some nuclear data on the studied reactions and associated decay data of products are presented in Table 1. The results of the cross section measurements are given in Fig. 3 - 6 and in Tables 2 and 3.

Table 1. Decay data of activation products

Nuclear reaction	Q-value (MeV)	Initial spin	Final spin	Half-life of product T1/2	γ-ray Energy	Abundance (%)
Ag-109(n,2n)Ag-108m	-9.186(4)	1/2-	6+	127(21)y	433.94	90.5(6)
					614.28	89.9(21)
					722.94	90.9(21)
Eu-151(n,2n)Eu-150	-7.935(4)	5/2+	5-	35.80(10)y	333.97	96.0(30)
					439.40	80.4(34)
					584.27	52.6(33)
Eu-153(n,2n)Eu-152m2+g	-8.553(4)	5/2+	3-	13.33(4)y	344.28	25.68(19)
					778.91	12.96(7)
					964.13	14.62(6)
					1408.01	20.85(8)
W-182(n,nα)W-178m2	-1.773(4)	0+	16+	31(1)y	213.43	81.7(18)
					325.57	94.1(18)
					426.36	96.9(20)
Mo-98(n,γ)Mo-99	+5925.6(23)	0+	1/2+	65.94(1)h	140.51	89.4(2)

3.1. Ag-109(n, 2n)Ag-108m

No experimental data on this reaction cross-section has been reported before IAEA CRP. The first results were reported at the IAEA Argonne Meeting in 1989 [8]. Our new results are presented in Fig. 3 along with the results of JAERI [9], IAE Beijing [10] and ANL/LANL/JAERI [11]. There is a rather good agreement of the data of the four scientific groups at the 14.8-14.9 MeV neutron energy. The data of IAE Beijing group are a little higher than our results. For all data the half-life of 127 years was used. New measurements carried out at PTB gave for the Ag-108m another value of the half-life - 418 years.

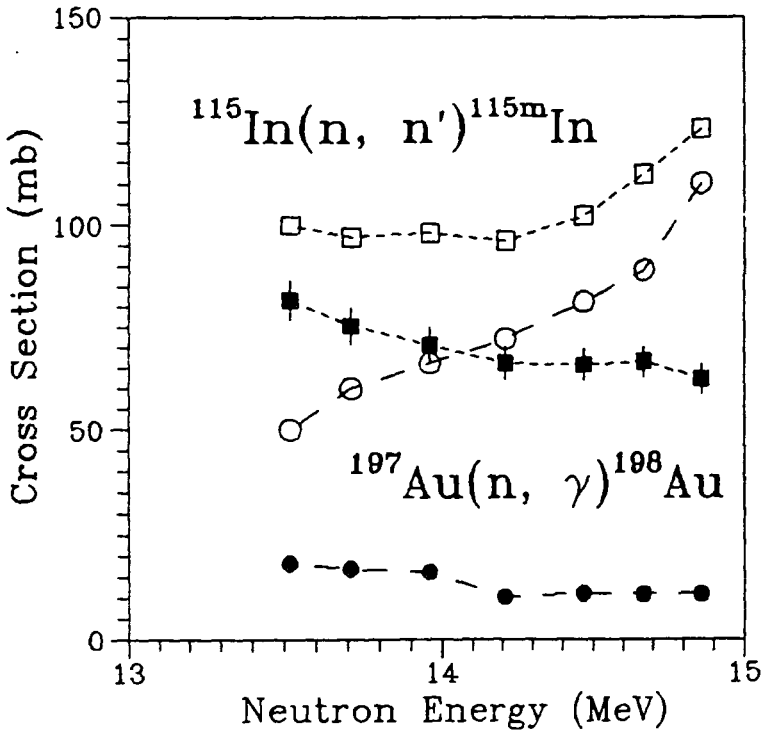

Fig. 2. Cross-section of the In-115(n, n')In-115m and Au-197(n, γ)Au-198 reactions.
● ■ - measured under the normal conditions
○ □ - measured with the scatterer

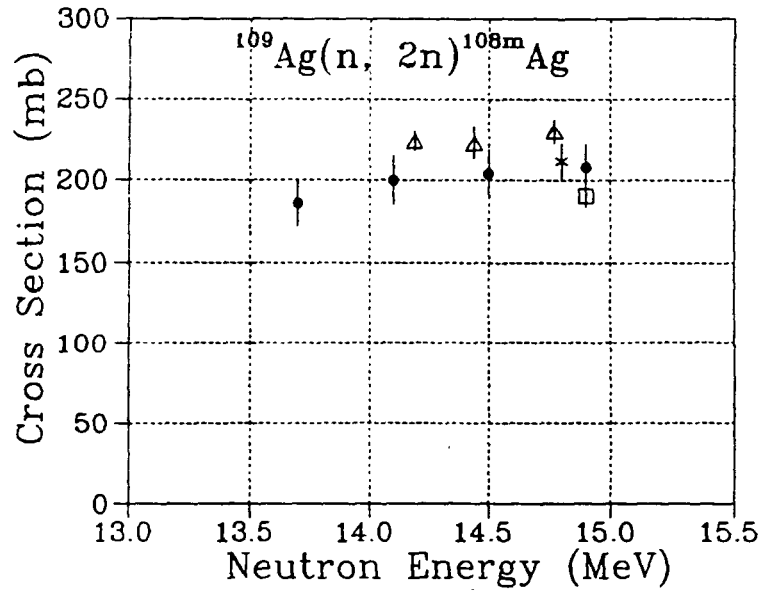

Fig. 3. Cross-section of Ag-109(n, 2n)Ag-108m
● - present data × - [9]
▲ - [10] □ - [11]

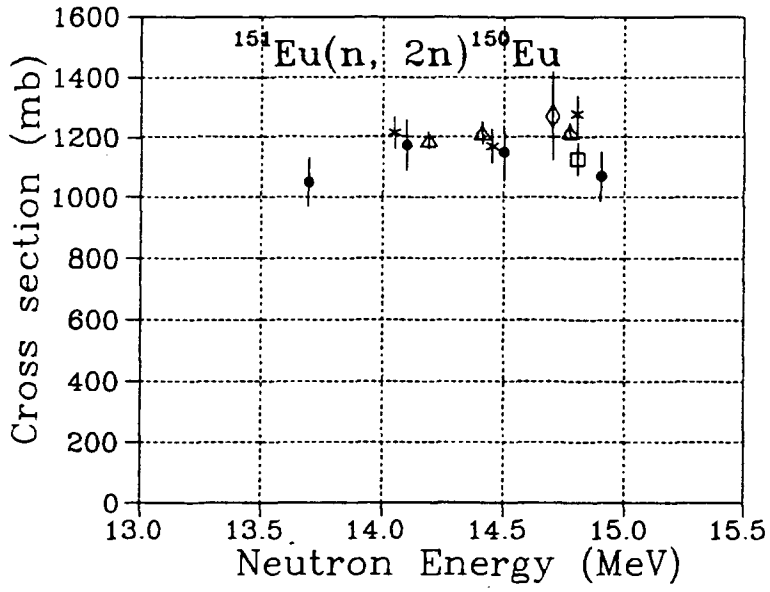

Fig. 4. Cross-section of Eu-151(n, 2n)Eu-150

● - present data × - [9]
□ - [11] ◇ - [12]
△ - [10]

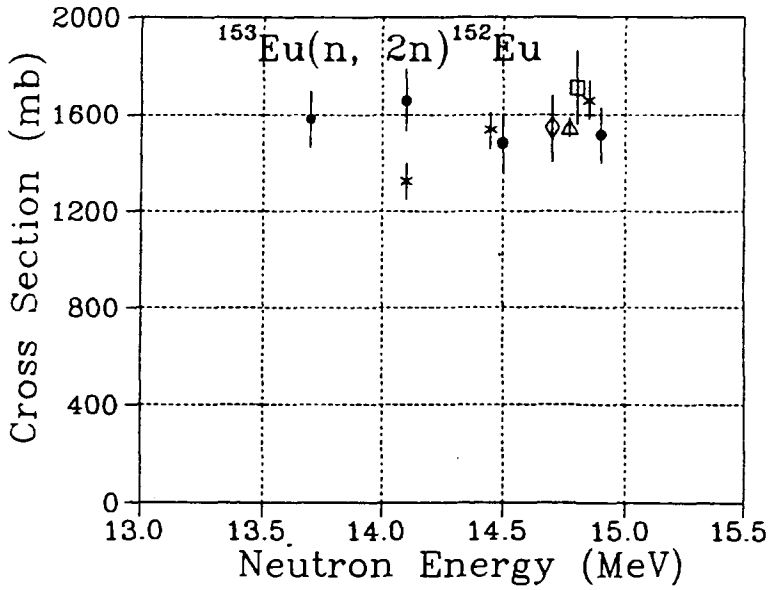

Fig. 5. Cross-section of Eu-153(n, 2n)Eu-152m2+g

● - present data × - [9]
△ - [10] □ - [11]
◇ - [12]

3.3. Eu-153(n, 2n)Eu-152

Our new experimental results for this reaction agree with our data reported earlier [8] within experimental errors. From Fig 5. it can be seen a good agreement of the cross sections obtained by various groups [9 - 12] with our experimental results (there is some difference only

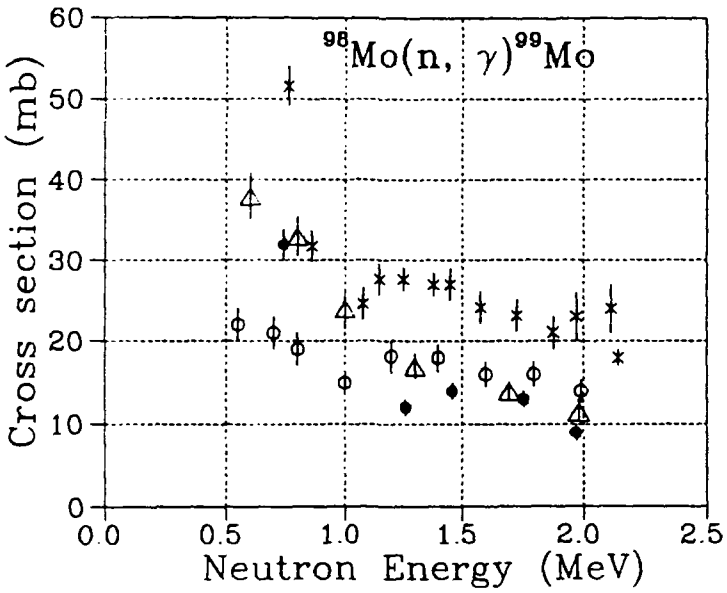

Fig. 6. Cross-section of Mo-98(n,γ)Mo-99

● - present data × - [13]

△ - [14] ○ - [15]

for E_n = 14 MeV). All data were obtained for the sum of the states m2+g as the state m2 (96 min) decays with 100% probability to the ground state.

3.4. W-182(n, n'a)Hf-178m2

The fluence measurements for this reaction were performed using W-182(n, 2n)W-181 reaction. We registrated gamma-rays with 152 keV energy (half-life 120.95 days). This gamma-ray branching was used as 0.097%.

After a cooling (150 days) the search of the 213, 325 and 426 keV gamma-lines was carried out. We could not detect these lines definitly and so now only the high limit of the cross section value can be given σ < 40 mb.

3.5. Mo-98(n,γ)Mo-99

The measurements were performed in the neutron energy range 0.75-2.0 MeV. The neutron fluence was determined by Au-197(n,γ) reference reaction, whose cross sections were taken from the ENDF-B/5 Standard File. In Fig. 6 results of Stupegia [13], Dovbenko [14], and Trofimov [15] are shown. The data of Ref [13] differ from results of the other groups. Our data and the data of Ref [14] and [15] agree rather well in the 1.5 - 2.0 Mev region and differ for the lower energies.

References

1. E.Cheng, Proc. IAEA Advisory Group Mtg. on Nucl Data for Fusion Reactor Techn. FRG 1986. IAEA TECDOC-457 IAEA Vienna p.16 (1988).

2. E Cheng, Nucl. Data for Science and Technology (Proc. of the Intern. Conf. MITO 1988, JAERI 1988 p.187.

3. M.Drosg, O.Schwerer, In: Handbook on Nuclear Activation Data Techn. rep. ser. N273 IAEA Vienna (1987).

4. L.C.Northcliffe, R.F.Shilling, NDT A7 (1970) p. 233.

5. T.V.Ryves, Europ. Appl. Res. Rep. Nucl. Sci. Techn. Vol.7 (1989) p.1241.

6. N.M.Kornilov et al, IAEA-TECDOC. Vienna 1985 p.135.

7. V.N.Manochin et al, In: Handbook on Nuclear Activation Data Techn. rep. ser. N273 IAEA Vienna (1987) p.305.

8. INDC(NDS)-232L. Activation Cross-Sections for the Generation of Long-Lived Radionuclides of importance in Fusion Reactor Technology. Proc. of the IAEA Cons. Meeting ANL 1989.

9. Y.Ikeda, A.Kumar, C.Konno, Proc. of the Intern. Conf on Nuclear Data for Science and Technology. Yulich 1991.

10. Lu Hanlin at al. INDC(NDS) 232/L, p.33.

11. J.W.Meadows at al. INDC(NDS) 232/L, p.79.

12. S.M.Qaim, Nucl. Phys. A190 (1974) p.319.

13. D.C.Stupegia et al. Journal of Nucl. Energy 22 (1968) p.267.

14. A.G.Dovbenko, V.A.Tolstikov, Atomic Energy (Rus), 26 (1969) p.67.

15. Yu.N.Trofimov and Yu.A.Nemilov, Nucl. Constants (Rus) 3/15 (1984) p.15.

"Activation Cross Sections for the Generation of Long-Lived Radionuclides of Importance in Fusion Reactor Technology"

Vienna, 11-12 November 1991
IAEA Room A2715

Agenda

Monday, 11 November

09:30-09:45 1. Opening of the Meeting (Room A2715)

- Adoption of Agenda

09:45-11:00 2. Progress reports of the CRP participants on experiments

- H. Vonach (Austria)

- Lu Hanlin (China)

  "Measurement of the cross section for $^{179}Hf(n,2n)^{178m2}$, $^{187}Re(n,2n)^{186g}Re$, $^{23}Na(n,2n)^{22}Na$ and $^{151}Eu(n,\gamma)^{152g}Eu$ reactions"

- S.M. Qaim (Germany)

  "Excitation functions of $^{151}Eu(n,2n)^{150m}Eu$ and $^{159}Tb(n,2n)^{158}Tb$ reactions"

11:00-11:15 Break

11:15-12:30 - J. Csikai (Hungary)

  "Measurements and calculations of some activation cross sections for the generation of long-lived radionuclides"

- M.V. Blinov (USSR)

- "Generation cross sections of some long-lived isomers for 14 MeV neutrons"

12:30-14:00 Lunch

14:00-15:30 - D.L. Smith (USA)

3. Recent Japanese measurements of activation cross sections for the generation of long-lived radionuclides

- Y. Ikeda (Japan)

  "Measurements of long-lived activation cross sections at 14.7 MeV in the inter-laboratory collaboration with ANL/LANL/JAERI"

15:30-15:45 Break

15:45-18:00 4. Discussions on technical problems with experiments

Tuesday, 12 November

09:30-11:00 5. Progress reports of the CRP participants on theoretical calculations

- G. Maino (Italy)

- M.B. Chadwick (UK)

"Theoretical calculations of isomer production cross sections using pre-equilibrium-equilibrium models"

11:00-11:15 Break

11:15-12:30 - D. Grudzevich (USSR)

"Evaluation of the isomer excitation functions for neutron induced reactions"

6. Recent Romanian activation cross-section calculations

- V. Avrigeanu

"Consistent activation cross-section calculations for all stable isotopes of Ti, V, Cr, Mn, Fe, Co and Ni"

7. Discussions on theoretical calculations

8. Activation cross section data needs for fission and fusion reactor technology

- E.T. Cheng (USA)

12:30-14:00 Lunch

14:00-15:30 9. Review of the data status of activation cross sections for the generation of long-lived radionuclides and its potential impact on the work of the CRP

10. Work programme of the CRP for 1992 - 1993

15:30-16:00 Break

16:00-18:00 Discussions of conclusions and recommendations

NOTIFICATION OF AN AGENCY-SPONSORED MEETING

Title of meeting: RCM on Activation Cross Sections for the Generation of Long-lived Radioactive Nuclides of Importance in Fusion Reactor Technology

Dates of meeting: 11-12 November 1991

Scientific Secretary: Wang DaHai (A-2309, x1707)

Place of meeting: IAEA Headquarters
Meeting Room: A2715

Secretary: E. Baumgartner (A-2314, x1710)

PARTICIPANTS	ADDRESS ABROAD
Austria	
Prof. Dr. H.K. Vonach No. 6242/CF	Institut für Radiumforschung und Kernphysik Boltzmanngasse 3 A-1090 Vienna
Dr. Maria Wagner	Institut für Radiumforschung Und Kernphysik Vienna
China	
Dr. Lu Hanlin No.5060/CF	Institute of Atomic Energy P.O. Box 275(3) Beijing 102413
Germany	
Dr. Syed M. Qaim No. 5061/CF	Institut für Chemie Forschungszentrum Jülich GmbH D-W 5170 Jülich
Hungary	
Prof. Dr. J. Csikai No. 4882/CF	Institute of Experimental Physics Kossuth University P.O. Box 109 H-4001 Debrecen
Japan	
Dr. Y. Ikeda	Fusion Reactor Laboratory Dept. of Reactor Engineering Japan Atomic Energy Research Inst. Tokai-mura, Naka-gun Ibaraki-ken, Japan
Dr. Y. Kanda	Dept. of Energy Conversion Engineering Kyushu University 33 Sakamoto, Kasuga Kasuga-shi Fukuoka-ken 816, Japan

PARTICIPANTS	ADDRESS ABROAD
Dr. H. Maekawa	Fusion Reactor Laboratory JAERI Tokai-mura, Ibaraki-ken
Italy	
Dr. G. Maino No. 6416/CF	E.N.E.A. Viale G.B. Ercolani, 8 I-40138 Bologna
Netherlands	
Dr. J. Kopecky	Department of Physics Netherlands Energy Research Foundation (ECN) 3, Westerduinweg NL-1755 ZG Petten
Romania	
Dr. V. Avrigeanu	Institute of Atomic Physics P.O. Box MG-6 R-76900 Bucharest-Magurele
United Kingdom	
Dr. Mark B. Chadwick No. 5062/CF	Present address MS B 243 Los Alamos National Laboratory Los Alamos, NM 87545
United States	
Dr. D.L. Smith No. 5064/CF	Applied Physics Division Bldg. D-314 Argonne National Laboratory 8700 South Cass Avenue Argonne, IL 60439
Dr. E.T. Cheng	TSI Research 225 Stevens Avenue Suite 110 Solana Beach, CA 92075
USSR	
Dr. M.V. Blinov No. 5677/CF	V.G. Khlopin Radium Institute Ul Rentgena 1 St. Petersburg 197022
Dr. D. Grudzevich on No. 6719/CF	Institute of Atomic Energetics Ploshchad Bondarenko SU-249 020 Obninsk

PARTICIPANTS	ADDRESS ABROAD
USSR continued	
Dr. A.V. Ignatyuk	Fiziko-Energeticheskij Institute Obninsk

Nuclear Data Section

J.J. Schmidt
D.W. Muir
A. Pashchenko
N. Kocherov
H.D. Lemmel
S. Ganesan